UNIVERSIDAD AUTONÓMA DE MADRID

Faculty of Sciences
Department of Molecular Biology

The role of the Crc/Hfq/CrcZ-CrcY global regulatory system on the regulation of metabolic and cellular processes in *Pseudomonas putida*

Doctoral Thesis
Ruggero La Rosa
Madrid 2015

UNIVERSIDAD AUTONÓMA DE MADRID

Facultad de Ciencias
Departamento de Biología Molecular

The role of the Crc/Hfq/CrcZ-CrcY global regulatory system on the regulation of metabolic and cellular processes in *Pseudomonas putida*

Tesis Doctoral

Memoria presentada para optar al grado de
Doctor Internacional en Microbiología

Director de tesis:
Dr. Fernando Rojo

Este trabajo se ha realizado gracias a una beca predoctoral de la Fundación "La Caixa"

Este trabajo se ha realizado en el Centro Nacional de Biotecnología CNB-CSIC

Index


Crc
system
medium
Introduction
Results
Conclusions
Experimental
procedures
putida
hierarchy
consumption
Pseudomonas
translation
Chapter
Crc/Hfq
metabolism
discussion
carbon
succinate
Inactivation
growth
LB
mRNAs
Role
CrcZ
sources
glucose
gene
CCR
leads
acids
phaC1
Influence CrcY
Crc/CrcZ-CrcY
proteins
mixture
subtilis
glycolytic
RNAs
accumulation
Repression
pyruvate
PHA
initiation
protein
complete
flux
levels
regulated
growing
forces
Levels
Carbon
metabolites
production
carbon/nitrogen
cell
ndex
Figures
Effect
secreted
sugars
Binding
Genes
different
helps
C/N
cells
polyhydroxyalkanoates
Materials
ATP
acetate
present
transcriptome
assimilation
Hierarchy
papers
analysis
PTSNtr
Constraint-based
inhibit
rerouting
terminal
KT2440
regulator
carboxylic
provided
greater
mRNA
published
balanced
Summary
identified
phosphotransfer
inhibits
Bacillus
gluconeogenic
NADH
conditions
secretion
sRNAs
Escherichia
profile
Analysis
Cyo
Crc/Hfq-CrcZ/CrcY
integration
regulatory
reveals
Supplementary
global
coli
ratios
phaF
phaI
crc
NADPH
NMR
Compounds
Catabolite
compounds
Resumen
small
controlling
Annexes
Objectives
oxidase
amino
Discussion
Conclusiones
References

GENERAL INDEX

Index of Figures

Summary

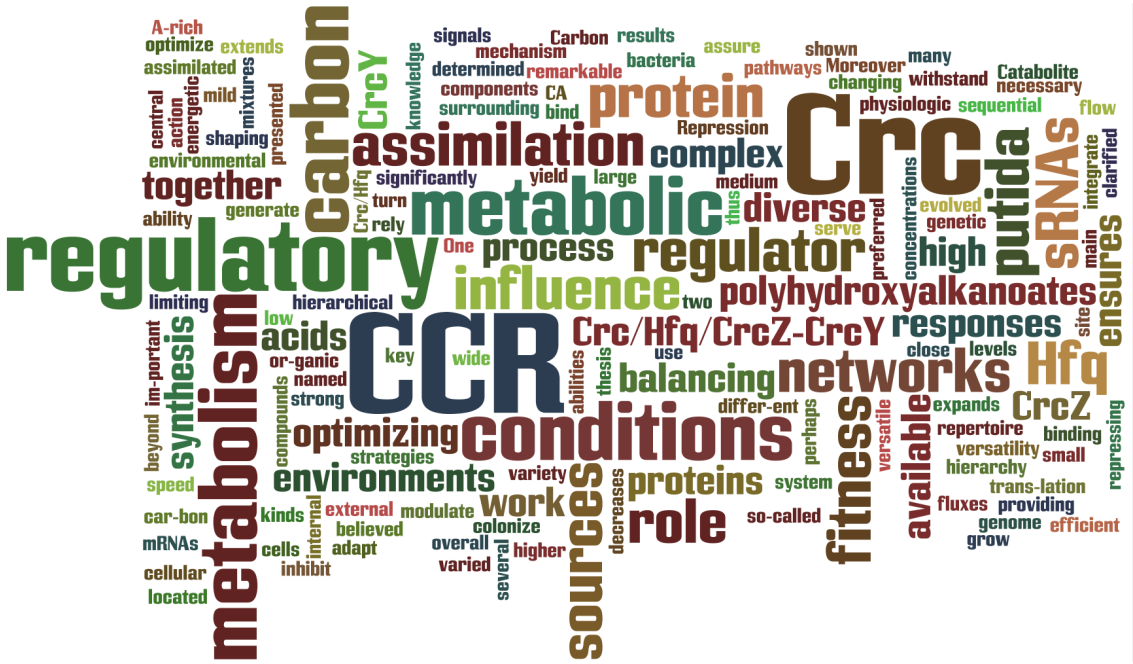
regulatory
metabolism
carbon
CCR
Crc
assimilation
metabolic
protein
conditions
influence
networks
regulator
Crc/Hfq/CrcZ-CrcY
responses
polyhydroxyalkanoates
fitness
sources
role
optimizing
environments
balancing
proteins
work
process
diverse
complex
putida
sRNAs
Hfq
CrcZ
CrcY
ensures
together
synthesis
acids
available
high
Repression
Carbon
signals
mechanism
determined
remarkable
bacteria
pathways
Moreover
shown
assure
results
components
surrounding
bind
CA
knowledge
physiologic
sequential
flow
withstand
Catabolite
necessary
changing
many
optimize
extends
assimilated
mixtures
mild
energetic
central
action
shaping
environmental
presented
generate
ability
limiting
hierarchical
low
key
wide
use
close
levels
site
integrate
clarified
main
genetic
evolved
concentrations
preferred
serve
thus
medium
large
yield
significantly
turn
rely
Crc/Hfq
One
two
differ-ent
perhaps
versatile
expands
repertoire
versatility
hierarchy
trans-lation
fluxes
providing
genome
grow
efficient
binding
small
repressing
system
so-called
variety
strategies
decreases
proteins
modulate
colonize
overall
varied
several
higher
external
internal
believed
adapt
inhibit
cells
kinds
car-bon
mRNAs
cellular
located
speed
beyond
im-portant
or-ganic
named
strong
compounds
abilities
thesis
A-rich

Metabolically versatile bacteria have evolved diverse strategies to adapt and to colonize different environments and niches. This ensures high fitness and the ability to withstand changing surrounding conditions and diverse kinds of stresses. These abilities rely on a varied genetic repertoire and on complex regulatory networks that integrate external and internal signals, providing efficient responses. *Pseudomonas putida* possesses a large genome and a remarkable metabolic and physiologic versatility, with several regulatory networks that assure metabolic responses for surviving in a wide variety of environments. One of the main regulatory networks that serve to optimize metabolism, growth speed and cellular fitness is the so-called Carbon Catabolite Repression (CCR). This regulatory mechanism ensures that, when mixtures of carbon sources are available at sufficient concentrations, those with higher energetic yield are preferentially assimilated, limiting the use of those that are less preferred. This process allows a hierarchical and sequential assimilation of the carbon sources available, optimizing metabolism and the overall fitness. In *P. putida*, the Crc and Hfq proteins and the CrcZ and CrcY small RNAs are key components of CCR. The Crc and Hfq proteins work together to inhibit the translation of some mRNAs that present an A-rich sequence, named CA motif, located close to the ribosome binding site. In turn, Crc/Hfq action is antagonised by the CrcZ and CrcY sRNAs. The levels of these two sRNAs are low in media that generate high CCR conditions and increase significantly when CCR decreases; it is believed that the function of these sRNAs is to bind the Hfq protein, perhaps together with Crc, sequestering them when their effects are not necessary.

The work described in this thesis expands our knowledge on the influence of CCR, and in particular of the Crc/Hfq/CrcZ-CrcY system, in shaping *P. putida* metabolism according to environmental conditions. The results presented illustrate the role of the Crc regulator in controlling several metabolic processes. We have determined the hierarchy of assimilation of organic acids and amino acids when cells grow in a complex medium, where CCR is strong, and the role of the Crc protein in regulating this process. We have also clarified the influence of the Crc regulator in balancing the carbon fluxes through central metabolic pathways under mild CCR conditions, optimizing metabolism. Moreover, we have shown that the Crc/Hfq/CrcZ-CrcY regulatory network can modulate the synthesis of polyhydroxyalkanoates, which are important storage compounds, thus balancing carbon flow. The influence of the Crc protein in the synthesis of polyhydroxyalkanoates extends the role of this regulator beyond that of repressing the uptake and assimilation of non-preferred carbon sources.

Resumen


represión
catabólica
Crc
metabolismo
regulador
condiciones
función
pequeños
biológica
eficacia
fuentes
diversas
fuerte
sistema
RNAs
asimilación
putida
Hfq
CrcZ
CrcY
Crc/Hfq/CrcZ-CrcY
proceso
compuestos
carbono
resultados
optimizando
ambientales
células
regulación
capacidad
cambiantes
características
importantes
proteina
influencia
llamada
traducción
medio
bacterias
respuestas
clave
inicio
cuya
supervivencia
genoma
disponibles
fisio-lógica
facilitan
clarificado
cata-bólica
reguladora
redes
implican
trabajan
rico
varios
tesis
determinados
balance
preferidos
menos
jerárquica
significativamente
limitando
crece
solo
moderada
diferentes
CA
mRNAs
adaptarse
elevada
describe
aseguran
dos
niveles
piensa
adecuadas
competitiva
región
secuestrándolas
bajos
obtenidos
ecosistemas
situaciones
concentraciones
flujo
grande
secuencia
controla
ambiente
necesario
ácidos
confieren
metabolicen
versátil
célula
inhibir
señales
destaca
permite
regulan
mejor
conjunto
protei-nas
adeninas
aumentan
aminoácidos
quizá
derivan
preferentemente
rutas
ambientes
centrales
aquellas
través
expresión
carbonados
rendimiento
metabólica
modular
sino
ilus-tran
nueva
motivo
frente
desarrollado
facilita
mostramos
junto
acción
fisiolo-gicas
versatilidad
energético
influye
componentes
colonizarlos
crecimiento
antagonistas
flujos
global
tipos
gran
optimizar
He-mos
suficientes
rica

Las bacterias que tienen un metabolismo versátil han desarrollado diversas estrategias para adaptarse a diferentes ambientes, y colonizarlos. Entre ellas destaca la capacidad de resistir condiciones ambientales cambiantes y diversos tipos de estrés, características que confieren una elevada eficacia biológica. *Pseudomonas putida* tiene una gran versatilidad metabólica y fisiológica, características que derivan de un genoma grande cuya expresión está controlada por diversas redes de regulación global que aseguran respuestas adecuadas frente a señales fisiológicas y del medio ambiente. Esto facilita su supervivencia en condiciones y ecosistemas muy variados. Una de las redes de regulación más importantes para optimizar el metabolismo, la velocidad de crecimiento y la eficacia biológica es la llamada represión catabólica. Este mecanismo regulador asegura que, cuando las células disponen de diversas fuentes de carbono en concentraciones suficientes, se metabolicen preferentemente aquellas que facilitan un mejor rendimiento energético, limitando el uso de otros compuestos menos preferidos. Este proceso regulador permite una asimilación secuencial y jerárquica de las fuentes de carbono disponibles, optimizando el metabolismo y la capacidad competitiva de la bacteria. En *P. putida*, las proteínas Crc y Hfq, y los RNAs pequeños CrcZ y CrcY, son componentes clave de la represión catabólica. Crc y Hfq trabajan juntas para inhibir la traducción de determinados mRNAs que tienen una secuencia rica en adeninas (llamada motivo CA) en la región de inicio de la traducción. Los RNAs pequeños CrcZ y CrcY regulan la acción de Crc y Hfq, actuando como antagonistas. Los niveles de estos dos RNAs son bajos en situaciones que generan una fuerte represión catabólica, pero aumentan significativamente cuando la represión disminuye. Se piensa que la función de CrcZ y CrcY es unir la proteína Hfq, quizá junto con Crc, secuestrándolas cuando su efecto no es necesario.

El trabajo que se describe en esta tesis aporta información nueva sobre la influencia de la represión catabólica, y en particular del sistema Crc/Hfq/CrcZ-CrcY, en la adaptación del metabolismo de *P. putida* a condiciones ambientales cambiantes. Los resultados obtenidos ilustran la función de la proteína reguladora Crc en el control de varios procesos metabólicos. Hemos analizado la jerarquía de asimilación de diversos ácidos orgánicos y aminoácidos cuando la célula crece en un medio rico, en el que la represión catabólica es muy fuerte, y la función de Crc en este proceso. También hemos clarificado la influencia del regulador Crc en el balance de los flujos de metabolitos a través de las rutas metabólicas centrales, optimizando el metabolismo cuando las células crecen en condiciones en las que la represión catabólica es moderada. Además, mostramos que el sistema regulador Crc/Hfq/CrcZ-CrcY puede modular la síntesis de polihidroxialcanoatos, que son compuestos de reserva importantes. En conjunto, los resultados implican que este sistema regulador no solo controla el transporte y asimilación de fuentes de carbono, sino que influye en todo el proceso del flujo de compuestos carbonados.

Introduction

Pseudomonas putida

Pseudomonads are ecologically versatile bacteria that can survive in many different environments. They are Gram-negative rod-shaped γ-protobacteria and are frequently present in complex environments. Some strains are pathogenic to animals (*Pseudomonas aeruginosa*) or to plants (*Pseudomonas syringae*), while others are usually non-pathogenic and can even be beneficial for plants and the environment (*Pseudomonas putida* or *Pseudomonas fluorescens*). *Pseudomonas putida* mt-2 was isolated in Japan by Hosokawa as a strain able to degrade metatoluate (Nakazawa, 2002). This strain contained the TOL plasmid pWW0 which encodes the metabolic pathway for toluene and xylene catabolism. The strain KT2440, used in the studies presented in this thesis, is a derivative of mt-2 cured of the TOL plasmid (Regenhardt et al., 2002). It contains a 6.2 Mb genome in which 76.9% of its genes have an accredited function (Nelson et al., 2002). Interestingly it contains no less than 670 genes coding for proteins with functions related to transport and binding, which support its growth on no less then a hundred different carbon sources (Daniels et al., 2010), among them aromatic and linear hydrocarbons, chlorinated and nitrated organic compounds, pesticides, herbicides, sugars, carboxylic acids and amino acids (Jimenez et al., 2002). These metabolic traits rely on the presence of more than 80 genes coding for dioxygenases, monooxygenases and oxidoreductases which ensure an efficient growth on aromatic and recalcitrant substrates. Interestingly, *P. putida* does not contain a canonical glycolysis (Embden-Meyerhof-Parnas pathway) and catabolizes C_3-C_6 sugars via the Entner-Doudoroff pathway (ED) and via the pentose phosphate pathway (PPP). PPP is moreover the major source of NADPH, which ensures a strong resistance to oxidative stress in this bacterium (Chavarria et al., 2013a; Kim and Park, 2014). The tricarboxylic acid cycle (TCA) is connected to the ED pathway via the pyruvate shunt, which plays a fundamental role in modulating the fluxes through glycolysis and gluconeogenesis. These pathways represent the metabolic core of *P. putida*. Accordingly with the presence of numerous pathways for the catabolism of carbon sources of different energetic and chemical characteristics and a limited number of pathways of central carbon metabolism, *P. putida* metabolic organization can be considered an example of bow-tie functional metabolism (Fig. 1). The nutrients are catabolized to produce energy, redox cofactors, and the biomass precursor metabolites, which are then synthesized into larger building blocks which support growth (Fig. 1) (Csete and Doyle, 2004; Sudarsan et al., 2014).

Metabolism plays a central role in cell behaviour and many cellular processes are strictly connected with metabolism and depend on its efficiency. Since its discovery, *P. putida* has been widely used for biotechnological applications including bioremediation of contaminated areas, quality improvement of fossil fuels, biocatalytic production of fine chemicals, production of bioplastics, and as agents of plant growth promotion and plant pest control. Moreover, KT2440 strain is officially classified as GRAS (generally regarded as safe) and its use is considered biosafe for biotechnological applications. The first metabolic model of *P. putida* was published in 2008 and represented a step forward in metabolic engineering studies for biotechnological application (Nogales et al., 2008).

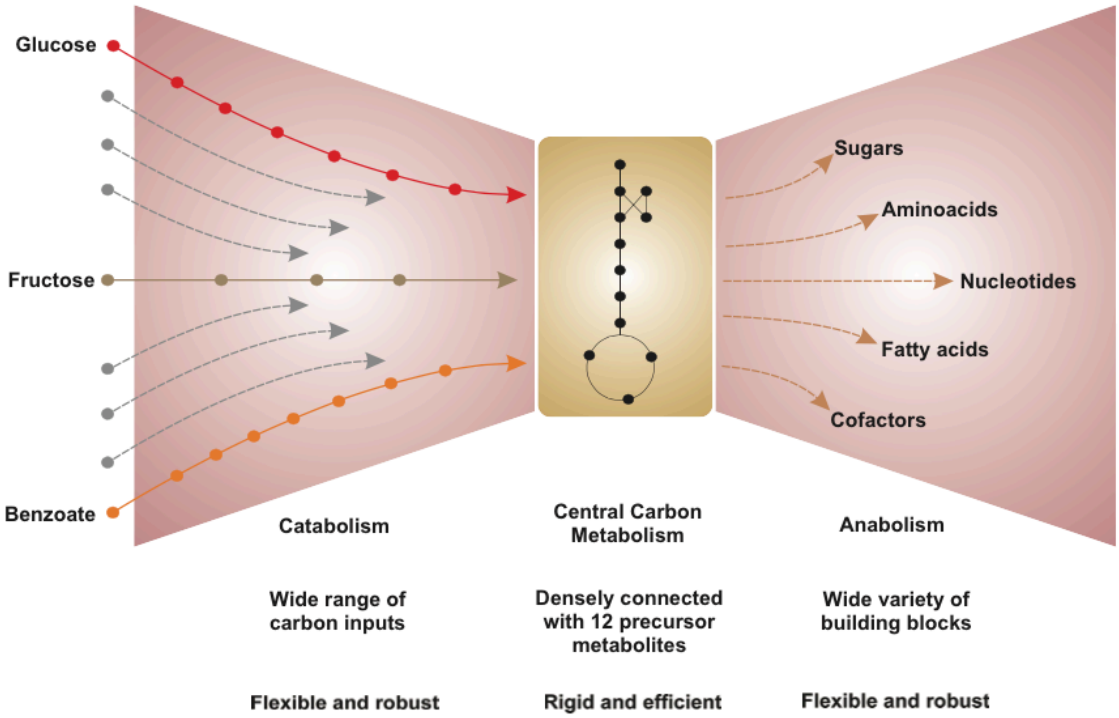

Fig. 1 Functional structure and organization of carbon metabolism in *P. putida*.
The metabolic network structure is organized as a "bow tie." The bow tie can be decomposed into three modules; i.e., the catabolic and anabolic reactions are organized as fan-in and fan-out parts of the bow tie, and the knot part of the bow tie is comprised by the 12 biomass precursor metabolites that form the central carbon metabolism (Sudarsan et al., 2014).

Pseudomonas putida skills rely to a large extent on its high metabolic versatility and on complex regulatory systems that control metabolic and cellular processes, allowing at the same time responding to different kinds of stress and to rapid changes in the environment. Not surprisingly, 12.7% of its genes code for proteins related to regulatory functions and signal transduction. Several distinct regulatory networks participate in the coordination of gene expression under different conditions (Cases and de Lorenzo, 2005). In particular, cell regulation relies on the presence of local and global regulators that optimize physiological and metabolic traits according to fluctuations in the environment. One of the major regulatory mechanisms that balance gene expression, cell metabolism and cellular processes is the so-called carbon catabolite repression (CCR).

Carbon Catabolite Repression

Bacteria such as Pseudomonads, which can use many different compounds as carbon sources, have developed sophisticated regulatory mechanisms to ensure that when mixtures of these compounds are available, those with higher energetic yield are preferentially used. These regulatory mechanisms, globally known as Carbon Catabolite Repression, control the uptake of these substrates and the induction of the corresponding catabolic pathways. They therefore coordinate and optimise metabolism, and maintain a proper balance between the uptake and consumption of the available compounds. It is believed that this helps microorganisms compete in environments in which the availability of carbon sources fluctuates, allowing for optimised growth when food is plentiful. Once the preferred substrates are consumed, the CCR mechanisms are switched off and the cells metabolise those remaining (Deutscher, 2008; Gorke and Stulke, 2008; Rojo, 2010). CCR also influences other aspects of cell biology such as antibiotic sensitivity and virulence of opportunistic pathogens such as *P. aeruginosa* (Linares et al., 2010). Biofilm formation, which is strictly dependent on metabolism, is positively regulated by the CCR system (O'Toole et al., 2000). CCR can also compromise the use of microbial cells in industrially important biotransformation processes, as the production of polyhydroxyalkanoates (Vinuselvi et al., 2012; La Rosa et al., 2014). Therefore, a better understanding of CCR can lead to a better control of virulent pathogens and to higher production of bacterial bioactive molecules.

CCR in *Escherichia coli* and *Bacillus subtilis*

In many organisms, CCR is achieved by a combined activity of global and operon-specific regulatory mechanisms. The two most studied mechanisms of CCR are those of the model organisms *Escherichia coli* and *Bacillus subtilis*. The first studies on CCR recall to Jacques Monod experiments on diauxic growth of *E. coli* in presence of glucose and lactose as carbon sources (Monod, 1941). Cells use preferentially glucose over lactose limiting its assimilation until glucose is completely depleted. A key element involved in glucose assimilation and lactose repression is the phosphoenolpyruvate-carbohydrate phosphotransferase system (PTS) which couples glucose uptake to its phosphorylation. Briefly, the system is composed by several enzymes that transfer a phosphoryl group from phosphoenolpyruvate (PEP) to glucose (Fig. 2A). When glucose is present at high concentration the $EIIA^{Glc}$ enzyme is in a de-phosphorylated state because the phosphoryl group is rapidly transferred to glucose to render glucose-6-phosphate. In this metabolic state, the ratio between PEP and pyruvate is low and the dephosphorylated $EIIA^{Glc}$ binds to transporters for non-preferred compounds repressing the uptake of the corresponding metabolites. When glucose is present at low concentration, the PEP/pyruvate ratio increases and $EIIA^{Glc}$ is mostly in its phosphorylated form, which is unable to associate to and repress transporters for non-preferred compounds. This kind of CCR is called “inducer exclusion”. The complete activation of the non-preferred catabolic routes requires the transcriptional activation of the corresponding pathways by the cAMP-CRP complex. Phosphorylated $EIIA^{Glc}$ associates to a soluble unknown factor and to the adenylate cyclase enzyme controlling the pool of cAMP

present in the cytoplasm. The CRP regulator associated with cAMP dimerizes and activates the transcription of the target genes (Fig. 2A). Therefore, CCR in *E. coli* relies both on the phosphorylation state of $EIIA^{Glc}$ and on the pool of cAMP (Gorke and Stulke, 2008; Rojo, 2010).

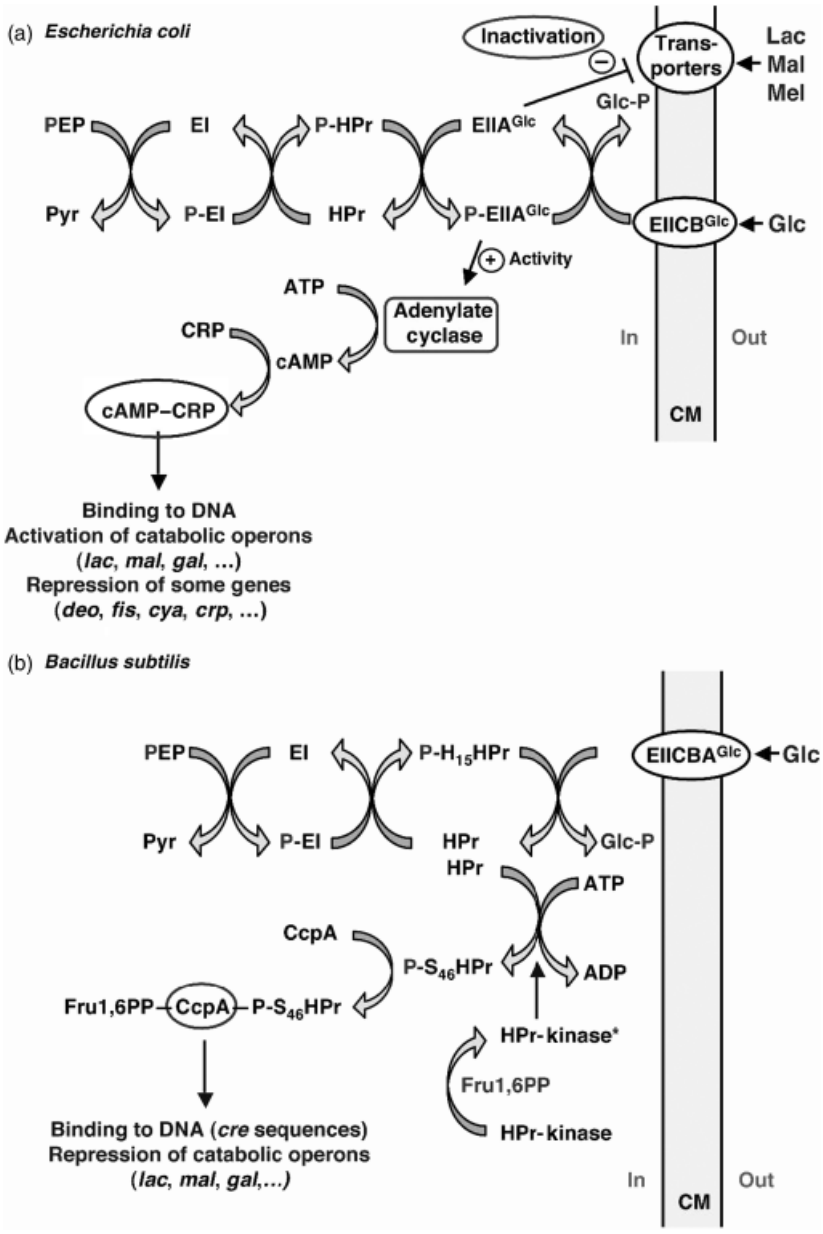

Fig. 2 Sugar transport and CCR in *Escherichia coli* and *Bacillus subtilis*.
In both *E. coli* (**A**) and *B. subtilis* (**B**), the transport of glucose (Glc) through the cytoplasmic membrane (CM) is coupled to its phosphorylation by a multiprotein phosphorelay system named the PTS. In *E. coli*, CCR is mainly determined by the phosphorylation state of the $EIIA^{Glc}$ enzyme and on the pool of cAMP. In *B. subtilis*, CCR is determined by the phosphorylation state of the HPr enzyme, on the levels of fructose-1,6-bisphosphate. See text for a complete description (Rojo, 2010).

As in *E. coli*, glucose is a preferred substrate for *Bacillus subtilis*. Although the PTS system involved in glucose uptake is similar to that of *E. coli*, the molecular mechanisms underlying CCR are different. The key players of CCR in *B. subtilis* are the HPr protein along with the CcpA transcriptional regulator. Briefly, during high glycolytic activity (high level of glucose), the cytoplasmic levels of the metabolite fructose-1,6-bisphosphate increase. This causes the phosphorylation of the HPr protein on residue Ser46 by the HPrK kinase/phosphatase. HPr is part of the PTS system and when it is phosphorylated on Ser46, it can associate to the CcpA protein. The complex formed by the P-Ser46-HPr and the CcpA proteins binds to the catabolite responsive sequences (*cre*) of the target genes repressing the transcription of numerous catabolic pathways and therefore limiting the uptake of the corresponding carbon sources (Fig. 2B). Under conditions of nutrient limitation, the phosphatase catalytic activity of the HPrK prevails and it dephosphorylates the P-Ser46-Hpr protein, releasing repression (Fig. 2B). In addition to HPr, *B. subtilis* triggers CCR through the HPr-like Crh protein or using other CcpA homolog proteins. Therefore, the CCR mechanism used by *B. subtilis* to regulate metabolism is based on sensing the levels of fructose-1,6-bisphosphate and the energetic status of the cell through the phosphorylation state of the HPr protein (Gorke and Stulke, 2008; Rojo, 2010).

CCR in Pseudomonas putida

Three apparently independent CCR systems have been identified in *Pseudomonas putida*. One of them includes the Crc and Hfq proteins and the CrcZ-CrcY small RNAs. A second system is based on the PTS^{Ntr} phosphotransfer system. Finally, a regulatory system that receives information from the Cyo terminal oxidase seems to affect several catabolic genes as well.

The Crc/Hfq/CrcZ-CrcY global regulatory system

The Crc/Hfq system

The Catabolite Repression Control (Crc) protein is a key player in CCR in *Pseudomonas*. It is a 30 Kda (259 amino acids) protein the structure of which has been characterised in the case of the *Pseudomonas aeruginosa* (Milojevic et al., 2013) and *Pseudomonas syringae* proteins (Sharma et al., 2015). Crc was firstly identified in *P. aeruginosa* where mutant strains in the Crc regulator showed increased mannitol and glucose consumption in the presence of succinate, along with higher activity of the corresponding catabolic pathways (Wolff et al., 1991). The Crc protein has a key role in optimising carbon metabolism and growth by inhibiting (mainly) the expression of the genes involved in the uptake and/or assimilation of non-preferred carbon sources (Moreno et al., 2009a; Moreno et al., 2010; Hernandez-Arranz et al., 2013). When *P. putida* grows in the presence of a preferred carbon source, the Crc regulator favours its assimilation, inhibiting the expression of genes involved in the transport and assimilation of the less preferred compounds (Fig. 3). Crc controls gene expression post-transcriptionally, promoting the inhibition of the translation of mRNAs containing an AAnAAnAA motif where 'n' is any ribonucleotide. This motif is known as Catabolite Activity (CA) motif and it is present close to the ribosomal binding site of the target mRNAs (Fig. 3) (Yuste and Rojo, 2001; Moreno et al., 2007; Moreno and Rojo, 2008; Moreno et al., 2009a; Sonnleitner et al., 2009). Although Crc was previously believed to directly recognize and bind the CA motif, recent insights have demonstrated that the purified Crc protein cannot bind RNA on its own (Sonnleitner and Blasi, 2014; Moreno et al., 2015). Rather, it is now clear that it is the Hfq RNA chaperone who recognises and binds the CA motif, the role of Crc being to facilitate Hfq binding via a mechanism still not fully understood (Sonnleitner and Blasi, 2014; Madhushani et al., 2015; Moreno et al., 2015).

Hfq is a small and abundant protein found in many bacterial genera, with functions related to post-transcriptional gene regulation. In *E. coli,* Hfq can facilitate the annealing of a small RNA (sRNA) with a target mRNA. If the annealing changes mRNA structure in a way that occludes the access of ribosomes to the ribosome-binding site (RBS) of the mRNA, the result is that Hfq and the sRNA repress translation initiation. However, if the change produced in the mRNA structure facilitates a more effective exposure of the RBS to the ribosomes, the final

outcome is an activation of translation. Hfq can also protect some sRNAs from ribonuclease cleavage or, contrarily, it can induce the cleavage of the sRNAs or of their target mRNAs (Morita et al., 2005; Aiba, 2007; Vogel and Luisi, 2011; De Lay et al., 2013; Holmqvist and Vogel, 2013). Hfq therefore behaves as an RNA-chaperone that ultimately regulates the expression of many genes.

In *E. coli*, Hfq forms hexamers and recognizes with high affinity AU-rich sequences containing the canonical 5'-AA$^{C}/_{U}$ AA$^{C}/_{U}$ AA$^{C}/_{U}$-3' motif, which is highly similar to the CA motif present in Crc-regulated mRNAs in *Pseudomonas*. It is believed that this is the reason why preparations of Crc protein containing small amounts of Hfq protein as contaminant were able to generate ribonucleoprotein complexes with RNA probes containing the CA motif, which led to the erroneous interpretation that Crc can bind RNA on its own and inhibit translation initiation. It was recently shown that the *P. aeruginosa* Hfq protein can directly recognise the CA motif at a target RNA *in vitro*, preventing the assembly of a translation initiation complex (Sonnleitner and Blasi, 2014). Our laboratory has shown that the Crc protein stimulates Hfq binding to RNAs that contain a CA motif (Moreno et al., 2015). In addition, we showed that Crc can form a specific ternary complex that contains, in addition to Crc, the Hfq protein and a target RNA containing a CA motif (Moreno et al., 2015). This suggests that Crc and Hfq create a ternary complex at target mRNAs that can inhibit translation initiation, eliciting CCR (Fig. 3) (Moreno et al., 2015).

The Hfq regulon is wider than that of Crc and contains many Crc regulated genes and genes with biological functions not related with Crc regulation. Crc-null and Hfq-null *P. putida* strains are both impaired in CCR, but inactivating the *hfq* gene generates much stronger pleiotropic effects than inactivating *crc*. In other words, the Hfq protein mediates Crc-dependent catabolite repression, but it possibly has other functions as well (Moreno et al., 2015).

Crc/Hfq activity is highest in cells growing exponentially in a nutrient-rich media such as Lysogenic Broth (LB), but vanishes when cells reach to the stationary phase of growth. However, expression of the *crc* gene and the levels of the Crc protein, change little throughout growth in LB medium, or in a minimal salts medium containing succinate as the carbon source (Ruiz-Manzano et al., 2005; Yuste et al., 2006; Moreno et al., 2015). Although Crc expression is similar irrespective of the growth medium and the growth phase, its activity strongly varies accordingly to these elements (Fig. 3).

The CrcZ and CrcY small RNAs

Crc activity strongly depends on the culture medium and on the growth phase. In cells growing exponentially in a nutrient-rich media Crc activity is very high, opposite to what is observed in stationary phase cells or in nutrients-limited media, where CCR is not active. Albeit these differences in activity, the levels of the Crc and Hfq proteins vary little irrespective of the conditions. The strength of the Crc-dependent catabolite repression is indeed inversely proportional to the levels of one or more small RNAs (sRNAs). In *Pseudomonas aeruginosa* one such sRNA, named CrcZ, has been identified, while *P. putida* contains, in addition to the CrcZ sRNA, a homologous sRNA called CrcY (Fig. 3). In *Pseudomonas syringe* a third sRNA named CrcX has been identified and it seems to be specific of this species (Filiatrault et al., 2013). In other

Pseudomonads other combinations of similar sRNAs can also be found. Since these sRNAs contain several CA motifs it has been proposed that they may antagonise Crc by sequestering Hfq, perhaps in combination with Crc (Fig. 3). This could modulate the availability of Hfq, and perhaps of Crc, when their effect is not needed, for example when a poor carbon source is used (Sonnleitner et al., 2009; Moreno et al., 2012; Sonnleitner and Blasi, 2014; Moreno et al., 2015). However, this model is still in need of more definitive experimental proofs. The possible advantage of having several Crc antagonists, rather than one, is not fully clear. One possibility is that redundancy helps to obtain a rapid and strong increase in the levels of the antagonists under certain conditions reducing the risk of loss of an important component of the global regulatory network. Another possibility is that each sRNA responds to a different signal although the levels of the two *P. putida* sRNAs vary in parallel (Moreno et al., 2012). The levels of these small RNAs fluctuate according to the carbon and nitrogen source being used, the growth rate and the growth temperature (Moreno et al., 2012; Fonseca et al., 2013; La Rosa et al., 2014; Valentini et al., 2014; La Rosa et al., 2015). During conditions that elicit a strong CCR response (exponential growth in LB medium), the levels of the sRNAs are low and a considerable amount of Hfq/Crc are free to bind the target mRNAs, repressing their translation. When CCR is not needed, for example in LB during stationary phase or in nutrient-limited media, the level of the sRNAs increases, thereby reducing the amounts of free Hfq/Crc proteins to levels in which they are unable to repress the translation of the target mRNAs (Fig. 3). The latest data indicate that Crc is unable to bind directly to the RNA, but that it may form part of a complex in which, at least temporarily, the Hfq protein, who is primarily responsible for the recognition of the CA motif, is present. RNA motility shift assays have moreover demonstrated the ability of Crc and Hfq to form a stable ternary complex with the small RNA CrcZ (Moreno et al., 2015). Therefore, the available *in vivo* and *in vitro* data support that the sRNAs CrcZ and CrcY antagonize the Hfq/Crc-mediated CCR.

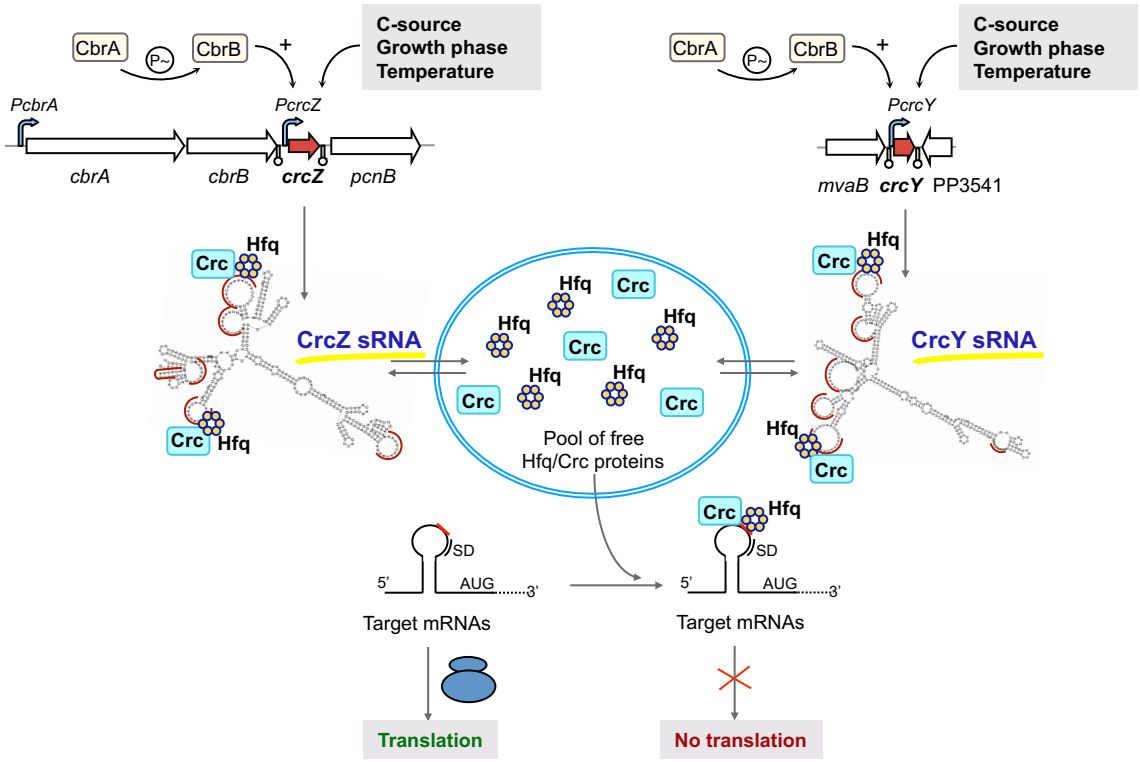

Fig. 3 Model of regulation of the Crc/Hfq system by the sRNAs CrcZ and CrcY.
Model showing how the co-ordinated action of the CrcZ and CrcY sRNAs can regulate the pool of Crc/Hfq proteins. These sRNAs, the levels of which vary according to growth conditions and the temperature, trap the Hfq protein and perhaps Crc as well, thereby impeding Hfq binding to target mRNAs to inhibit translation initiation. The CA motifs can be immediately upstream from the Shine-Dalgarno sequence, or overlapping the AUG initiation codon, depending on the mRNA considered. Modified from (Moreno et al., 2012; Sonnleitner and Blasi, 2014; Moreno et al., 2015).

The *P. putida* CrcZ and CrcY sRNAs are 368 nt in length and contain six repeated Catabolite Activity motifs (Fig. 3). Transcription of *crcZ* and *crcY* sRNAs occurs from the RpoN-dependent promoters *PcrcZ* and *PcrcY*, respectively, and relies on the CbrA/CbrB two-component regulatory system (Fig. 3). The CbrA/CbrB regulators belong to the family of the NtrB-NtrC two-component system. Its precise role in Pseudomonads is not fully clear but seems to be responsible for the carbon/nitrogen balance along with the regulation of the assimilation of a large number of substrates as carbon or nitrogen source, in stress tolerance and biofilm formation (Amador et al., 2010). In *P. aeruginosa*, mutant strains in *cbrB* and *crcZ* genes have overlapping but not identical phenotypes, suggesting the presence of other still uncharacterized CbrB targets (Sonnleitner et al., 2012). The *cbrA-cbrB* genes are located upstream of *crcZ*. CbrA is a sensor histidine kinase that phosphorylates the CbrB response regulator in response to an as yet unclear signal (Fig. 3) (Hoch, 2000). The activity of CbrB as a transcriptional activator increases greatly when phosphorylated. In *P. aeruginosa*, CbrB recognizes and binds the palindromic sequence TGTTAC-N_{14}-GTAACA, located between positions -151 and -125 relative to the initial transcription site of *crcZ* (Abdou et al., 2011). Similarly, in *P. putida* palindromic sequences were identified between positions -148 and -123 and between -147 and -108 relative to the initial transcription site of respectively *crcZ* and *crcY* sRNAs (Moreno et al., 2012; Garcia-Maurino et al., 2013). Transcription initiation from the *PcrcZ* and *PcrcY* promoters re-

quires CbrB, the IHF DNA-binding protein, and the RNA polymerase containing the σ^{54} factor (RpoN) (Sonnleitner et al., 2009; Moreno et al., 2012; Garcia-Maurino et al., 2013). RpoN (σ^{54}), originally described as involved in nitrogen metabolism, regulates also the expression of genes involved in the assimilation of various carbon sources, in the formation of flagella and in the synthesis of cofactors (Potvin et al., 2008). A canonical RpoN-dependent promoter contains the highly conserved consensus sequence -24(GG)/-12(GC) and requires a transcriptional activator to initiate transcription (Thony and Hennecke, 1989). In addition, many RpoN-dependent promoters require binding of IHF at a site located between the transcriptional activator and RNA polymerase.

Genes regulated by the Crc/CrcZ-CrcY system

Using a bioinformatic approach, more then 340 putative CA motifs were predicted in *Pseudomonas* strains (Browne et al., 2010). Most of them are located on genes coding for transcriptional regulators, membrane transport proteins and enzymes related to carbon metabolism. The possible functionality of many of these CA motifs still needs experimental validation. Examples of Crc-repressed genes are the *bkd* operon for the assimilation of aromatic amino acids (Hester et al., 2000a; Hester et al., 2000b), the degradation pathways for benzoate, 4-hydroxybenzoate, 4-hydroxyphenilpyruvate (Morales et al., 2004; Moreno and Rojo, 2008), the genes implicated in the assimilation of alkanes present in the OCT plasmid (Yuste and Rojo, 2001), or the genes of the toluene metabolism coded on the pWW0 plasmid (Aranda-Olmedo et al., 2005; del Castillo and Ramos, 2007; Moreno et al., 2010). Crc/Hfq regulation is in many cases exerted through a multi-tier strategy, directly repressing the translation not only of a mRNA coding for a catabolic enzyme, but also that a mRNA coding for a protein involved in the transport of the catabolite and/or that of the transcriptional regulator that activates the expression of all pathway genes (transporter and catabolic enzymes). Lowering the levels of the transcriptional regulator below those needed for a full activation indirectly lowers the expression of all genes in the pathway (Fig. 4). Two examples are the genes required to assimilate benzoate or *n*-alkanes, the expression of which is regulated by the BenR or AlkS transcriptional activators. Crc/Hfq inhibit translation of the mRNAs for *benR* and *alkS*, lowering the expression of *ben* and *alk* operons (Fig. 4) (Hernandez-Arranz et al., 2013). The resulting mechanism allows a fast amplification of Crc regulation and allows the cells to rapidly adapt to changes in the environment. Similar multi-tiered regulation has been identified or predicted for genes involved in the transport and assimilation of other carbon sources, represented in Fig. 4. Inactivation of the *crc* gene leads to changes (obviously indirect) in the mRNA levels of about 7-8% of the *P. putida* genes (Moreno et al., 2009b; La Rosa et al., 2015). This clearly indicates that Crc regulon is rather wide and that most of the target genes are still unidentified.

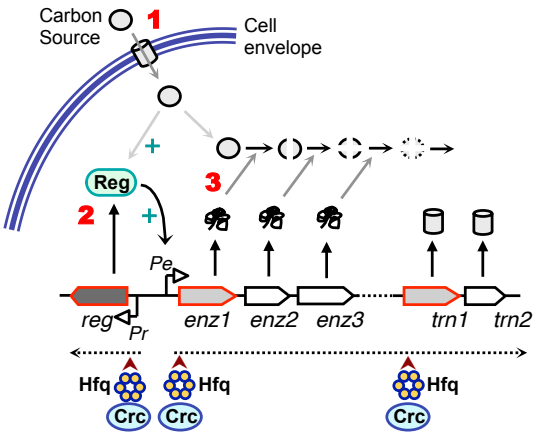

Substrate	1 Transport	2 Regulator	3 Enzyme
- Benzoate	BenF	BenR	BenA
- Toluene	XylN	XylR	XylAM
- Alkanes		AlkS	AlkB
- Vanillate	VanP*	VanR*	VanA*
- Nicotinate	NicT*	NicR*	NicA*
- 4OHBenz	PcaK* PacP*		PobA*
- Phenylacetate	PhaK*		PhaE*
- Gallate	GalT* GalP*		GalB*
- Val/Leu/Ile	BraC*	BkdR*	BkdA1A2*
- Phe	PhhT*	PhhR*	PhhA*
- Glucose	OprB-1* GstABD*	GltR-2*	Zwf1*

Fig. 4 Model for multi-tier regulation of catabolic pathways by Crc and Hfq.
The Crc/Hfq proteins may inhibit the translation of the mRNAs of genes corresponding to uptake proteins (element 1; generically denoted as '*trn*'), the specific transcriptional activators of pathway genes (element 2; denoted as '*reg*'; the activator usually recognizes the substrate or one of its metabolic intermediates as effector), and/or particular enzymes of the pathway that transform the initial substrate into central metabolites, usually that involved in the first step (element 3; generically denoted as '*enz*'). The simultaneous inhibition of more than one of these elements presumably allows for tighter, more versatile regulation. Crc/Hfq-regulated elements are indicated in red. The Hfq binding sites (red arrowheads) can be located at the 5' end or at internal sites in the mRNA (indicated as a dotted line). *Pe*, promoter for the structural genes; *Pr*, promoter for the regulatory gene. The box on the right shows some examples of genes belonging to the catabolic pathways for the indicated substrates, and that either are known to be regulated by Crc/Hfq (gene name with no asterisk) or show presumed Hfq targets that overlap the translation initiation region but that have not been experimentally confirmed (gene name with an asterisk). Modified from (Hernandez-Arranz et al., 2013).

PTS^{Ntr} phosphotransfer system

Pseudomonas putida contains two types of Phosphoenolpyruvate:carbohydrate-phosphotransferase systems (PTS). One of them, the sugar-related phosphotransfer system (PTS^{Fru}), regulates fructose uptake. The second one, named the nitrogen-related PTS (PTS^{Ntr}) system, is unrelated to the transport of metabolites but rather has a regulatory function, modulating carbon metabolic fluxes *via* a post-translational mechanism (Pfluger-Grau and de Lorenzo, 2014).

The fructose PTS^{Fru} transporter is encoded by the *fruA* and *fruB* genes, the expression of which is repressed by the Cra regulator under gluconeogenic conditions (succinate as carbon source) (Chavarria et al., 2013b). When cells are in presence of fructose as sole carbon source, fructose-1-phosphate accumulates in the cytoplasm and the Cra repressor is inactivated (Chavarria et al., 2014). Under these conditions, phosphoryl groups are transferred from phosphoenolpyruvate (PEP) to the components of the PTS^{Fru} branch, allowing for the coupled transport and phosphorylation of fructose to the cytoplasm. Phosphoryl groups can, under certain conditions, also be transferred from the PTS^{Fru} branch to the PTS^{Ntr} system. In *P. putida*, the PTS^{Ntr} system is involved in the CCR mediated by glucose that controls the expression of the toluene degradation pathway specified in the pWW0 plasmid (Cases et al., 2001), and has an influence as well on the accumulation of polyhydroxyalkanoates (Velazquez et al., 2007). The PTS^{Ntr} system is composed by the PtsP, PtsO and PtsN proteins. Unlike the PTS^{Fru}, it seems that the phosphoryl group is not transferred to any specific substrate. When PstN is in its phosphorylated form (PstN-P), it physically contacts the pyruvate dehydrogenase (PDH) complex regulating its activity and ultimately modulating central carbon metabolic fluxes influencing the amount of acetyl-CoA produced in the cell (Pfluger-Grau et al., 2011; Chavarria et al., 2012). Therefore, the ratio between PtsN/PtsN-P ultimately regulates metabolism through a protein-protein interaction between the PstN-P and the PDH complex.

Cyo terminal oxidase

A third regulatory system involved in CCR and global metabolic regulation has been described in *P. putida,* which relies on the Cytochrome *o* ubiquinol oxidase (Cyo). Cyo is one of the terminal oxidases of the electron transport chain of *P. putida* and mutant strains in which the *cyo* genes have been inactivated show a decrease in the CCR that controls the expression of the phenol degradation pathway of *P. putida* H (Petruschka et al., 2001), or of the pathway for the assimilation of *n*-alkanes specified in the *P. putida* OCT plasmid (Dinamarca et al., 2002). In *P. putida* KT2440, at least five terminal oxidases for aerobic respiration have been described, namely Cyo, CIO, Cbb3-1, Cbb3-2, and Aa3, although only Cyo appears to be involved in CCR (Morales et al., 2006). Albeit the mechanism of repression is still unclear, there is a correlation between the expression of the Cyo terminal oxidase and the CCR effect that inhibits expression of the alkanes and phenol degradation pathways, both of which are non-preferred carbon

sources. Expression of the genes coding for the Cyo oxidase vary depending on the carbon source being used and on the oxygen levels. During exponential growth in a rich medium under vigorous aeration, conditions that generate a strong CCR effect, Cyo expression is elevated. However, when cells enter into the stationary phase of growth, expression of the *cyo* genes greatly decrease, and CCR fades away as well. The expression of Cyo is also high when cells are cultivated in a minimal salts medium in presence of carbon sources that generate catabolite repression, such as succinate (Dinamarca et al., 2002). It should be noted that, aside from CCR, Cyo levels also influence the composition of the respiratory chain. The affinity of Cyo for oxygen is low and, under oxygen limiting conditions, expression of the *cyo* genes is low, in part because of the repression exerted by the ANR global regulator (Ugidos et al., 2008). However, it is thought that there are other factors involved in Cyo expression that are still unknown. Therefore, Cyo on the one-side functions as a terminal oxidase of the electron transport chain, and on the other belongs to a global regulatory system that integrates signals from the electron transport chain, the aeration state and/or the redox state, probably sending information to other regulatory elements that ultimately control the expression of genes involved in the metabolism of some specific compounds.

Objectives

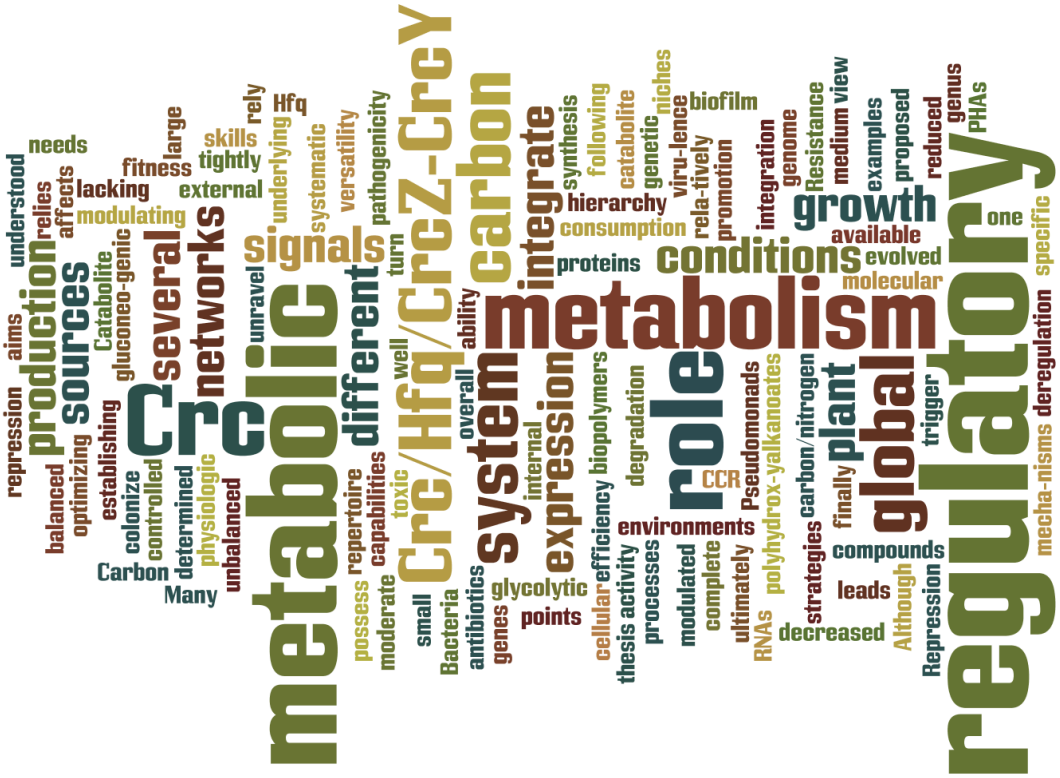
regulatory
metabolism
metabolic
Cr
global
role
carbon
Crc/Hfq/CrcZ-CrcY
system
integrate
networks
several
signals
different
conditions
growth
plant
expression
production
sources
regulation
Resistance
genome
integration
biofilm
hierarchy
consumption
proteins
synthesis
following
catabolite
genetic
viru-lence
rela-tively
promotion
medium view
examples
proposed
reduced
genus
PHAs
one
specific
available
evolved
molecular
trigger
finally
Pseudomonads
polyhydrox-yalkanoates
carbon/nitrogen
strategies
compounds
leads
decreased
Repression
Although
mecha-nisms
deregulation
environments
degradation
biopolymers
efficiency
cellular
thesis activity
processes
modulated
complete
ultimately
RNAs
CCR
internal
overall
ability
well
toxic
repertoire
capabilities
possess
moderate
small
Bacteria
antibiotics
genes
glycolytic
points
Carbon
Many
balanced
optimizing
establishing
colonize
controlled
determined
physiologic
unbalanced
repression
aims
understood
needs
production
sources
Catabolite
gluconeo-genic
relies
affects
lacking
modulating
fitness
external
large
skills
tightly
rely
Hfq
underlying
systematic
versatility
pathogenicity
turn
unravel

Bacteria have evolved strategies to colonize different environments and niches. This ability relies on their metabolic and physiologic versatility, which is in turn determined by their genetic repertoire and the regulatory networks that integrate different metabolic and regulatory internal and external signals. Pseudomonads possess a large genome the expression of which is tightly controlled by several regulatory networks. Resistance to antibiotics, production of biofilm, virulence, degradation of toxic compounds, synthesis of biopolymers, promotion of plant growth and plant pathogenicity are examples of the capabilities of the genus. Many of these skills rely on cell's metabolism and are ultimately modulated by Carbon Catabolite Repression. The Crc and Hfq proteins, and one or more small RNAs, integrate the metabolic needs with the available carbon sources, optimizing metabolism and cellular processes. The deregulation of CCR leads to a reduced metabolic efficiency and decreased overall fitness. Although the molecular mechanisms underlying the role of Crc in modulating the expression of several specific genes is relatively well understood, a systematic view is lacking on how Crc finally affects metabolism, and which are the metabolic signals that trigger Crc activity.

The proposed thesis aims to unravel the following points:

1. The role of Crc/Hfq/CrcZ-CrcY global regulatory system in establishing the hierarchy of consumption of carbon sources from a complete medium

2. The role of Crc/Hfq/CrcZ-CrcY global regulatory system in the integration of gluconeogenic and glycolytic metabolism under moderate carbon catabolite repression conditions

3. The role of Crc/Hfq/CrcZ-CrcY global regulatory system on the production of polyhydroxyalkanoates (PHAs) under balanced and unbalanced carbon/nitrogen growth conditions

Results

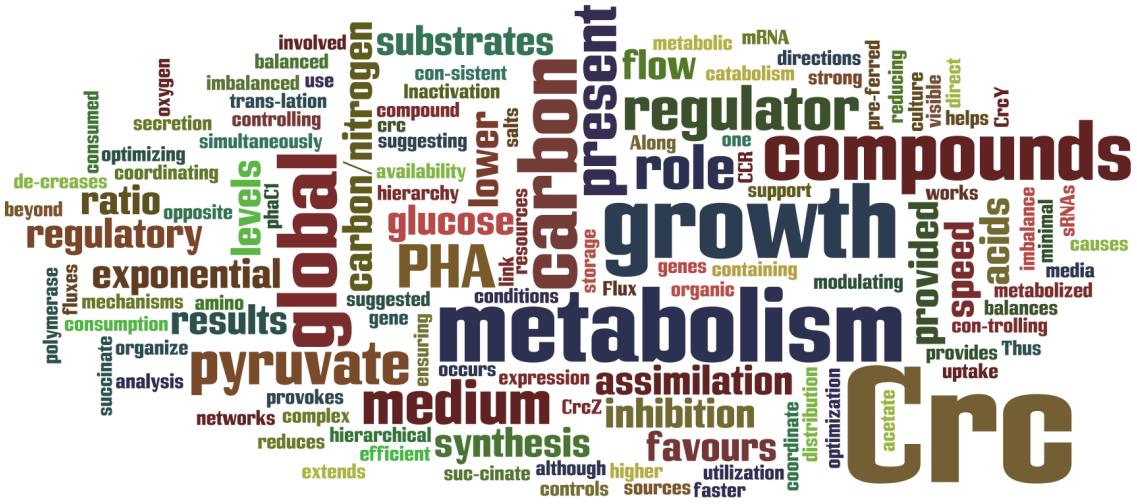

The results of this thesis are presented as separated chapters entitled:

Chapter 1:

The role of the Crc regulator in controlling the hierarchy of consumption of carbon sources from a complete medium.

Chapter 2:

The Crc/CrcZ-CrcY global regulatory system helps the integration of gluconeogenic and glycolytic metabolism.

Chapter 3:

The Crc protein inhibits the production of polyhydroxyalkanoates under balanced carbon/nitrogen growth conditions.

Chapter 1

The role of the Crc regulator in controlling the hierarchy of consumption of carbon sources from a complete medium

The results described in this chapter form part of a manuscript that is currently under preparation:

La Rosa, R., Behrends, V., Williams, H., Bundy, J., and Rojo, F. (2015) The role of the Crc regulator in controlling the hierarchy of consumption of carbon sources from a complete medium in *Pseudomonas*.

Introduction

Complex media such as LB (Lysogeny broth) are frequently used to culture bacteria because of their high nutritional value, which allows high growth rates and yields for many bacterial species, including Pseudomonads. LB contains tryptone (a tryptic digest of casein) and yeast extract as source of amino acids, peptides, vitamins and other organic compounds. Probably due to the presence of carbon sources that allow for an efficient growth, LB medium generates a strong carbon catabolite repression response while cells grow exponentially. In the case of *Pseudomonas putida*, growth in LB has been observed to elicit a strong CCR on the expression of genes involved in the assimilation of less-preferred carbon sources such as *n*-alkanes, toluene, xylene, phenol or benzoate (reviewed in Rojo, 2010). When provided as mixtures, as it occurs in complex growth media, amino acids exert a clear catabolite repression control over the assimilation of sugars and hydrocarbons (Hester et al., 2000a; Aranda-Olmedo et al., 2005; Moreno et al., 2009b). Since the amino acids present in the LB medium are the main carbon and nitrogen source for cells, it could be presumed that these are the nutrients that generate the CCR response. However, several data suggest that not all amino acids are equally preferred. For example, branched-chain keto acids are less preferred than other amino acids, or that succinate or glucose (Hester et al., 2000a; Hester et al., 2000b; Moreno et al., 2009b). Furthermore, metabolomic analyses directed to monitor the assimilation of amino acids by *Pseudomonas aeruginosa* when cultivated in different complex media have shown that cells assimilate the amino acids in a sequential and hierarchical manner. The order of uptake of the diverse amino acids was similar, but not identical, in different complex media analysed, although the general trend observed was that asparagine, aspartate, alanine and glutamate are assimilated first, while other amino acids are assimilated at a later stage (Palmer et al., 2007; Behrends et al., 2009; Frimmersdorf et al., 2010; Behrends et al., 2013a).

In the case of *P. putida*, the information available on the order of assimilation of the amino acids present in complex media derives mostly from data on gene and protein expression obtained through transcriptomic and proteomic approaches (Moreno et al., 2009b). These analyses suggested that, in cells growing exponentially in LB medium, amino acids such as proline, alanine, glutamate, glutamine, histidine, arginine, lysine, aspartate and asparagine are preferred over valine, isoleucine, leucine, threonine, phenylalanine, tyrosine, glycine or serine. Moreover, this same work showed that the Crc/Hfq/CrcZ-CrcY regulatory system has an important role in repressing the expression of genes required for the uptake and/or assimilation of these apparently non-preferred amino acids. Overall, inactivation of the *P. putida crc* gene lead to a deregulated expression of no less than 99 proteins and 92 genes in cells growing exponentially in LB medium. Interestingly, 28% of these genes or proteins are involved in the transport of substrates across the membrane, and 36% have functions related to energy metabolism (Moreno et al., 2009b).

Despite much information is available on the Crc regulon, and many Crc/Hfq regulated genes have been identified (Moreno et al., 2009b; Browne et al., 2010; Sonnleitner et al., 2012), the information on how Crc controls and optimizes the metabolic fluxes derived from the assimilation of the carbon sources present in the LB medium is still very incomplete. In addition,

although gene expression data can be very useful to grasp which compounds are being preferentially metabolized, a definitive proof requires a parallel monitoring of the depletion of the different compounds present in the growth medium. Therefore, a global metabolic footprint analysis was undertaken with the aim of getting a more precise view on the hierarchy of assimilation of the compounds present in the LB medium by *P. putida*, and the role of the Crc/Hfq/CrcZ-CrcY regulatory system in orchestrating this hierarchy.

Results and discussion

Compounds identified in LB medium by NMR

LB is usually considered to be an undefined medium because its specific composition can vary from different suppliers, labs or batches and, moreover, because light exposure and autoclaving time can lead to amino acid degradation and deamination (Sezonov et al., 2007). As mentioned in the introduction, LB contains tryptone, an enzymatic digest of casein that provides peptides and free amino acids, and yeast extract which, in addition to amino acids, provides vitamins, nucleotides, and other nutrients. Previous analyses of the composition of this medium involved an hydrolytic treatment that converted all peptides into free amino acids (Sezonov et al., 2007). In this work, we have analysed the composition of LB without a previous hydrolytic treatment, using NMR technology. This approach has allowed identifying free low-molecular-weight compounds such as amino acids, sugars and organic acids, although information on peptides was not obtained due the lack of specific NMR profiles that could be used as reference (Beckonert et al., 2007). The concentration of the different compounds was determined relative to that of the internal standard, 2,2-dimethyl-2-silapentane-d_6-5-sulfonic acid (DSS).

In the batch of LB used, amino acids accounted for 88.5% of the total compounds characterized. Eighteen of the twenty common amino acids were identified with the exception of glutamine and cysteine. In the case of amino acids, concentrations ranged between that of histidine (0.4 relative mM) to that of leucine (3.8 relative mM; Fig. 5A). The uncommon amino acid pyroglutamate, which is a cyclized derivative of L-glutamic acid, was also identified (Fig. 5A). Globally, free amino acids were present at a concentration of 26.8 relative mM. Among the organic compounds that presumably derive from the yeast extract, we were able to detect carboxylic acids (acetate, formate, succinate), sugars (glucose, glycerol, trehalose), and nitrogenated bases (adenosine, uracil, uridine) (Fig. 5B). Carboxylic acids and sugars were more abundant than nitrogenated bases (Fig. 5B). Globally, these compounds represented an 11.5% of the total amount of compounds detected, and their concentration was 3.5 relative mM.

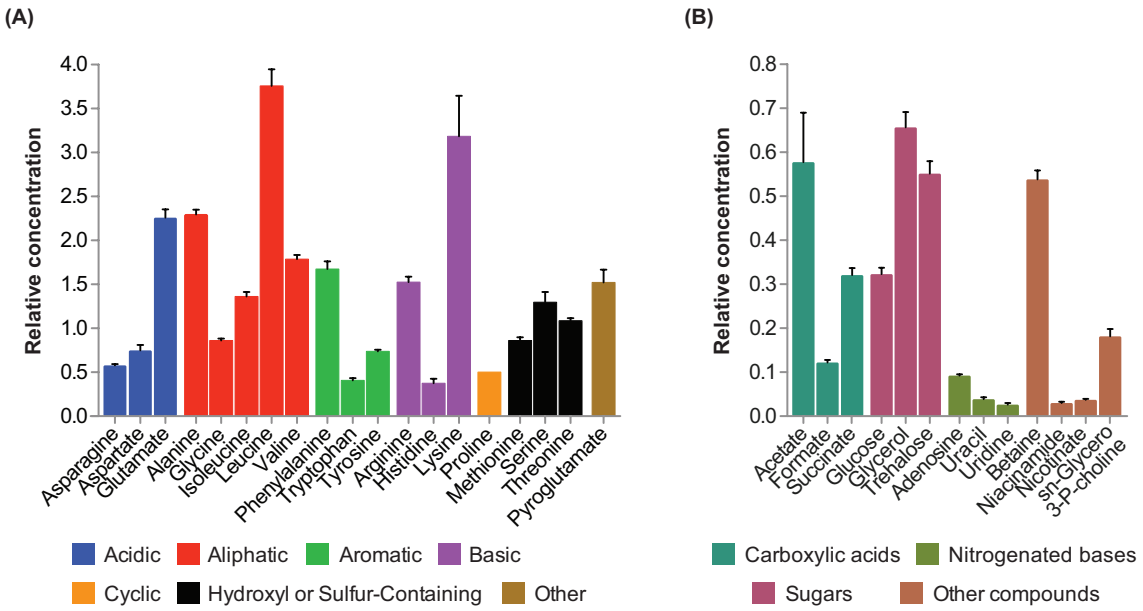

Fig. 5 Compounds detected in the Lysogeny broth (LB).
Free amino acids (**A**) and organic acids (**B**) detected in the LB medium used, grouped according to their chemical characteristics. Nine replicas of the same batch of LB were analysed using NMR spectroscopy as described (Beckonert et al., 2007). Concentrations represent integral values of characteristic resonances relative to the internal standard 2,2-dimethyl-2-silapentane-d_6-5-sulfonic acid (DSS). Error bars represent the standard deviation (SD) of the mean.

Hierarchy of assimilation of the compounds present in the LB medium by *P. putida* KT2440

When cultivated in LB medium in aerated flasks, the wild type strain *P. putida* KT2440 grew exponentially at a rate of 0.86 ± 0.01 h^{-1} up to a turbidity (A_{600}) above 1, moment in which growth rate started to decline, eventually ceasing at a turbidity close to 4 (Fig. 6A). To analyse which compounds from the LB medium were consumed, and at which moment of the growth phase, sixteen samples of culture supernatants were collected throughout growth (time points indicated in Fig. 6A). The compounds present in these sample supernatants were subsequently analysed using NMR technology. Earlier work has shown that the decrease in concentration of most metabolites in a culture supernatant due to cell growth can be fitted to a four-parameters nonlinear sigmoid model, of which three parameters can be related to biologically meaningful information (Behrends et al., 2009; Behrends et al., 2013a; Behrends et al., 2014). The first parameter, indicated as "t_{50} value", is the time point at which 50% of a given compound has been consumed. The second parameter is the "assimilation time" and indicates the amount of time in which a compound decreases from 75% to 25% of its initial concentration; it represents how fast a metabolite is consumed. The combination of these two parameters represents the "uptake window" in which each metabolite is consumed. A third parameter is the "amplitude" of the decrease in concentration of a given metabolite and, when combined with its assimilation time, it allows deducing the "uptake rate", which represents the speed at which a metabolite is consumed (See *Experimental procedures*). The curves representing the decrease in concentration of the amino acids, carboxylic acids and sugars identified in our assays are shown in Fig. 7. After

fitting each data set to a sigmoid model, the t_{50} value, the assimilation time and the uptake rate were calculated for most compounds (Fig. S1).

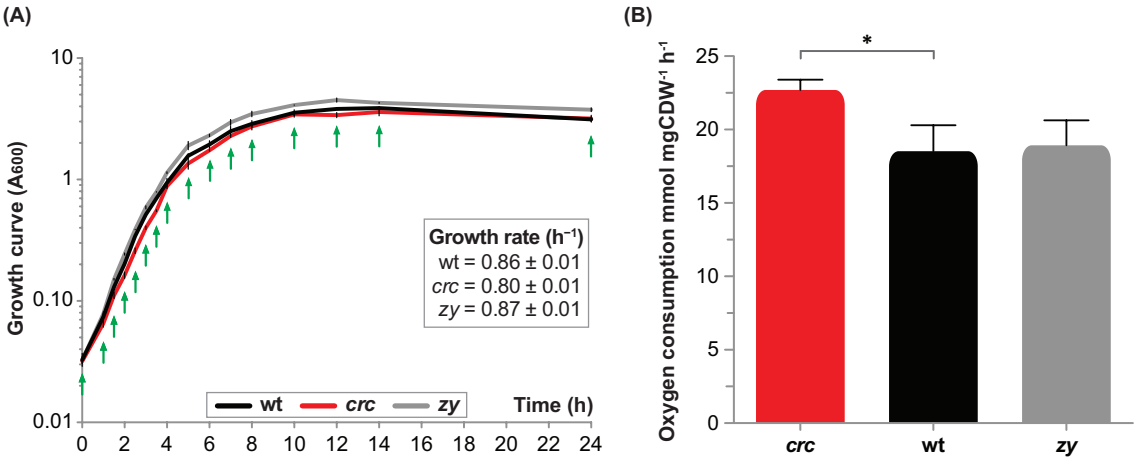

Fig. 6 Influence of the Crc/CrcZ-CrcY regulatory system on the growth rate and oxygen consumption of *P. putida* cultivated in LB medium.
(**A**) *P. putida* strains KT2440 (wild type, black line, indicated as 'wt'), KTCRC (Crc-null derivative of KT2440; red line, indicated as '*crc*') and KT2440-ZY (CrcZ- and CrcY-null derivative of KT2440, grey line, indicated as '*zy*') were cultivated in LB medium for 24 hours. Growth was followed by measuring turbidity at 600 nm. Black bars indicate the standard deviation. Growth rate (h^{-1}) of the three strains during exponential phase is indicated in the grey box; values correspond to the mean ± the standard deviation of three independent measurements. Green arrows indicate the time points at which samples of supernatant were collected for NMR analyses. (**B**) The specific oxygen consumption was calculated during mid exponential phase ($A_{600} = 0.6$). Values correspond to the mean ± the standard deviation of three measurements and are indicated as mmol $mgCDW^{-1}\,h^{-1}$. The asterisks indicate that a significant difference exists between the samples compared (in brackets), with a P value of <0.007.

Early during the growth (low t_{50} values), a group of nine compounds (formate, glucose, succinate, glycerol, asparagine, serine, aspartate, proline and glutamate) were consumed, being essentially exhausted after 3-4 hours of growth, while cells were growing exponentially (Fig. 7A-B and Fig. 8). However, the uptake rates clearly differed: glycerol, glutamate, aspartate, proline and serine were assimilated faster, while glucose, formate, succinate or asparagine were assimilated at a comparatively slower rate (Fig. 7A-B and Fig. S1). Interestingly, some compounds were consumed right from the start (formate, glucose, asparagine), while the assimilation of glutamate or aspartate required a lag time of 2 to 2.5 hours that was followed by their disappearance from the culture supernatant (Fig. 7A-B). The 2.5 h lag for glutamate is remarkable, given that it was one of the most abundant compounds detected in the LB and, once its assimilation started, it was consumed very fast (Fig. 7B and Fig. S1). Glutamate has a central role in the carbon/nitrogen metabolism and its peculiar consumption could be related to their balance (Valentini et al., 2014). Formate, which showed the lowest t_{50} value and was present at a very low concentration (0.1 relative mM; Fig. 7A and Fig. 8B), can be transformed by a formate dehydrogenase that generates CO_2 and reduced NADH, which can in turn be directly used as energy source to feed the electron transport chain (Roca et al., 2008; Roca and Ramos, 2009; Roca et al., 2009). It is worth noting that, although the sequential assimilation of the different

compounds should force cells to adapt their metabolism accordingly, during exponential phase cells were able to maintain a fairly constant growth rate.

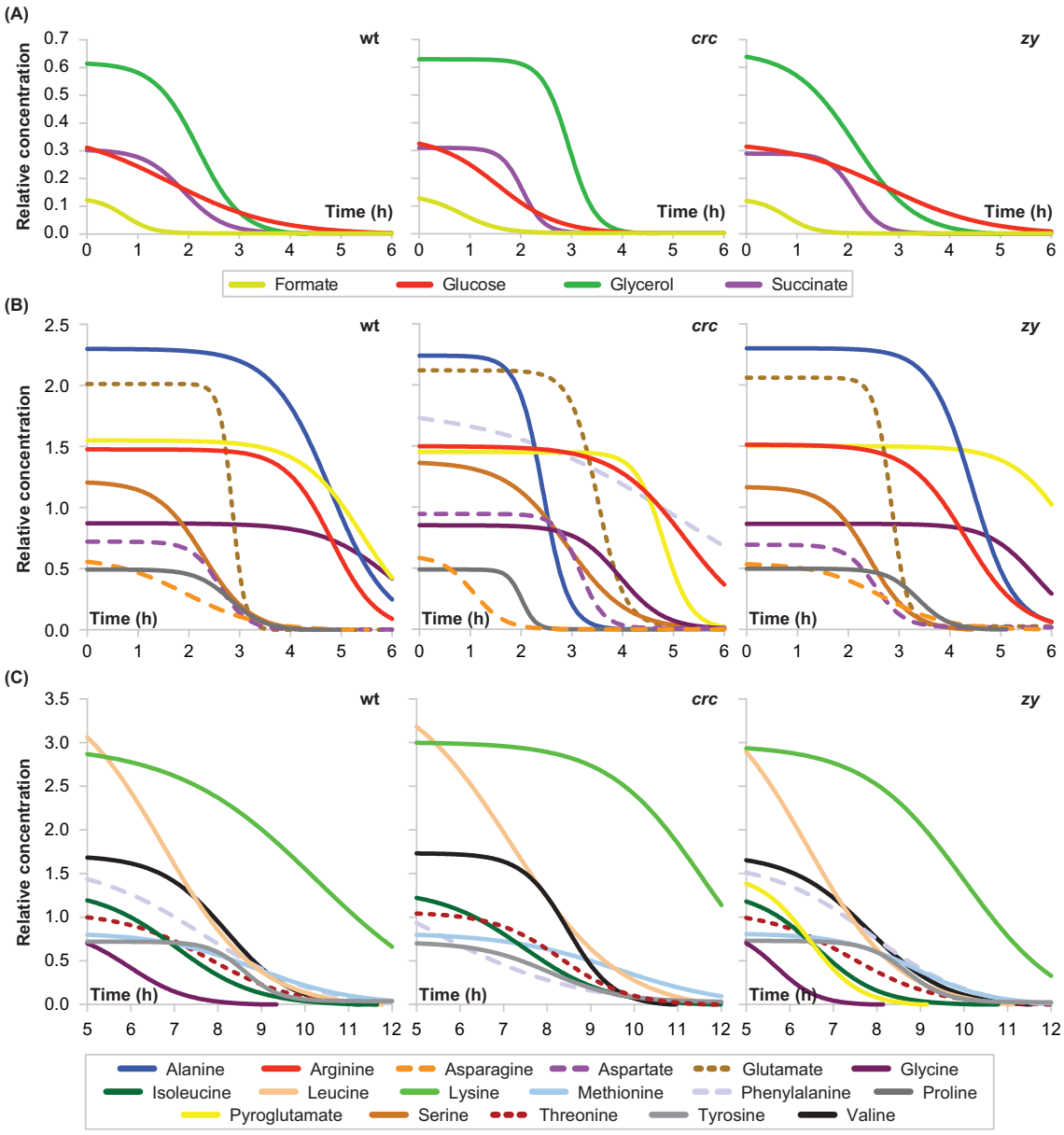

Fig. 7 Consumption of amino acids and organic acids during growth of *P. putida* in LB medium, and influence of the Crc/CrcZ-CrcY regulatory system.
Curves represent the sigmoid model fits of metabolites concentration. (**A**) Use of organic acids during exponential growth (between 0 and 6 hours of growth). (**B, C**) Use of amino acids during exponential growth (**B**; between 0 and 6 hours of growth), or upon entry into stationary phase (**C**; between 6 and 24 hours of growth). The indicated concentrations represent the integral values of the characteristic resonances for each compound relative to the internal standard DSS. The *P. putida* strains used were KT2440 (wild type, indicated as 'wt'), KTCRC (Crc-null derivative of KT2440, indicated as '*crc*') and KT2440-ZY (CrcZ- and CrcY-null derivative of KT2440, indicated as '*zy*').

Once this first group of compounds had been consumed, which allowed cells to reach to mid-exponential phase, a group of several amino acids started to be assimilated. In this case, their t_{50} values were very heterogeneous (see Fig. 8B). During the late exponential phase of growth (hours 4 to 6), alanine, arginine and pyroglutamate were taken up, their concentration declining by 50% after 4.8, 4.8 and 5.5 hours, respectively (Fig. 8B), a moment in which growth rate started to decline (Fig. 6A). The consumption of glycine soon followed.

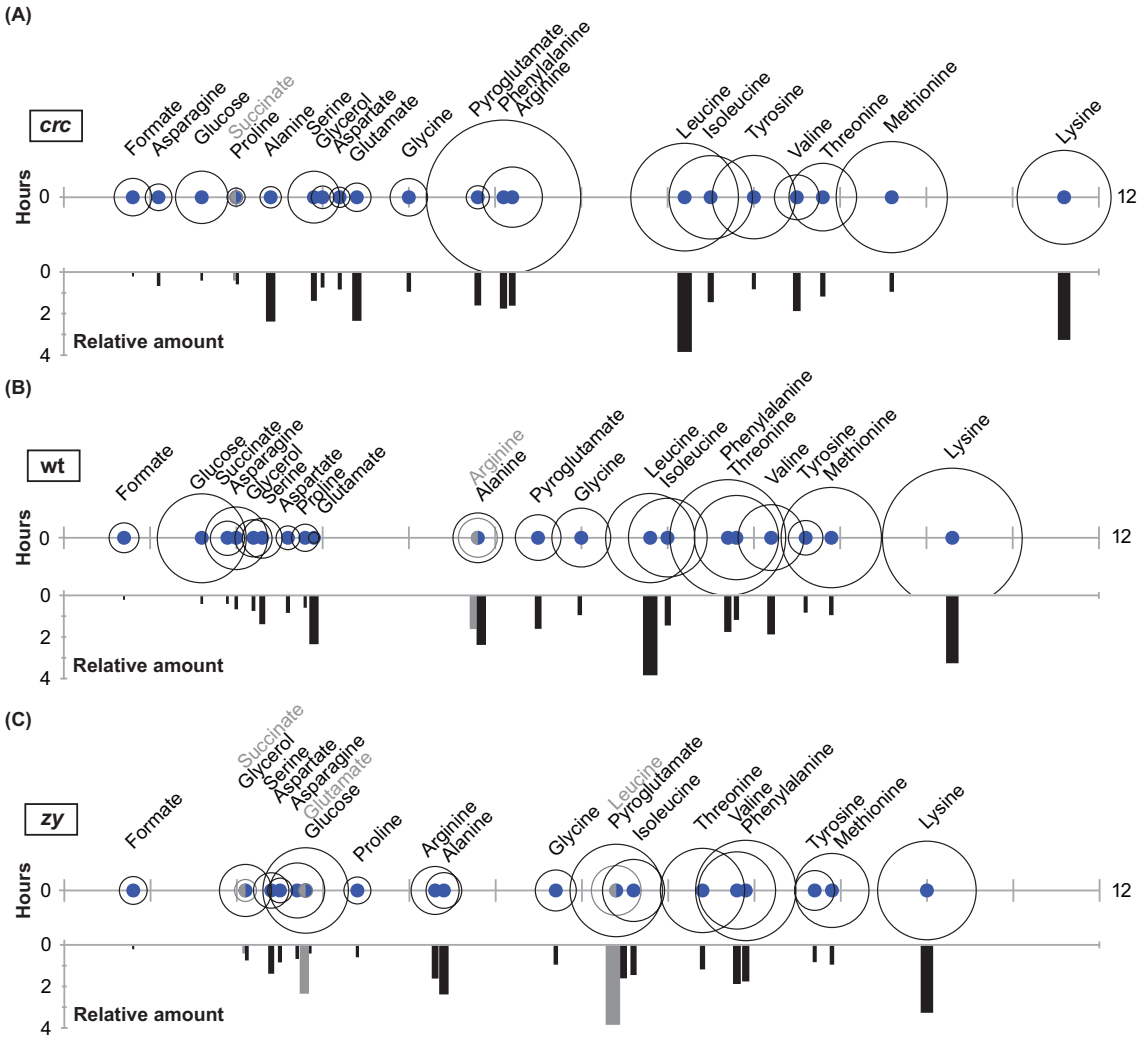

Fig. 8 Uptake parameters of the assimilated compounds.
Dots (blue or grey) indicate the t_{50} value (time at which the concentration of the metabolite has decreased to 50% of the initial value) for each compound, while the circles (black or grey) represent the speed of assimilation (time needed to detect a reduction in the compound concentration from 75% to 25% of the initial value). The relative amount of each compound, expressed as mM relative to the DSS standard, is indicated below the corresponding dot (Y-axis in mM; the area of the rectangle is proportional to the concentration value). (**A**) Plot corresponding to *P. putida* KTCRC (Crc-null derivative of KT2440, indicated as '*crc*'). (**B**) Plot corresponding to *P. putida* strain KT2440 (wild type, indicated as 'wt'), (**C**) Plot corresponding to KT2440-ZY (CrcZ- and CrcY-null derivative of KT2440, indicated as '*zy*').

The transition from the exponential to the stationary phase of growth (about 6 to 9 hours of culture; Fig. 6A) was characterised by the consumption of leucine, isoleucine, valine, phenylalanine, threonine, tyrosine and methionine, all of which were essentially exhausted at hour 9, which corresponded to the start of the stationary phase (Fig. 7C and Fig. 8B). There onwards, cells seemed to rely on the consumption of lysine, an abundant amino acid which consumption was prolonged during several hours. We note that *P. putida* has also transport systems for di- and tripeptides (Cascieri and Mallette, 1976; Kiely et al., 2008), the contribution of which was not studied here.

Role of Crc in the hierarchy of consumption of sugars and carboxylic acids

To study the influence of the Crc protein, and of the CrcZ and CrcY sRNAs, on the consumption of the different components of the LB medium throughout growth, culture supernatants of Crc-null and CrcZ/CrcY-null strains derived from KT2440 were analysed using the global metabolic footprinting approach described above for the wild type strain. The growth rate of the KT2440 derivative bearing an inactivated *crc* allele, and therefore lacking the Crc regulator, was 7.5% lower than that of the wild type strain, but after 24 hours the total biomass was comparable in the two strains (Fig. 6A). In spite of its lower growth rate, during exponential phase the Crc-null strain consumed 22.5% more oxygen than the wild type (Fig. 6B). A KT2440 derivative lacking both CrcZ and CrcY sRNAs, in which CCR is constitutive and very strong (Moreno et al., 2012), showed growth rate and oxygen consumption values very similar to those of the wild type strain (Fig. 6A-B). These results suggest that Crc activity favours a more efficient metabolism that leads to a higher growth rate with lower oxygen consumption.

Inactivation of the *crc* gene increased the uptake rate of glucose by 1.7-fold and that of succinate by 1.9-fold, but had little influence on their hierarchy of assimilation (Fig. 8A-B and Fig. S1). In the case of glycerol, however the lack of Crc led to a 1.7-fold increase in the uptake rate but delayed the moment in which it started to be consumed, increasing the t_{50} value by 0.8 h (Fig. 8A-B and Fig. S1). Glucose concentration was relatively low (0.3 relative mM) and its depletion started immediately in both wild type and the Crc-null strains. Glucose enters the periplasmic space through the OprB1 porin and then it can be either transported to the cytoplasm by the GstABCD transport system, or converted to gluconate in the periplasm, which in turn can be either transported to the cytoplasm by a dedicated transporter or further oxidised to 2-ketogluconate in the periplasm (del Castillo et al., 2007). Gluconate was not found in the culture supernatants, suggesting that most of glucose is assimilated rather than converted to gluconate and then expelled back to the culture medium. As mentioned above, although glucose depletion started immediately after the cells were inoculated, the uptake rate was very low (Fig. 8A-B and Fig. S1). Inactivation of the *crc* gene increased the uptake rate, although assimilation was still slow in comparison to that of other compounds and its hierarchy of assimilation remained unchanged (Fig. 7A, Fig. 8A-B and Fig. S1). In the CrcZ/CrcY-null strain, in which Crc-dependent CCR is very strong, glucose consumption was delayed, taking 2.8 hours to achieve a 50% reduction of its initial concentration (as compared to 1.6 hours for the wild type or the Crc-null strains) (Fig. 8C and Fig. S1). The increase in glucose uptake in the Crc-null strain and the delay in the CrcZ-CrcY-null strain is consistent with other reports showing that

Crc inhibits the expression of the genes coding for the OprB1 porin and the GstABCD transporter (del Castillo et al., 2007; del Castillo et al., 2008; Moreno et al., 2009b; La Rosa et al., 2015). It is worth noting that, in contrast to the general view that glucose is not a preferred compound for *P. putida*, our results show that this sugar is co-metabolized during the first hours of exponential growth, in spite of the clear -albeit partial- repression that Crc imposes on its uptake and metabolism.

Succinate is one of the preferred compounds for Pseudomonads and during aerobic growth its uptake relies on two transporters: the DctA transporter, which is active at mM concentrations of succinate, and the high affinity DctPQM transporter, which is more important at μM concentrations. Expression of the high affinity DctPQM transporter, but not that of the low affinity DctA transporter, is inhibited by Crc (Valentini et al., 2011; Valentini and Lapouge, 2013; La Rosa et al., 2015). In LB, succinate concentration was similar to that of glucose (0.3 relative mM; Fig. 5B), a concentration at which the high affinity DctPQM transporter should play the main role in succinate uptake. Succinate assimilation, which occurred early during the exponential phase, was about twice faster in the absence of the Crc regulator while the CrcZ/CrcY-null strain behaved essentially as the wild type (Fig. 7A, Fig. 8, and Fig. S1). Overall, these results suggest that, under the conditions tested, Crc exerts a mild -though detectable- repression on the expression of the DctPQM transporter. Interestingly, the uptake rate of succinate was 3.9 to 2.5 higher than that of glucose, which agrees with succinate being preferred over glucose by *P. putida* (Fig. S1; further information on the influence of the Crc/CrcZ-CrcY system on glucose and succinate uptake and metabolism are provided in the next chapter of this thesis).

Like glucose and succinate, glycerol was also consumed early during growth, its concentration declining by 50% within the first 2.2 hours. The strain lacking the Crc regulator delayed glycerol consumption, showing a lag of about 2 hours before consumption started. After this lag, the Crc-null strain showed an uptake rate higher than that of the wild type strain (Fig. 7A, Fig. 8A and Fig. S1). Again, the CrcZ/CrcY-null strain behaved as the wild type. These consumption profiles suggest that the Crc/CrcZ-CrcY system favours, rather than inhibits, glycerol consumption. Glycerol uptake involves the GlpF facilitator and a phosphorylation by the GlpK glycerol kinase to render glycerol-3-phosphate (Escapa et al., 2013; Nikel et al., 2014). Expression of the *glpF* and *glpK* genes is inhibited by the GlpR transcriptional repressor. Interestingly, *glpF*, *glpK* and *glpR* mRNAs all show putative CA motifs within their translation start sites that are indicative of regulation by the Crc/Hfq system. However, whether these motifs are bona-fide Hfq binding sites, and whether Crc/Hfq indeed regulate translation of these mRNAs, has not been experimentally determined. The earlier start of glycerol assimilation in the wild type strain as compared to the Crc-null strain suggests that Crc/Hfq might inhibit translation of *glpR* mRNA, having less -or no- effect on translation of *glpF* and *glpK* mRNAs. However, this possibility needs to be further explored.

Trehalose, a disaccharide formed by a 1,1-glucoside bond between two α-glucose units, was also detected in the LB medium. Although *P. aeruginosa* is known to assimilate this sugar (Behrends et al., 2009), *P. putida* KT2440 appeared to be unable to do it, since trehalose concentration remained constant throughout growth irrespective of the strain used (wild-type, Crc-null or CrcZ/CrcY-null).

Role of Crc in the hierarchy of consumption of amino acids

Inactivation of the *crc* gene had a clear impact on the hierarchy and speed of assimilation of several amino acids, leading to altered t_{50} values and uptake rates for most of them (Fig. 7, Fig. 8 and Fig. S1). Interestingly, the Crc-null strain showed a much more disperse pattern of assimilation of the carbon sources without a clear separation between the groups as visible in the wild type strain (Fig. 8A-B). The pattern of amino acids consumption of the strain lacking the CrcZ and CrcY sRNAs was in most cases very similar to that of the wild type strain, which is consistent with the presence of a strong Crc-dependent repression.

The changes in the time and speed of assimilation of some amino acids upon inactivation of the *crc* gene did not always correlate with the changes in the expression of the genes presumably involved in their transport and utilization. *Pseudomonas putida* has several porins and transport systems for amino acids; while some of them have a strong preference for particular amino acids, other ones have broader substrate specificity. The contribution of each system for the assimilation of a particular amino acid has been studied in only very few cases, which complicates assigning changes in the hierarchy of assimilation of each amino acid to variations in the expression of a particular transport system. Moreover, there are increasing reports showing that changes in the fluxes of metabolites through catabolic pathways do not always correlate with parallel changes in gene expression. In many cases, the metabolic demand is satisfied even if the expression of the genes involved changes (Chubukov et al., 2013; Sudarsan et al., 2014).

Asparagine, which was present at a low concentration (0.6 relative mM), was consumed earlier (t_{50} decreased by 0.9 h) and faster (2.3-fold higher uptake rate) by the Crc-null strain (Fig. 8A). This amino acid can be internalised by the AatJQMP transporter for acidic amino acids, albeit with a low affinity (Sonawane et al., 2006; Singh and Rohm, 2008). The Aat system is formed by a periplasmic solute binding protein (AatJ), two cytoplasmic membrane proteins that function as permeases (AatQ and AatM), and an ATP-binding subunit (AatP). Expression of the *aatJQMP* genes increases when the *crc* gene is inactivated and cells are cultivated in LB (Moreno et al., 2009b). The assimilation of asparagine involves its conversion to aspartate, reaction that can occur either in the periplasm by the AnsB asparaginase, or in the cytoplasm by the AnsA asparaginase (Sonawane et al., 2003a). In cells growing in LB medium, inactivation of *P. putida crc* gene reduced the expression of *ansB* by and increased that of *ansA* by 2-3 fold (Moreno et al., 2009b). Therefore, the more efficient consumption of asparagine by the Crc-null strain could derive from a combination of a more effective transport and higher levels of the AnsA asparaginase in the cytoplasm.

Proline was also consumed earlier (t_{50} decreased by 0.8 h) and faster (2.2-fold higher uptake rate) by the Crc-null strain than by the wild type strain (Fig. 7, Fig. 8A and Fig. S1). In *P. putida*, proline assimilation involves its uptake, mediated by the PutP protein, and its conversion into glutamate by the PutA enzyme (Vilchez et al., 2000a; Vilchez et al., 2000b). Inactivation of the *crc* gene is known to reduce expression of these two genes in cells growing in LB (Moreno et al., 2009b). This, however, did not seem to impair proline depletion in our assays, but rather accelerated its consumption. Proline was present in the LB at a relatively low concentration (0.5 relative mM), so that perhaps the amount of PutP and PutA proteins present is the Crc-null strain are still enough to manage the assimilation of small amounts of this amino acid.

The assimilation of alanine, which in the wild type strain did not start until the late exponential phase of growth, occurred earlier (the t_{50} was 2.4 h lower) and more then twice faster in the Crc-null strain (Fig. 8A-B and Fig. S1). Alanine is imported by the LIV-I high-affinity branched-chain amino acid transport system (Hoshino and Kose, 1990; Hoshino et al., 1992). This system includes two intrinsic membrane proteins and the BraC periplasmic binding protein, the amounts of which increase when the *crc* gene is inactivated in *P. putida* KT2440 (Moreno et al., 2009b). Once internalised, alanine is assimilated through its direct conversion to pyruvate by the product of gene PP_1872, the expression of which is apparently not affected by Crc (Moreno et al., 2009b). Therefore, it seems that the faster assimilation of alanine by the Crc-null strain could derive from a more efficient transport of the amino acid.

Glycine, which the wild type strain consumed only after its entry into the stationary phase, was also assimilated earlier by the Crc-null strain (the t_{50} was 2 h lower), at a time when exponential phase ceased and cells prepared to enter the stationary phase of growth (Fig. 8A-B and Fig. S1). Glycine can be converter either to serine, or to CO_2 + NH_3 by the glycine-cleavage enzyme system that transfers a one-carbon unit to tetrahydrofolate. Strain KT2440 has two sets of genes coding for a glycine-cleavage system, and the Crc/Hfq regulators apparently inhibit the expression of one of them (Moreno et al., 2009b). Albeit no information on the glycine uptake system is available to date, the higher expression in the Crc-null strain of this glycine-cleavage system may explain the faster assimilation of glycine.

In the strain lacking the Crc regulator, pyroglutamate showed a reduction in the t_{50} value (0.7 h lower) and a doubled uptake rate relative to the wild type strain (Fig. 8A). Pyroglutamate is non-canonical amino acid whose catabolism generates glutamate at the expense of ATP. Interestingly, pyroglutamate uptake rate was among the highest in all the strains (Fig. S1), which could indicate a role in cellular metabolism that is still unexplored.

The aromatic amino acids phenylalanine and tyrosine use a common uptake system and assimilation pathway, since phenylalanine is converted to tyrosine, which is then further processed in several enzymatic steps, finally rendering fumarate (Arias-Barrau et al., 2004). Expression of the gene involved in the uptake and assimilation of these two aromatic amino acids is inhibited by the Crc/Hfq regulators in cells growing in LB medium (Moreno et al., 2009b). This explains why phenylalanine and tyrosine were consumed earlier during growth by the Crc-null strain (the t_{50} were 2.6 h and 0.6 lower; Fig. 8A). However, the uptake rate was lower in both cases, and tyrosine consumption appeared to start only after phenylalanine concentration (an abundant amino acid) significantly decreased (Fig. 7B-C). This suggests a possible competition for transport.

Inactivation of the *crc* gene delayed or lowered, the consumption of several amino acids. For example, aspartate and glutamate showed a moderate increase in their t_{50} values (0.5 to 0.6 h greater), although once assimilation started, this was fast (Fig. 7B, Fig. 8A-B and Fig. S1). The uptake rate of aspartate was comparable in the Crc-null and the wild type strains, although that of glutamate decreased by 2.6 fold upon inactivation of the *crc* gene. These amino acids enter the cell mainly though the AatJQMP transporter for acidic amino acids, which has a high affinity for aspartate and glutamate and low affinity for asparagine and glutamine (Sonawane et al., 2006; Singh and Rohm, 2008). As described above, in cells growing in LB medium, expression of the genes coding for this transport system increases when the *crc* gene is inactivated (Moreno et al., 2009b). This is in contrast with the delay in their assimilation observed in the Crc-null strain (Fig. 7B, Fig. 8A-B and Fig. S1). *Pseudomonas putida* KT2440 genome encodes no less

than 26 porins, most of which are poorly characterised. Growth of KT2440 in glutamate induces the expression of the OprD porin (PP_1206) (Ochs et al., 1999; Sonawane et al., 2003b). Although this porin is specifically involved in the uptake of basic amino acids (Trias and Nikaido, 1990), its induction by glutamate suggests that it may facilitate -perhaps indirectly- glutamate uptake as well. Interestingly, when cells are cultivated in LB, expression of OprD decreases more than two fold upon inactivation of the *crc* gene (Moreno et al., 2009b), which may impair the uptake of glutamate and aspartate. This may explain as well the somewhat delayed assimilation of arginine by the Crc-null strain since, as mentioned above, this amino acid traverses the outer membrane through OprD (Trias and Nikaido, 1990).

Serine assimilation was somewhat delayed and its uptake rate decreased in the absence of a functional Crc regulator (Fig. 8A), which is consistent with the observation that expression of the *sdaC* gene, coding for the serine transporter, is lower in the Crc-null strain than in the wild type strain (Moreno et al., 2009b).

Regarding threonine, its assimilation requires its conversion to glycine, and Crc has no known effect on the genes responsible for this reaction. Therefore, its delayed consumption, which was small, might be due to impaired transport.

The case of the branched-chain amino acids leucine, isoleucine and valine is noteworthy. Their assimilation did not start until cells reached the stationary phase of growth, indicating that they are non-preferred compounds (Fig. 7C). The Crc regulator has been identified as a negative regulator of the genes involved in their transport and assimilation (Hester et al., 2000a; Hester et al., 2000b; Moreno et al., 2009b). However, inactivation of the *crc* gene did not improve the assimilation of any of these three amino acids, suggesting that other factors, perhaps unknown regulatory systems, also impact on their consumption.

Lysine, which represent the less preferred amino acid (last amino acid consumed in all the strains) is believed to cross the outer membrane through the OprD porin (Trias and Nikaido, 1990), the levels of which decrease in the Crc-null strain (Moreno et al., 2009b). Thereafter it gains access to the cytoplasm though two ABC transporters that are apparently not regulated by Crc. Lysine catabolism can occur through two interconnected pathways, the aminovalerate (AMV) and the aminoadipate (AMA) pathways (Revelles et al., 2005). Crc exerts a moderate inhibition on the expression of two genes of the AMV pathway, favouring lysine processing through the AMA pathway (Moreno et al., 2009b). The delayed lysine consumption (Fig. 8A and Fig. S1) by the Crc-null strain might derive either from an impaired uptake by OprD, or from a sub-optimal distribution of the amino acid through the AMA and AMV pathways.

As mentioned above, the behaviour of the CrcZ/CrcY-null strain was in most cases similar to that of the wild type, but with some exceptions. The consumption of asparagine and proline was slightly delayed (their t_{50} were 0.7 h and 0.6 h higher) (Fig. 8C and Fig. S1). The slower assimilation of asparagine is consistent with the strong repression of the AatPMJQ transporter that could be expected from the high activity of the Crc regulator in this strain. Assimilation of pyroglutamate was delayed as well in the CrcZ/CrcY-null strain (the t_{50} was 0.9 h higher), albeit the uptake rate was similar to that of the wild type strain once assimilation started (Fig. 8C). The fact that the assimilation of pyroglutamate was anticipated in the Crc-null strain while delayed in the CrcZ/CrcY-null strain suggests that Crc could regulate its transport or its catabolism, none of which have been studied in detail in *P. putida* (Tamber et al., 2006). The uptake window of arginine was instead slightly anticipated by 0.5 hours relative to the wild type strain

(Fig. 8C). Again this result is consistent with the opposite behaviour of the Crc-null strain, which agrees with Crc having a role in regulating the arginine transport system.

Inactivation of the *crc* gene leads to acetate and pyruvate secretion

Small amounts of acetate (about 0.6 relative mM) were detected in the LB medium. The wild type strain consumed this acetate within the first 4 hours of growth (Fig. 9A). However, during the end of the exponential growth (from 6-8 hours of growth), acetate concentration increased again, suggesting some excretion of this compound to the culture medium, although consumption was again evident as cells entered into the stationary phase, being completely consumed soon after. The CrcZ/CrcY-null strain behaved as the wild type (Fig. 9A). However, the culture supernatants from the Crc-null mutant showed a constant increase in acetate concentration during the first 6 hours of growth, until cells prepared to enter the stationary phase. At this time point, acetate concentration was three times higher in the supernatants of the Crc-null strain than in those of the wild type strain. Acetate excretion by the Crc-null strain seemed to be most active during the early exponential growth (Fig. 9B). When cell growth ceased, acetate concentration decreased steeply, suggesting a fast assimilation (Fig. 9A).

The Crc-null strain, but not the wild type, also secreted pyruvate to the culture medium during exponential growth (Fig. 9C). Unlike acetate, pyruvate was not present in the LB medium before inoculating *P. putida*. The increase in pyruvate concentration was very fast during early exponential growth, and peaked during the mid exponential phase (Fig. 9D). Then onwards, pyruvate concentration dropped fast, suggesting that it was no longer secreted and, moreover, it was consumed. Interestingly, pyruvate concentration, at its peak, was about twice that of acetate, and reached a relative value of about 3.5 mM.

Pyruvate excretion has been previously observed in several *P. aeruginosa* strains under conditions of metabolic imbalance. For example, strain PA14 secretes pyruvate in the late stationary phase under aerobic/microaerobic growth conditions, probably to balance redox conditions (Price-Whelan et al., 2007). Also, strains isolated from cystic fibrosis patients with mutations at the *aceE* and *aceF* genes, which code for the pyruvate dehydrogenase complex that transforms pyruvate into acetyl-CoA, were observed to excrete pyruvate (Behrends et al., 2013b). Interestingly, when growing exponentially in LB, the *P. putida* Crc-null strain showed a higher expression of several genes that transform different compounds to pyruvate, as for example those coding for the enzymes transforming serine into pyruvate (Sda2), sugars to pyruvate (Entner-Doudoroff pathway), or oxaloacetate to pyruvate (OadA) (Moreno et al., 2009b). The Crc-null strain also showed an earlier consumption of alanine, an abundant amino acid that is directly transformed to pyruvate by alanine transaminase. An excessive production of pyruvate, which cannot be fully handled by the enzymes of the TCA cycle, could be the reason why the Crc-null strain excreted this compound.

It seems therefore that the excretion of acetate and pyruvate by the Crc-null strain are a consequence of the deregulated expression of several key genes involved in the assimilation of carbon sources, which produces a metabolic imbalance that leads to the accumulation of inter-

mediates such as acetate and pyruvate, that leak out of the cell during early exponential growth, and are recovered and consumed again during the late exponential phase of growth.

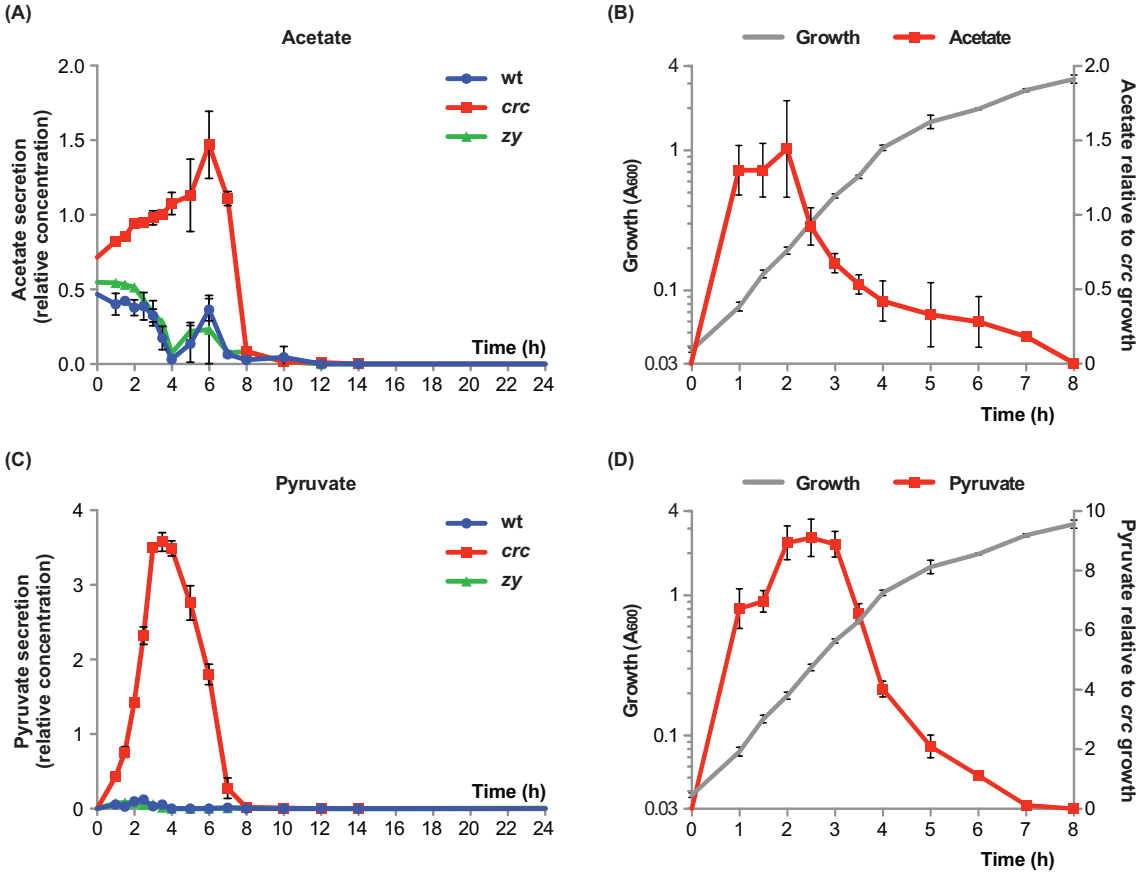

Fig. 9 Influence of the Crc/CrcZ-CrcY regulatory system on the excretion of acetate and pyruvate.
Transient secretion of acetate (**A**) and pyruvate (**C**), as revealed by NMR analyses, of the bacterial strains KT2440 (wild type, blue line, indicated as 'wt'), KTCRC (Crc-null derivative of KT2440; red line, indicated as '*crc*') and KT2440-ZY (CrcZ- and CrcY-null derivative of KT2440, green line, indicated as '*zy*'), cultivated in LB medium. Concentrations are indicated in mM, relative to that of the DSS internal standard. (**B**, **D**) Secretion of acetate (**B**) or pyruvate (**D**) relative to the growth of the Crc-null strain, indicated as relative µmol OD^{-1} h^{-1}. The growth curve of the Crc-null strain is also represented for comparison (grey line). Error bars represent the standard deviation (SD) of the mean.

Conclusions

Using a global metabolic footprint approach based on NMR technology, we have studied the changes in the composition of the culture medium when *P. putida* KT2440 is cultivated in LB medium. The same approach was also used to study the role of the Crc/Hfq/CrcZ-CrcY global regulatory system in controlling the uptake and assimilation of the carbon sources available to the cells. LB is a complex growth medium, rich in amino acids and with smaller amounts of other compounds such as organic acids, sugars, nitrogenated bases, vitamins, etc., the amounts of which can vary depending of the source of the yeast extract used to prepare the medium. The available panel of reference NMR profiles allowed detecting 19 amino acids (cysteine and glutamine could not be distinguished), as well as several sugars and organic acids and other less abundant compounds. By collecting culture supernatants at 16 time points after cells were inoculated in a strongly aerated flask, and analysing the composition of the supernatant in each of these samples, we observed that the wild type *P. putida* KT2440 strain makes a sequential and hierarchical use of the different compounds available. Sugars such as glucose or glycerol, which were detected in low but significant amounts, organic acids such a formate or succinate, and a selected group of amino acids including asparagine, serine, aspartate, proline and glutamate, were assimilated during the first 3 hours of culture, allowing cells to reach a turbidity (A_{600}) of about 0.4. Thereafter, there was a gap of about 1.5 to 2 hours until cells started to assimilate different amino acids in a sequential fashion. It is unclear what cells consumed during this 1.5 h gap, since growth rate did not change until cells prepared to enter into the stationary phase, which occurred when cells had been growing for about 5 h and turbidity reached to a value of about 1.5. We cannot discard the possibility that during this 1.5 h gap cells metabolised compounds not detected in our NMR analyses. The amino acids consumed during late exponential phase, and the onset of the stationary phase (hours 4-8 of culture), were arginine, alanine, pyroglutamate, glycine, leucine, isoleucine, phenylalanine and threonine. Thereafter, the turbidity remained constant at a value of about 3.5, and cells consumed valine, tyrosine, methionine and lysine. It is worth noting that lysine, one of the most abundant amino acids, was the least preferred compound, being consumed slowly during the stationary phase of growth.

Inactivating the *crc* gene led to a small decrease in growth rate and cells reached to similar turbidity values in stationary phase. However, oxygen consumption during mid exponential growth was 22.5% higher than that of the wild type strain, suggesting that the lack of Crc leads to a sub-optimal, less efficient configuration of metabolism. In addition, the time and speed of utilization of the different compounds changed significantly relative to that seen for the wild type strain. Although a clear sequential pattern of consumption was still detected, compounds such as glucose, proline, asparagine, alanine, phenylalanine, pyroglutamate and glycine were consumed earlier and/or faster, while assimilation of glycerol, succinate, formate, glutamate, aspartate, arginine, lysine, methionine, threonine, serine, valine, leucine and isoleucine showed little changes or was delayed. The assimilation of the carbon sources was much more dispersed and a gap between the compounds consumed was only visible when growth rate started decline after exponential phase. Interestingly, during the early exponential growth the Crc-null strain excreted significant amounts of pyruvate and acetate. Since the wild type strain secreted very

little acetate, and no pyruvate at all, the behaviour of the Crc-null strain suggests that the lack of Crc generates a metabolic configuration leading to an overflow of metabolites towards pyruvate, derived from the unregulated production of several enzymes that convert sugars or different amino acids to pyruvate.

The pattern of assimilation of the different compounds by the strain lacking the CrcZ and CrcY sRNAs was in most cases rather similar to that of the wild type strain. Lack of these two sRNAs is believed to strengthen Crc-dependent CCR, perhaps by increasing the amount of Hfq available to bind mRNAs containing a CA motif (Sonnleitner and Blasi, 2014; Moreno et al., 2015). Therefore, the behaviour of the CrcZ/CrcY-null strain is consistent with Crc -and therefore, Hfq- being responsible for the alterations detected in the pattern of consumption of the compounds present in the LB medium.

Interestingly, albeit *P. putida* and *P. aeruginosa* are phylogenetically related, the hierarchy of consumption of carbon sources of the two bacteria presents dissimilarities. The most evident correspond to the assimilation of compounds during the transition and stationary phase, which therefore indicate a similar influence of the Crc/Hfq/CrcZ-CrcY system on the management of carbon sources during exponential phase.

Overall, the results presented emphasise the key role of the Crc protein in helping *P. putida* to adapt to and get the most from an environment that is in constant change due to the sequential consumption of the available substrates which, in most cases, are rapidly depleted once their assimilation starts. The lower growth rate and higher oxygen consumption of the Crc-null strain, and its secretion of key compounds from the central metabolism, strongly suggest that lack of Crc leads to an unbalanced metabolism. Nevertheless, it should be stressed that although the absence of Crc altered the time and speed of assimilation of several compounds, these were still consumed in a sequential and hierarchical manner, suggesting that other regulatory processes exist in addition to the Crc/Hfq system. Additional Crc-independent CCR systems have been described in *P. putida*, such as those involving the PTS^{Ntr} proteins (Cases et al., 2001; Pfluger-Grau and Gorke, 2010) and the Cyo terminal oxidase (Dinamarca et al., 2002), although their relevance seems to be smaller. It would not be surprising to learn about the existence of new still uncharacterized regulatory systems that help to coordinate metabolism in Pseudomonads.

Experimental procedures

Bacterial strains and culture media
Pseudomonas putida strains were cultivated at 30°C with vigorous shaking in LB medium (tryptone, 10 g l^{-1}; yeast extract, 5 g l^{-1}; NaCl, 10 g l^{-1}). The *P. putida* strains used were KT2440 (wild type; Franklin et al., 1981), KTCRC (a KT2440 derivative containing an inactivated *crc* allele; Hernández-Arranz et al., 2013), and KT2440-ZY, which derives from KT2440 by deletion of the *crcZ* and *crcY* genes (La Rosa et al., 2015). Antibiotics were added when needed at the following concentrations: tetracycline 10 μg ml^{-1} and gentamicin 10 μg ml^{-1}.

Measurement of oxygen consumption
Pseudomonas putida strains KT2440, KTCRC and KT2440-ZY were grown in 50 ml flasks with strong aeration until cultures reached to a turbidity (A_{600}) of 0.6. At this point, 0.5 ml of the cultures were diluted 1:2 with preheated fresh medium and the respiration rate measured using an oxygraph (Hansatech, United Kingdom) fitted with a Clark's type oxygen electrode, according to the manufacturer's instructions (Sevilla et al., 2013). The dry weight of the samples was used as the reference parameter. The consumption rate is expressed as mmol O_2 consumed per mg of cell dry weight per hour.

Metabolite footprinting (NMR sampling)
Cells were inoculated in LB medium and cultured overnight at 30ºC. This culture was used to inoculate three separate 250 ml flasks containing 50 ml of fresh LB, up to a turbidity (A_{600}) of 0.03. Cells were allowed to grow with vigorous aeration and, at different time points (0, 1, 1.5, 2, 2.5, 3, 3.5, 4, 5, 6, 7, 8, 10, 12, 14, 24 hours after inoculation), samples were collected. The turbidity was recorded and 0.7 ml of cell suspension were centrifuged at 16000 x *g* for 5 minutes at room temperature. Thereafter, 0.6 ml of supernatant was collected and stored at -80°C until used for NMR analysis. To this end, samples were defrosted at room temperature and 520 μl of supernatant were mixed with 130 μl of NMR buffer (0.25 M phosphate buffer, pH 7, in 100% ^2H_2O (D_2O) containing 0.2 mM 2,2-dimethyl-2-silapentane-d_6-5-sulfonic acid (DSS) as internal standard). Samples were centrifuged for at 16000 x *g* for 5 minutes at room temperature and 600 μl of the supernatant were transferred to NMR tubes.

Nuclear magnetic resonance spectroscopy
Spectra were acquired on a Bruker Avance DRX600 NMR spectrometer (Bruker BioSpin, Rheinstetten, Germany), with a magnetic field strength of 14.1 T and a resulting ^1H resonance frequency of 600 MHz, equipped with a 5-mm inverse flow probe. Samples were introduced using a Gilson flow-injection autosampler. Spectra were acquired following the approach described by (Beckonert et al., 2007). Briefly, a one-dimensional NOESY pulse sequence was used for water suppression; data were acquired into 32 K data points over a spectral width of 12 kHz, with 8 dummy scans and 64 scans per sample, and an additional longitudinal relaxation recovery delay of 3.5 s per scan, giving a total recycle time of 5 s. After acquisition, spectra were Fourier transformed, phased in and normalized to DSS in Chenomx NMR Suite 8.0 (Chenomx, Inc., Edmonton, Alberta, Canada). Peaks were assigned using Chenomx NMR Suite 8.0 spectral database and using spectral information obtained in previous studies (Behrends et al., 2009).

Non-linear fitting of metabolites concentration
Nonlinear regression of the data against time was achieved using a four parameters sigmoid curve model as indicated in (Behrends et al., 2009; Behrends et al., 2014). This resulted in fitting each variable with four parameters: the "amplitude" of the curve (change in relative concentration over the fitted time), the "offset" (relative concentration at the starting time point), the "t_{50}" (time at which the concentration has changed by half the amplitude) and the "assimilation time" (time during which the relative concentration decreases from 75 % to 25 % of the initial value). Cut-offs were imposed for t_{50} (1 to 24 h), assimilation time (0 to 3 h) and fitting of the results ($R^2 > 0.96$). The "uptake rate" for each metabolite was calculated dividing half of the initial concentration by the assimilation time. The uptake rate represents the speed of consumption of a compound when its concentration decreases from 75% to the 25% of the initial value. The uptake rate is indicated as mmol h^{-1}.

Chapter 2

The Crc/CrcZ-CrcY global regulatory system helps the integration of gluconeogenic and glycolytic metabolism

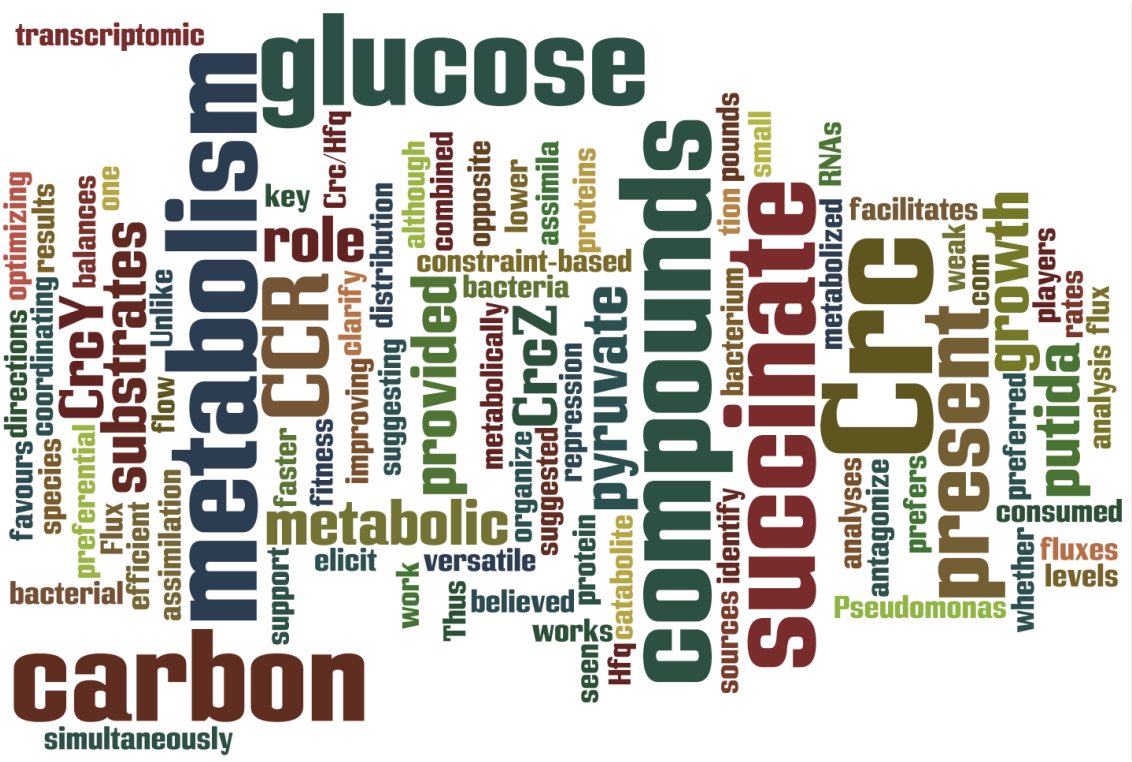

This chapter has been published as:

La Rosa, R., Nogales, J., and Rojo, F. (2015) The Crc/CrcZ-CrcY global regulatory system helps the integration of gluconeogenic and glycolytic metabolism in *Pseudomonas putida*. *Environ Microbiol*. DOI:10.1111/1462-2920.12812

Introduction

Bacteria have evolved regulatory mechanisms to optimize metabolism accordingly to the nutrients present with the aim of improving growth speed, fitness and the chances of survival in their environment. *Pseudomonas putida* is present in different and diverse environments and is able to use, as carbon and energy sources, diverse types of compounds: organic acids, sugars, amino acids and small peptides, alkanes, aromatic compounds, etc. The consumption and metabolism of some of these compounds is regulated by the Crc/CrcZ-CrcY regulatory system that controls and defines the hierarchy of consumption when different carbon sources are present. As previously presented, this regulatory system is composed by the Crc/Hfq regulators and by the two sRNAs CrcZ and CrcY. The levels of CrcZ and CrcY fluctuate according to the carbon source used and the growth phase and their levels are indicative of the CCR strength. The transcription of *crcZ* and *crcY* occurs from RpoN-dependent promoters (*PcrcZ* and *PcrcY* respectively) that rely on the CbrA/CbrB two-component regulatory system, which in turn responds to an as yet unclear signal (Sonnleitner et al., 2009; Moreno et al., 2012; Garcia-Maurino et al., 2013). The mutation of CbrA/CbrB system, or the deletion of the sRNAs, leads to a constitutive state of catabolite repression in which cells are unable to sense and regulate the fluxes of carbon sources coming from the exterior. Recently, to investigate the levels of CCR imposed by different carbon sources, transcriptional fusions of *PcrcZ* and *PcrcY* promoters to the *gfp* reporter gene were used to determine the amount on CCR in different growth conditions (Valentini et al., 2014). The activity of the promoters *PcrcZ* and *PcrcY* were greatest in cells growing at the expense of a poor carbon source such as oxaloacetate, and lowest when cells were cultivated in a complete medium such as LB (Fig. 10). This is consistent with the knowledge that cells cultivated in rich undefined media tightly regulate the consumption of metabolites, which is not needed with a poor carbon source. Most of the carbon sources generate a moderate CCR and the levels of CrcZ and CrcY are intermediate between those of oxaloacetate and those of LB (Fig. 10) (Valentini et al., 2014).

Accordingly, when glucose or succinate were provided to a minimal salts medium, the activity of promoter *PcrcZ* was intermediate between that seen when OAA was the carbon source used, and when cells were cultivated in LB medium (Fig. 10A-B) (Valentini et al., 2014). In *P. aeruginosa*, succinate elicits a strong CCR effect and is preferred over glucose (MacGregor et al., 1992; Hester et al., 2000b). The activity of *PcrcZ* in cells using succinate is about half that seen in cells using glucose, suggesting that the levels of free Crc/Hfq are higher in succinate-using cells (Fig. 10A) (Valentini et al., 2014). Indeed, in presence of succinate, the repression imposed by the Crc/Hfq system on *bkdR* and *amiE* genes expression, implicated in the metabolism of branched-chain amino acids (*bkd* operon) and of aliphatic amides (*ami* operon), respectively, was noteworthy (Hester et al., 2000b; Sonnleitner et al., 2009).

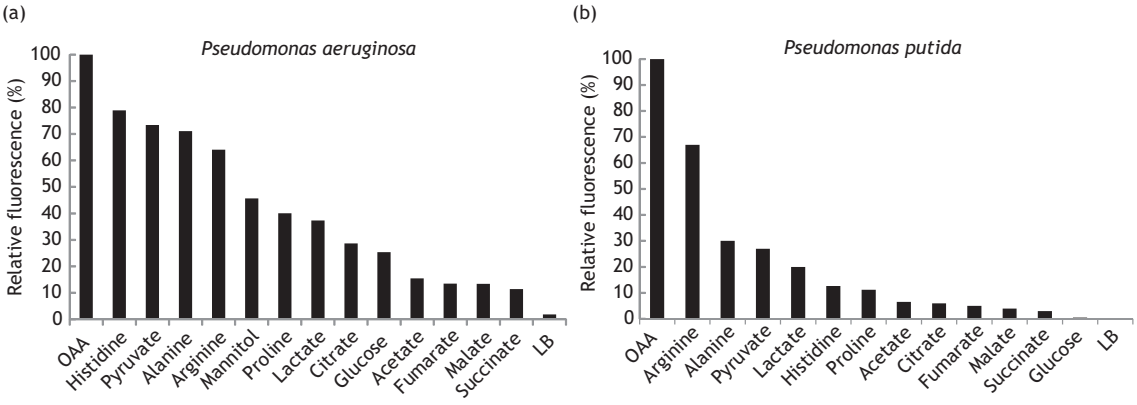

Fig. 10 *crcZ* induction is carbon source dependent in *P. aeruginosa* and *P. putida*.
Expression of the *P. aeruginosa* PAO1 *PcrcZ–gfp* reporter fusion measured in (**A**) *P. aeruginosa* PAO1 and (**B**) *P. putida* KT2442 grown to exponential phase (OD_{600} ~ 0.3) in minimal salts medium containing different carbon sources, or in LB medium, as indicated. Values are given as percentage of expression in the OAA condition and are mean values of duplicate experiments with an SD of ± 10 %. Modified from (Valentini et al., 2014).

In *P. putida*, however, succinate appears to be a weak repressor of non-preferred substrates such as alkanes and branched-chain amino acids, and the expression of *alkB* (alkane dehydrogenase) or *bkdR* (branched-chain amino acids transcriptional regulator) was only slightly diminished in the presence of succinate (Yuste et al., 1998; Hester et al., 2000b). Moreover the joint levels of CrcZ and CrcY in cells growing exponentially at the expense of succinate are rather high, suggesting a weak Crc-mediated CCR response (Moreno et al., 2012). Nevertheless, under certain conditions succinate exerts a clear CCR effect on the expression of genes required for the assimilation of toluene by *P. putida* (Duetz et al., 1994; Duetz et al., 1996). Duetz and colleagues, indicated that cells growing in the presence of non-limiting concentrations of succinate showed a decreased expression of genes coding for enzymes implicated in toluene degradation (*xyl* operon) in response to the addition of o-xylene or 2,3 dimethyl benzoate (a non metabolizable compound that activates the *xyl* operon). Moreover they indicated that the blockage was at the transcriptional level (Duetz et al., 1994; Duetz et al., 1996).

Glucose, although a preferred carbon source for many bacterial genera (Deutscher, 2008; Gorke and Stulke, 2008), is not at the top of the preference list for Pseudomonads. Indeed, the expression of the genes for the uptake and assimilation of glucose is strongly inhibited by the Crc/Hfq regulatory system when cells grow in a complex medium as LB (Moreno et al., 2009b). Glucose, although not being on top of *P. putida* preference, when supplemented with other substrates, in turn inhibits the assimilation of less preferred compounds such as toluene (Holtel et al., 1994; Cases et al., 1999; del Castillo and Ramos, 2007; Busch et al., 2010), methylphenol (Muller et al., 1996) and phenylacetic acid (Schleissner et al., 1994).

It seems, therefore, that compounds such as succinate or glucose, which in *P. putida* behave as weak repressors, can have a regulatory effect on the assimilation of other substrates. However, no information was available on the regulatory interactions affecting succinate and glucose metabolism when both compounds are simultaneously present in the growth medium. The choice between these two carbon sources is of interest since it means deciding between a metabolism focused on glucose consumption (glycolytic), or one directed towards gluconeogenesis (succinate consumption and the synthesis of sugars).

To clarify the preference for glucose or succinate in *P. putida*, and to determine whether Crc-dependent CCR has a role in coordinating metabolism when cells are confronted with a mixture of these compounds at non-limiting concentrations, metabolic, transcriptomic and constraint-based metabolic flux analyses were undertaken.

Results and discussion

Influence of Crc on cell growth when succinate and glucose are provided as carbon sources

When cultivated in minimal salts medium in aerated flasks, *P. putida* KT2440 grew about 15% faster when succinate was the carbon source than when glucose was provided (Fig. 11A-B). Inactivating the *crc* gene had a marginal effect on growth when either succinate or glucose was the carbon source. In agreement with earlier observations (Moreno et al., 2012), a mutant strain lacking the CrcZ and CrcY sRNAs, which is believed to have constitutive and strong Crc-mediated CCR, grew very slowly on succinate and even more slowly on glucose, and only after a long lag phase of adaptation (Fig. 11A-B). This suggests that Crc can influence the assimilation of both succinate and glucose when provided separately, although its effect in the wild type strain is small, presumably because the amounts of CrcZ and CrcY sRNAs are large enough to counteract its effect, ensuring that no inhibitory effect is exerted. This idea was reinforced after measuring the CrcZ and CrcY levels by real-time reverse-transcription PCR (RT-PCR) in wild type cells growing on succinate or glucose. In both situations (Fig. 12), the combined levels of CrcZ and CrcY were intermediate between a situation known to exert a strong CCR effect (exponential growth in a complete medium such as LB), and a condition in which CCR is absent (stationary phase in LB). CrcZ and CrcY levels were somewhat higher when succinate was the carbon source than when glucose was used, but under both conditions they were presumably high enough to assure a low Crc-mediated CCR. When both succinate and glucose were provided simultaneously at non-limiting concentrations (20 mM each), the wild type strain grew at a rate similar to that achieved when succinate was the sole carbon source (Fig. 11B-C). Inactivating the *crc* gene (strain KTCRC) led to an 11% fall in the growth rate, although the speed of depletion of succinate and glucose, and that of oxygen consumption, changed little (Table 1 and Fig. 11B-C). The reduction in growth rate suggests that Crc may have some role in optimising metabolism under these co-feeding conditions. In support of this, the levels of CrcZ and CrcY in wild type cells growing in the presence of the mixture of glucose and succinate were significantly lower than when only one of these compounds was present, which is diagnostic of a strong Crc-mediated CCR (Fig. 12). For both the wild type and *crc*-deficient strains, succinate was depleted from the medium significantly faster than glucose (Table 1 and Fig. 11C). Only after about 6 h of growth, when the succinate concentration had fallen to about 35% of its initial value, did its consumption apparently stop while that of glucose increased. This suggests that succinate was consumed preferentially over glucose during exponential growth, a preference that seems to cease when cells approach the stationary phase.

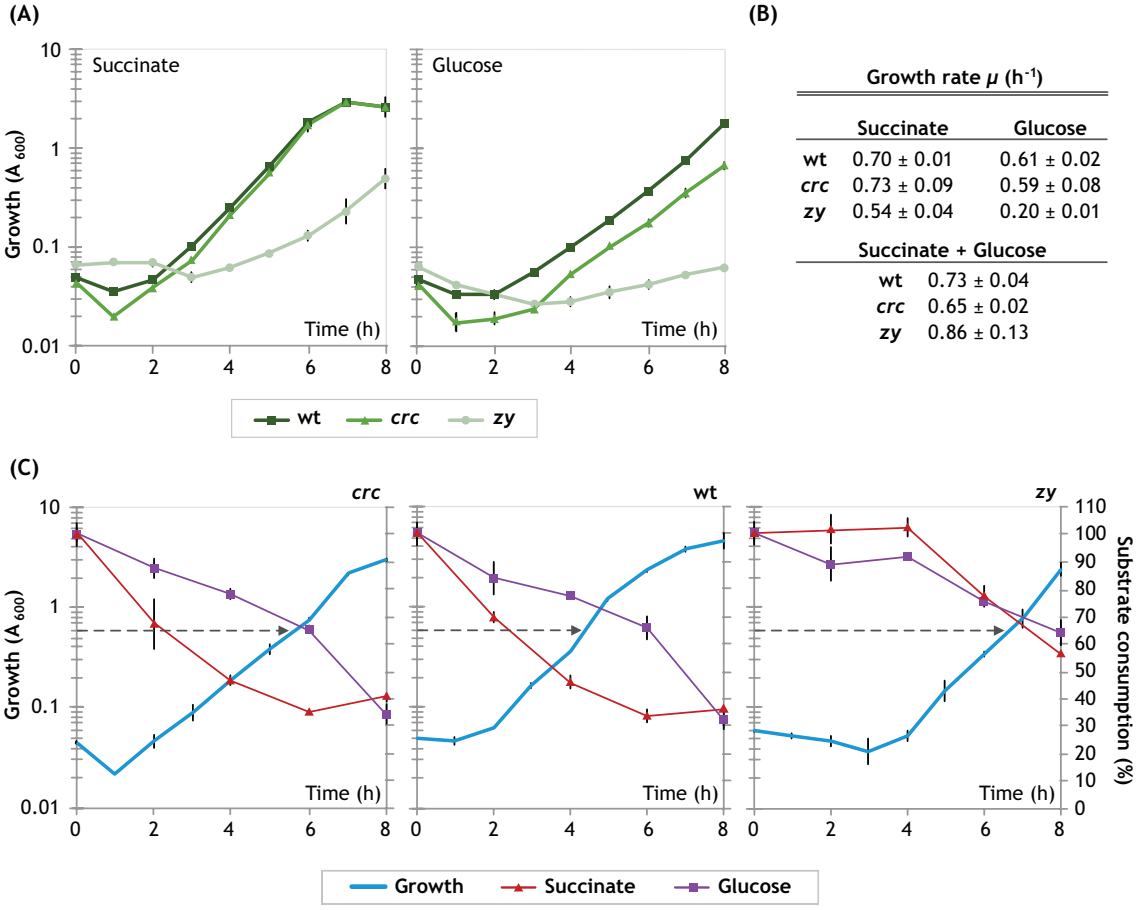

Fig. 11 Influence of Crc on the growth of *P. putida* using succinate, glucose, or both.
(**A**) *P. putida* strains KT2440 (wild type, dark-green line, indicated as 'wt'), KTCRC (Crc-null derivative of KT2440; green line, indicated as '*crc*') and KT2440-ZY (CrcZ- and CrcY-null derivative of KT2440, light-green line, indicated as '*zy*') were cultivated in minimal salts M9 medium supplemented with either 20 mM succinate or 20 mM glucose. Growth was followed by measuring the turbidity at 600 nm. Black bars indicate the standard deviation. (**B**) Growth rate of the three strains analysed when growing in the presence of 20 mM succinate, 20 mM glucose, or a mixture of both substrates (20 mM each). (**C**) The strains indicated above were cultivated in minimal salts M9 medium supplemented with a mixture of 20 mM of succinate and 20 mM glucose. Cell growth (A_{600}, blue line), and the depletion of succinate (red line) and glucose (violet line), expressed as the percentage remaining relative to the initial concentration of the substrate, are indicted as a function of time. The arrow indicates the moment in which cells were collected to purify total RNA for RNA-seq analyses.

The mutant strain KT2440-ZY, which lacks both CrcZ and CrcY, and therefore has an artificially strong Crc-mediated CCR, had a long lag time of about 4 h. However, after this adaptation period, growth was fast and succinate and glucose were consumed simultaneously, with succinate being spent at a rate double that of glucose (Table 1 and Fig. 11B-C). Adaptation did not seem to require mutations, since the same lag was observed when adapted cells were transiently cultivated in LB and reintroduced into minimal salts medium with succinate and glucose. In addition, no mutations in the *crc* gene were detected by PCR in any of several individual colonies isolated from cultures that had reached the stationary phase. It remains unclear what modifications allow this adaptation.

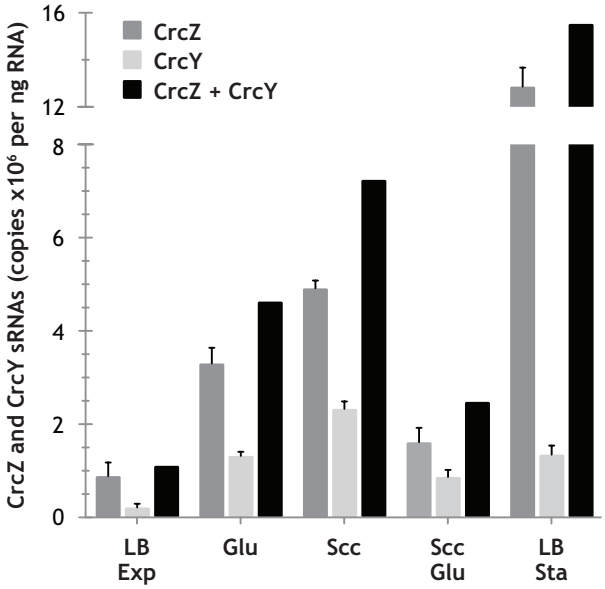

Fig. 12 Levels of CrcZ and CrcY sRNAs in *P. putida* KT2440 under different cultivation conditions.
Cells were cultivated (in triplicate) either in complete LB medium, or in minimal salts M9 medium supplemented with 20 mM succinate (Scc), 20 mM glucose (Glu) or both carbon sources at 20 mM each. Samples were taken either at mid-exponential phase (A_{600} = 0.6; "LB Exp", "Glu", "Scc" and "Scc-Glu"), or at the start of the stationary phase (A_{600} = 2.2; "LB Sta"). Total RNA was obtained and the levels of CrcZ and CrcY were determined by real-time RT-PCR. Error bars indicate the standard deviation. Black bars indicate the total amount of CrcZ+CrcY.

Table 1. Growth of *P. putida* strains KT2440 (wild type, indicated as 'wt'), KTCRC (Crc-null derivative of KT2440, indicated as '*crc*') and KT2440-ZY (CrcZ- and CrcY-null derivative of KT2440, indicated as '*zy*') in minimal salts M9 medium supplemented with a mixture of 20 mM succinate and 20 mM glucose.

Strain	Growth rate μ (h^{-1})[a]	Succinate uptake[b]	Glucose uptake[b]	Gluconate production[c]	Fumarate production[c]	Oxygen consumption[d]
wt	0.73 ± 0.04	4.66 ± 0.13	4.72 ± 0.10	1.07 ± 0.09	0.027 ± 0.001	20.4 ± 1.2
crc	0.65 ± 0.02	4.54 ± 0.08	5.38 ± 0.15	0.56 ± 0.03	0.038 ± 0.002	19.2 ± 3.6
zy	0.86 ± 0.13	8.18 ± 0.29	4.64 ± 0.25	1.56 ± 0.19	0.007 ± 0.001	19.2 ± 0.6

[a] Growth rate (μ) was determined during exponential growth; values correspond to the mean ± the standard deviation of three measurements

[b] Values correspond to the consumption observed during mid-exponential phase (between 4 and 6 h of growth for the wild type and Crc-null strains, and 6 to 8 h for the CrcZ/CrcY-null strain), and represent the mean ± the standard deviation of three measurements, indicated as mmol $gCDW^{-1}h^{-1}$

[c] Values correspond to the rate of gluconate or fumarate expulsion to the culture medium during mid-exponential phase (between 4 and 6 h of growth for the wild type and Crc-null strains, and 6 to 8 h for the CrcZ/CrcY-null strain), and represent the mean ± the standard deviation of three measurements, indicated as mmol $gCDW^{-1}h^{-1}$

[d] The specific oxygen consumption was calculated during mid exponential phase (A_{600} = 0.6). Values correspond to the mean ± the standard deviation of three measurements, indicated as mmol $mgCDW^{-1}h^{-1}$

Analysis of secreted metabolites

In *Pseudomonas*, after glucose enters the periplasmic space via the OprB-1 porin, its catabolism occurs through the simultaneous operation of three pathways that converge upon 6-phosphogluconate (6PGC) (del Castillo et al., 2007). In one of these pathways, glucose is transported directly to the cytoplasm via the ABC transport system encoded by the *gstABCD* genes, and is then converted first to glucose-6-P (G6P) and then to 6PGC (see Fig. 13). Alternatively, glucose can be oxidised to gluconate (GC) within the periplasm by glucose dehydrogenase (Gcd), the GC produced being either further oxidised to 2-ketogluconate (2KG) in the periplasm or transported into the cytoplasm and phosphorylated to render 6PGC. The 2KG remaining in the periplasm is also internalised and transformed to 6PGC. This molecule, the first common point of the three converging pathways, is further metabolised through the Entner-Doudoroff (ED) pathway (Fig. 13).

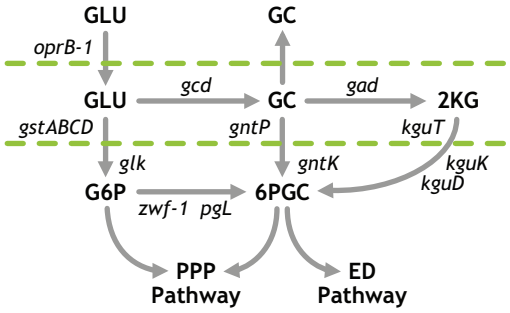

Fig. 13 Steps involved in the uptake and initial metabolism of glucose in *P. putida*.
The outer and inner membranes are indicated as green dashed lines; the space between them represents the periplasmic space. Abbreviations: GLU, glucose; GC, gluconate; 2KG, 2-keto-gluconate; G6P, glucose-6-phosphate; 6PGC, gluconate-6-phosphate; PPP, pentose phosphate pathway, ED, Entner-Doudoroff pathway.

This metabolic strategy means that measuring glucose depletion from the growth medium may not fully indicate its rate of metabolism, since a significant fraction could be transformed into GC or 2KG and extruded back into the medium rather than being internalised. Thus, the amounts of GC and 2KG in the growth medium were determined in parallel with glucose depletion. Table 1 shows that, when both succinate and glucose were present, about 22% of the glucose consumed by the wild type cells was expelled back to the growth medium as GC, an amount that decreased by nearly half when the *crc* gene was inactivated. The Crc protein mediates inhibition of the expression of the *gstABCD* genes that code for the ABC transport system responsible for glucose internalisation into the cytoplasm, but not that of the gene coding for the glucose dehydrogenase (*gcd*) that transforms glucose to GC (Moreno et al., 2009b). Therefore, the results suggest that, in the presence of both glucose and succinate, the Crc protein is able to reduce the direct import of glucose, which accumulates in the periplasm and is transformed into GC, which in turn leaks back to the growth medium. In support of this idea, glucose consumption was about 14% higher in the Crc-null mutant than in the wild type (Table 1), which sug-

gests that a somewhat larger fraction of the glucose is internalised and transformed to G6P, reducing the amount available to be transformed into GC. In addition, the strain lacking both CrcZ and CrcY, while able to consume as much glucose as the wild type, expelled about 50% more gluconate to the medium. However, and as explained below, the mRNA levels corresponding to the *gcd* gene were somewhat lower in the *crc* mutant strain than in the wild type, which may also help explain the lower production of GC in the Crc-null strain. The levels of 2KG in the growth medium were very low and could not be satisfactorily determined.

Under co-feeding conditions, the cells also expelled low but detectable amounts of fumarate to the growth medium (Table 1), suggesting that the tricarboxylic acids cycle (TCA) cannot accommodate all the flux of metabolites that derive from succinate and glucose assimilation, resulting in the accumulation of fumarate that is in part extruded. Inactivating the *crc* gene led to a 43% increase in the extrusion of fumarate to the culture medium. The strain lacking CrcZ and CrcY behaved in the opposite manner, the amount of fumarate detected in the medium being about a quarter that seen for the wild type. The levels of acetate, propionate, formate and pyruvate in the growth medium were also analysed, but in all cases were below detection limits.

Effect of Crc on the transcriptome profile of cells growing with a mixture of succinate and glucose

Although the Crc/Hfq regulatory system inhibits gene expression post-transcriptionally, it is known that the inactivation of the *crc* gene has a great impact on the transcriptome of the cell, at least in cells growing under conditions that elicit a strong CCR effect (Moreno et al., 2009b; Sonnleitner et al., 2012). This occurs, in part, because the Crc/Hfq system regulates the translation of mRNAs corresponding to many transcriptional regulators and to several membrane transporters that allow the internalisation of substrates that induce specific metabolic pathways. To obtain insight into the influence of Crc on cells growing in a minimal salts medium containing a mixture of succinate and glucose, the transcriptome profile of the wild type KT2440 strain was compared to that of its *crc* mutant derivative (strain KTCRC), and to that of its *crcZcrcY* mutant derivative (strain KT2440-ZY). Total RNA was obtained from exponentially growing cells (A_{600} = 0.6) and the transcriptomes analysed by RNA-seq deep sequencing, using two biological replicates for each strain. A given RNA was considered to be differentially expressed when its levels changed more than 1.8-fold between the two strains compared, with a *P* value of <0.001 (corrected for the fold discovery rate, FDR). With these cut-off values, inactivation of the *crc* gene changed the mRNA levels of 363 genes (7.4% of the genome) relative to the wild type strain. Similarly, 365 genes (8.2% of the genome) showed changes in their RNA levels when the *crcZ* and *crcY* genes were inactivated. Supplementary Table S1 shows a list of the differentially expressed genes. For both mutant strains, most of the genes affected were involved in energy metabolism, transport and the binding of substrates, or regulatory functions; many corresponded to hypothetical proteins or proteins with no known function (Fig. 14, Fig. S2 and Fig. S3). In the strain lacking the Crc protein, the levels of many mRNAs corresponding to genes involved in protein synthesis (mostly ribosomal proteins) were higher than in the wild type strain, likely indicating a higher protein turnover. This contrasts with the lower growth rate of the mutant strain and suggests less efficient growth. It is worth noting that the absence of

CrcZ and CrcY had a stronger effect on genes involved in transport and the binding of substrates than did the absence of Crc, and that in most cases the lack of both sRNAs led to a reduction in the levels of the affected mRNAs (Fig. 14). This is consistent with the proposal that, in this strain, Crc/Hfq-dependent CCR is very strong and reduces the uptake of many non-preferred substrates (Sonnleitner et al., 2009; Moreno et al., 2012).

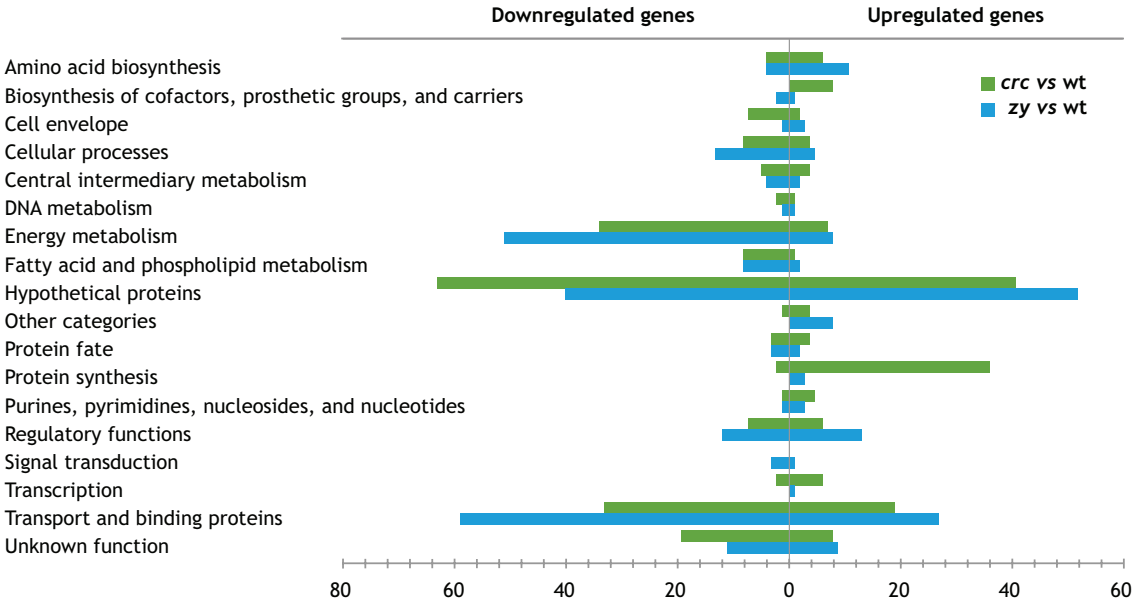

Fig. 14 Functional categories of the differentially expressed genes.
Genes showing elevated or reduced mRNA levels upon inactivation of the *crc* gene (in green), or of the *crcZ* and *crcZ* genes (in blue), and grouped into functional categories. The scale on the bottom indicates "number of genes".

The transcriptome profiles provided useful information on the impact of the absence of Crc, and of CrcZ and CrcY, on the expression of the genes involved in the transport of glucose and succinate. As mentioned above, under conditions of strong CCR, Crc co-inhibits the expression of genes involved in the initial uptake of glucose through the outer membrane (via OprB-1 porin) and its direct transport to the cytoplasm (GstABCD transporter), although the genes responsible for the production of GC and 2KG are apparently not regulated by Crc (Moreno et al., 2009b). The *gstABCD* and the *oprB-1* genes are believed to form an operon that is transcribed from the *PgstA* promoter, the expression of which is activated by the GltR-2 activator ((del Castillo et al., 2008); see Fig. 15A). GltR-2, in turn, activates the transcription of its own gene, as well as that of other genes involved in glucose assimilation (Fig. 15A). The *gltR-2* mRNA contains a putative CA box for Crc/Hfq-dependent regulation, and similar CA sequences can be predicted for the *gstA* and *oprB-1* translation initiation regions (and possibly at *gstD* as well; indicated in red in Fig. 15A). If Crc helps Hfq to inhibit the translation of *gltR-2* mRNA, reduction in the levels of the GltR-2 activator could result in the reduced transcription of the *gltR-2* gene itself and, as a consequence, of the *gstABCD-oprB-1* operon. When cells were cultivated in the presence of both glucose and succinate, the inactivation of the *crc* gene led to a small increase in the levels of *gltR-2* mRNA.

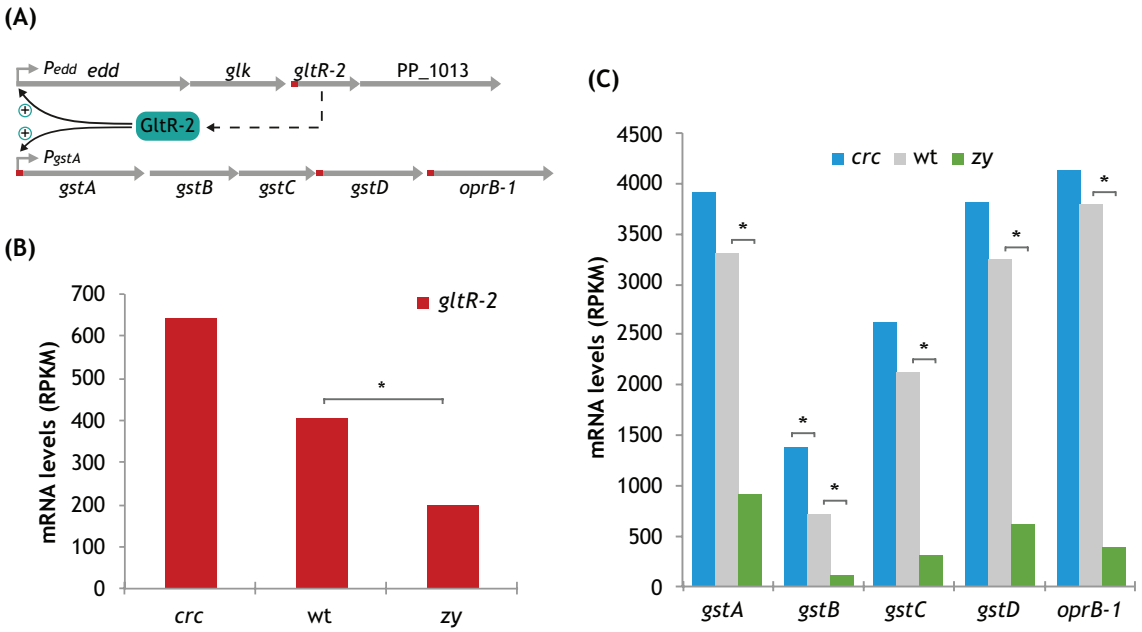

Fig. 15 Expression of the genes for glucose transport.
(**A**) The genes for glucose import through the outer membrane (*oprB-1*) and the inner membrane (*gstABCD*) are clustered in an operon transcribed from promoter *PgstA*, the activity of which requires the transcriptional activator GltR-2 encoded in a different cluster (del Castillo et al., 2008). The translation initiation regions of *gltR-2*, *gstA*, *gstD* and *oprB-1* mRNAs contain CA boxes indicative of Crc/Hfq-dependent regulation (indicated in red). (**B**, **C**) RNA levels corresponding to *gltR-2* (**B**), or to the *gstABCD-oprB-1* genes (**C**), in the KT2440 wild type strain (wt; grey bars in "C"), the Crc-null derivative (*crc*; blue bars in "C") and the CrcZ/CrcY-null derivative (*zy*; green bars in "C"), as derived from the RNA-Seq analyses. RNA levels are indicated as reads per kilobase per million reads (RPKM). RNAs were obtained from cells cultivated in M9 minimal salts medium supplemented with glucose and succinate, and collected at mid exponential phase (OD_{600} = 0.6). The asterisks indicate that a significant difference exists between the samples compared (in brackets), with a *P* value (corrected for FDR) of <0.001.

However, while detectable, this increase was below the threshold limits considered meaningful in the present analyses, although the absence of CrcZ and CrcY, which would be expected to increase the levels of Crc-dependent CCR, led to a clear reduction in *gltR-2* mRNA levels (Fig. 15B; Table S1). The behaviour of the *gstABCD-oprB-1* genes was similar: the absence of Crc led to a small increase in their mRNA levels, but again below the threshold considered meaningful, while the absence of CrcZ and CrcY led to a strong reduction (Fig. 15C; Table S1). Therefore, under the conditions tested, the Crc/Hfq regulatory system has a very small impact on the transcription of the *gstABCD-oprB-1* genes in the wild type strain. In other words, although Crc/Hfq can regulate these genes, the levels of CrcZ and CrcY are sufficiently high to antagonize their effect in the wild type strain under the growth conditions analysed. However, while mRNA levels remain unaffected, Crc/Hfq might compromise the translation of the *oprB-1* and *gstA* mRNAs, which contain clear CA motifs, therefore reducing the levels of the OprB-1 and GstA proteins, both of which are involved in glucose transport. Since glucose consumption in the Crc-null was 14% higher than in the wild type strain, this inhibitory effect of Crc/Hfq system probably exists, but must be small.

Inactivation of the *crc* gene reduced to about a half the mRNA levels of the gene coding for Gcd (which transforms glucose to GC), but had no effect on the mRNA levels of the gene responsible for the oxidation of GC to 2KG (Fig. 17; Table S1). This may partly explain the

reduction in GC production (47%) observed in the *crc* deficient strain compared to the wild type strain (Table 1).

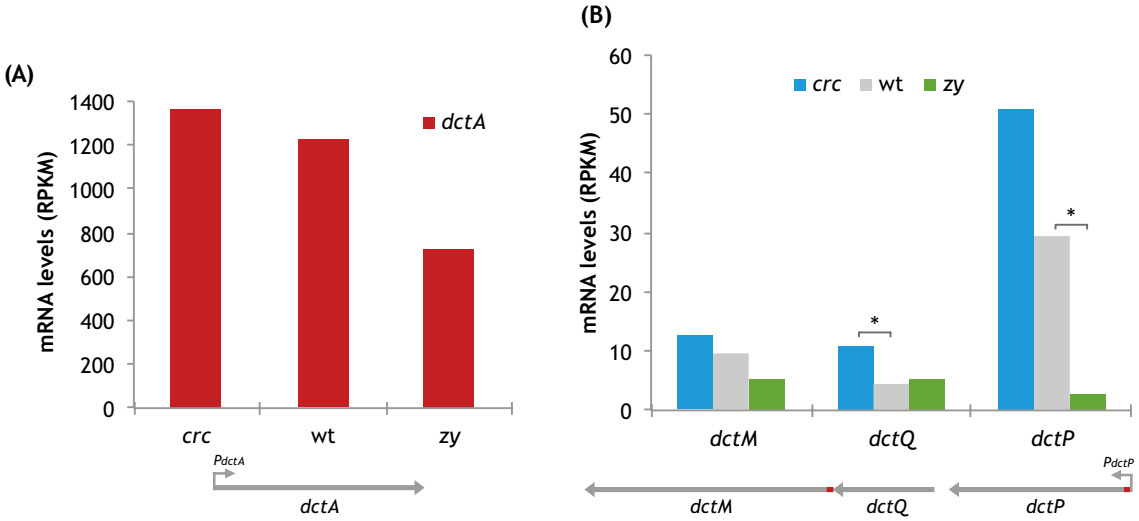

Fig. 16 Expression of the genes for succinate and fumarate transport.
The organisation of the *dctA* and *dctPQM* genes is indicated below the corresponding graph; promoters are indicated by arrows. The translation initiation regions of *dctP* and *dctM* mRNAs contain putative CA boxes (depicted in red) indicative of Crc/Hfq-dependent regulation. RNA levels corresponding to *dctA* (**A**), or to the *dctPQM* genes (**B**), in the KT2440 wild type strain (wt; grey bars in "B"), the Crc-null derivative (*crc*; blue bars in "B") and the CrcZ/CrcY-null derivative (*zy*; green bars in "B"), as derived from RNA-Seq analyses. RNA levels are indicated as reads per kilobase per million reads (RPKM). RNAs were obtained from cells cultivated in a minimal salts medium supplemented with glucose and succinate, and collected at mid exponential phase (OD_{600} = 0.6). The asterisks indicate that a significant difference exists between the samples compared (in brackets), with a *P* value (corrected for FDR) of <0.001.

Inactivating the *crc* gene did not affect the uptake of succinate (Table 1), suggesting that Crc has little influence on the expression of the genes involved in its transport under the conditions tested. In *P. aeruginosa*, the uptake of succinate and fumarate during aerobic growth relies mainly on two transporters, DctA and DctPQM (Valentini et al., 2011; Valentini and Lapouge, 2013). DctA is more efficient at millimolar concentrations of succinate, while DctPQM is a high affinity transport system more important at micromolar concentrations. Crc was shown to have a negative impact on expression of the high affinity DctPQM transporter and to stimulate the low affinity DctA system (Valentini and Lapouge, 2013). The *dctA* and *dctPQM* genes are also present in the *P. putida* KT2440 genome, although their regulation has not been described. The present transcriptomic analyses indicated that the mRNA levels of *dctA* were similar in the wild type and *crc*-deficient strains (Fig. 16A). The mRNA levels of the *dctPQM* genes were rather low - about 20 times lower than those of *dctA*. In addition, those of *dctP* and *dctQ* were almost twice higher in the Crc-null than in the wild type strain (Fig. 16B). With respect to *dctP*, inactivation of the CrcZ and CrcY sRNAs led to the opposite effect, i.e., to a strong reduction in its mRNA levels. The *dctP* translation initiation site contains a putative CA box indicative of Crc/Hfq-dependent regulation; the inhibitory effect of Crc/Hfq on *dctP* mRNA levels might reflect either reduced mRNA stability when its translation is inhibited, or the indirect inhibition

of *dctP* transcription by Crc/Hfq, perhaps derived from a Crc/Hfq-dependent repression of the regulatory system responsible for *dctP* transcription (a regulatory system that has not yet been characterised in *P. putida*). The present results, as well as the presence of a putative CA box in the *dctP* mRNA, suggest that the Crc/Hfq system regulates the expression of the DctPQM transport system in *P. putida* in a way analogous to that of *P. aeruginosa,* but that it has no effect on *dctA*, the transporter that one might think the most important under the growth conditions used here (millimolar concentrations of succinate). Therefore, Crc does not appear to limit succinate uptake under the conditions analysed.

In summary, the RNA-Seq analyses indicate that Crc has a detectable effect on the transcriptome of the cell when bacteria grow using a mixture of succinate and glucose, although its impact on the uptake of both substrates is weak. Inactivation of the *crc* gene, however, affected the mRNA levels of some important genes involved in central metabolism. For example, the absence of Crc doubled the levels of the mRNAs coding for subunits A and B of pyruvate carboxylase, which transforms pyruvate to oxaloacetate, and reduced by a half or more the mRNA levels of several genes coding for enzymes of the Krebs cycle and the glyoxylate shunt (summarised in Fig. 17). This might be connected to the 11% lower growth rate of the Crc-null strain compared to the wild type. In addition, inactivating the *crcZ* and *crcY* genes, which should exacerbate Crc inhibitory effects, led to a reduction in the expression of genes involved in the uptake and initial assimilation of glucose, reduction that apparently was not enough to block glucose consumption but sufficient to significantly increase GC secretion (Fig. 17B and Table 1). The clear increase in succinate consumption by this mutant strain (Table 1) suggests that metabolism was rewired to favour the use of this organic acid, although the impact on the mRNA levels of genes involved in its initial metabolism was not great. Thus, the influence of Crc on gene expression under the conditions analysed is subtle, although it does partly explain the impact of inactivating *crc* or the *crcZ*/*crcY* genes on the growth rate and uptake of succinate and glucose. However, the full explanation would have to take into account the complex regulatory processes that coordinate metabolism beyond transcriptional regulation, which comprise post-transcriptional and post-translational modifications, including allosteric enzymatic regulation driven by small molecules (Chubukov et al., 2014). In addition, metabolic fluxes are constrained not only by the levels of the relevant enzymes, but also by the availability of the metabolites that are the substrates of those enzymes, further increasing the complexity of the system. In fact, it has recently been observed that when *P. putida* uses glucose, fructose or benzoate as carbon source, remarkable changes occur in the fluxes of metabolites through central carbon metabolism, although these are not necessarily reflected in the mRNA levels of many of the enzymes involved (Sudarsan et al., 2014). As a way to tackle these problems, flux balance analyses were performed using an *in silico* method that calculates the flow of metabolites through a metabolic network on the basis of the genome-scale metabolic reconstruction of the microorganism of interest and a given number of experimentally provided constraints (Orth et al., 2010).

Constraint-based flux analysis reveals that Crc forces a rerouting of metabolism

Flux Balance Analysis (FBA) combined with Constraints-Based Reconstruction and Analysis (COBRA), is a mathematical method that allows a phenotype to be predicted from the genotype via its associated reaction fluxes (Patil et al., 2004; Feist et al., 2007; Feist et al., 2009; Lewis et al., 2012). It also affords a very useful computational framework for integrating *omics* datasets since it provides a mechanistic interpretation of the data (Hyduke et al., 2013; Saha et al., 2014). To gain additional insights into the metabolic control driven by Crc, an updated genome-scale model of *P. putida*, named *i*JN1411, was used as a computational platform for the integration and contextualisation of the available transcriptomic and metabolic data. Condition-specific models corresponding to the wild type, Crc-null and CrcZ/CrcY-null strains were constructed by applying, as additional constraints, the experimentally determined data for the uptake of glucose and succinate and the secretion of fumarate and gluconate (Table 1), and the available gene expression data. The Gene Inactivity Moderated by Metabolism and Expression (GIMME) algorithm was used to integrate the transcriptomic data (Becker and Palsson, 2008), as indicated in Experimental Procedures. It is important to note that the algorithm uses RNA-seq data to decide which genes are active via their mRNA levels being above a given threshold, but does not take into account differences between mRNA or protein levels. Finally, the solution space for each condition-specific model, in terms of flux distribution through individual reactions, was extensively computed by Markov chain Monte Carlo sampling (Schellenberger and Palsson, 2009). This analysis computes the probabilistic flux value for each single reaction in a given metabolic model, thus allowing the comparison of flux distributions between two or more condition-specific models through single reactions. Calculations were made with the objective of maximising the growth rate. Under succinate and glucose co-feeding conditions, the growth rates predicted by the FBA analyses were 0.61 h^{-1} for the wild type strain, 0.67 h^{-1} for the Crc-null strain, and 0.75 h^{-1} for the CrcZ/CrcY-null strain, values close to those observed experimentally (discrepancy 16.4%, 3% and 12.8%, respectively).

In *P. putida*, glucose is catabolised through the Entner-Doudoroff pathway (ED), in which the 6PGC generated from glucose is converted to pyruvate and glyceraldehyde-3-phosphate (G3P) in a two-step process catalysed by the enzymes Edd and Eda (see Fig. 17). Only a minor fraction of 6PGC is funnelled through the pentose phosphate pathway (PPP) (del Castillo et al., 2007; Chavarria et al., 2012; Sudarsan et al., 2014). Flux distribution predictions for the wild type under co-feeding conditions indicated that glucose was metabolised through the ED and PPP pathways at a ratio of about 1:1, suggesting that the simultaneous metabolism of succinate modifies glucose catabolism and, as a consequence, the carbon flux distribution is significantly altered during co-feeding.

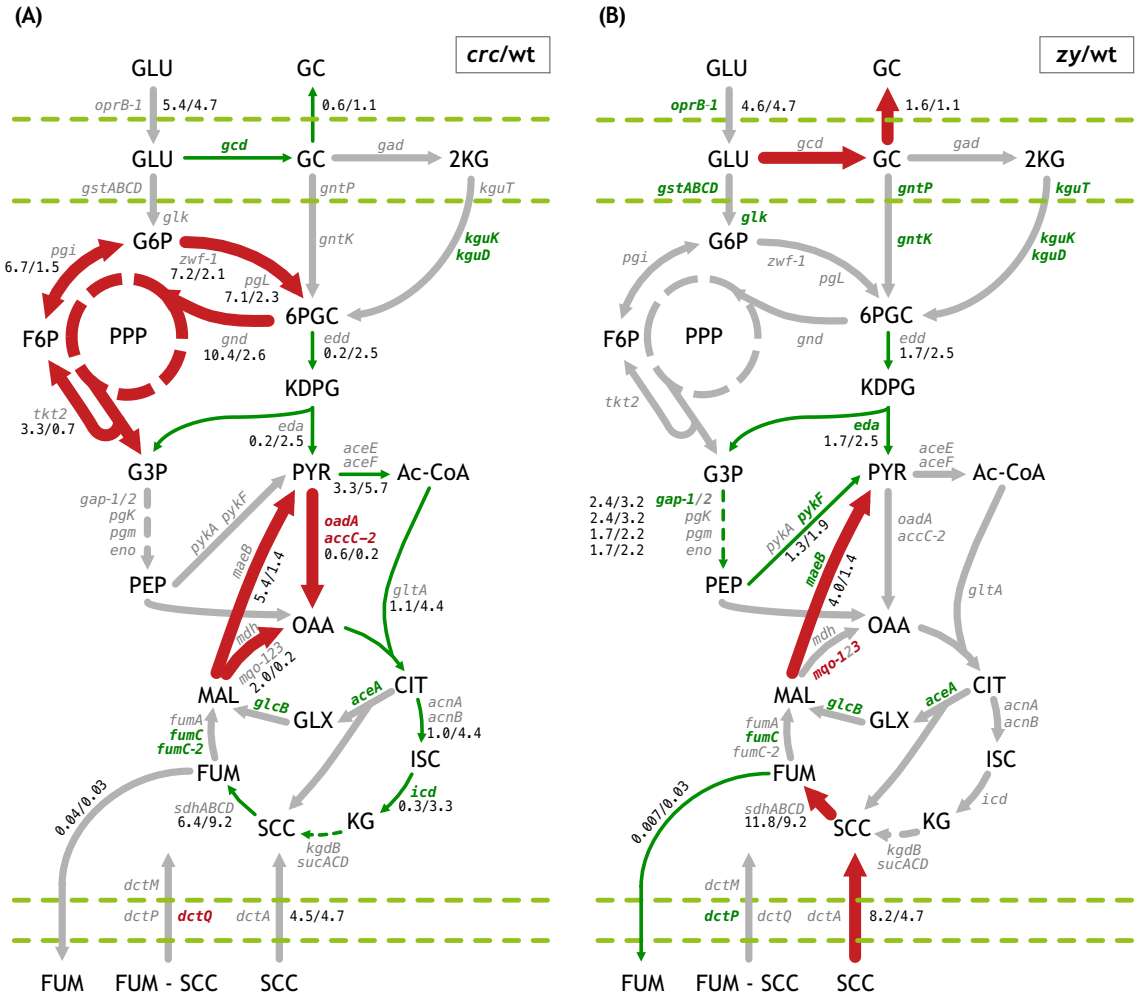

Fig. 17 Influence of Crc on the distribution of central metabolite fluxes, as determined by constraint-based analyses.
The diagrams summarise the reaction networks in cells growing exponentially in a minimal salts medium containing a mixture of glucose and succinate; the dashed green lines represent the inner and outer membranes. Modifications in the carbon flux resulting from the inactivation of the *crc* gene (**A**), or of the *crcZ* and *crcY* genes (**B**), are indicated by thick red arrows (increased flux), or thin green arrows (reduced flux); unaffected fluxes are shown in grey arrows. The numbers next to the arrows indicate the net flux (mmol $gCDW^{-1}$ h^{-1}) in the mutant and wild type strains (mutant/wild type). The genes showing elevated RNA levels (in red), or reduced RNA levels (in green) in the corresponding mutant strain relative to the wild type, as deduced from RNA-Seq analyses, are highlighted; those in grey showed no changes. Abbreviations: GLU, glucose; GC, gluconate; 2KG, 2-keto-gluconate; G6P, glucose-6-phosphate; 6PGC, gluconate-6-phosphate; F6P, fructose-6-phosphate; PPP, pentose phosphate pathway; G3P, glyceraldehyde-3-phosphate; KDPG, 2-dehydro-3-deoxy-6-phosphogluconate; PYR, pyruvate; Ac-CoA, acetyl-CoA; PEP, phosphoenolpyruvate; OAA, oxaloacetate; CIT, citrate; ISC, isocitrate; KG, α-ketoglutarate; SCC, succinate; FUM, fumarate; MAL, malate; GLX, glyoxylate.

Flux analysis of the Crc-null strain suggested that the amount of glucose metabolised through the PPP pathway was even higher. Thus, the fluxes moving through key enzymes of the PPP pathway (including its oxidative branch), such as those encoded by *gnd, tkt2, pgi*, *zwf-1* and *pgl*, were from 3.1 to 4.7 times stronger than in the wild type (see Fig. 17A). Accordingly, the flux of 6PGC towards pyruvate through the ED pathway (*edd*, *eda*) was 12.5 times lower in the Crc-null strain than in the wild type. Therefore, while in the wild type model some 65% of G6P

and 45% of 6PGC were generated through the PPP pathway, these values increased to 91% and 68% respectively in the Crc-null model (Fig. 18), suggesting a large flux of carbon recirculation in the PPP pathway in the Crc-null strain. The difference predicted by the condition-specific models was even greater for G3P since, in the wild type model, 19% of it was produced through the PPP pathway and another 73% through the ED pathway. These values were reversed in the Crc-null strain, in which 93% of G3P was produced through the PPP pathway and only some 6% via the ED enzymes (Fig. 18).

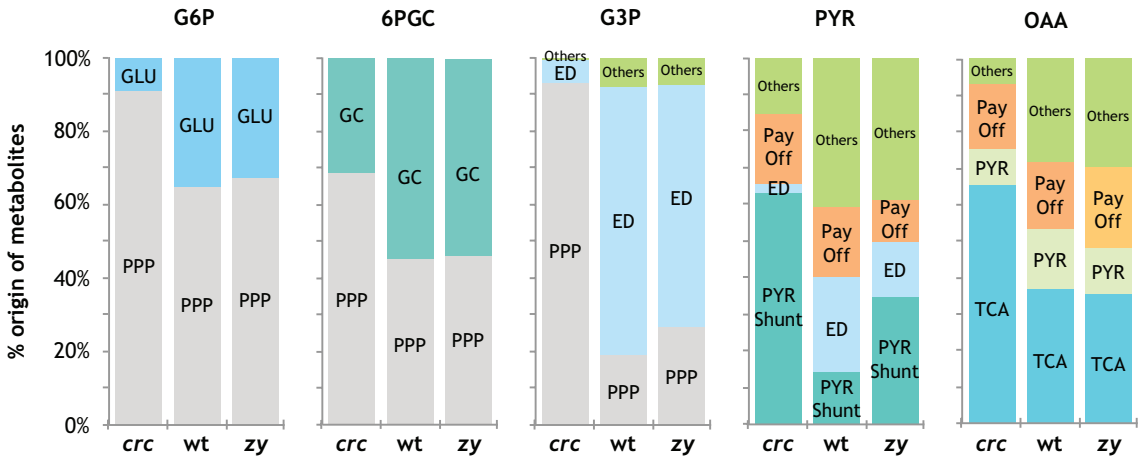

Fig. 18 Importance of different metabolic pathways in the synthesis of the indicated metabolites.
The *P. putida* strains KT2440, KTCRC and KT2440-ZY are indicated as wt, *crc* and *zy*, respectively. The relative contribution of different metabolites or pathways towards the synthesis of glucose-6-phosphate (G6P), gluconate-6-phosphate (6PGC), glyceraldehyde-3-phosphate (G3P), pyruvate (PYR) and oxaloacetate (OAA), was calculated from the fluxes of the reactions that generate each of these compounds, as indicated by the constraint-based metabolic reconstruction analyses. GLU, glucose; PPP, pentose phosphate pathway; GC, gluconate; ED, Entner-Doudoroff pathway; PYR shunt, pyruvate-shunt; TCA, tricarboxylic acids cycle; Pay-off, reactions converting G3P into PYR or OAA.

It should be noted that while succinate was consumed at similar efficiencies in the wild type and Crc-null strains (Table 1), the greater flux predicted for the Crc-null strain through the pyruvate shunt, driven by malic enzyme (MaeB), deviated an important amount of carbon away from the tricarboxylic acids cycle (TCA; see Fig. 17A). Accordingly, a stronger flux through the decarboxylative branch of TCA (which includes citrate synthase, aconitase, isocitrate dehydrogenase and oxoglutarate dehydrogenase activities) was predicted for the wild type model than for the Crc-null model (Fig. 17A). In support of this, pyruvate dehydrogenase (*aceE-F*), which transforms pyruvate into acetyl-CoA, was predicted to be less active in the Crc-null strain. This suggests that Crc might control the flux of succinate towards pyruvate, and that the wild type strain would preferentially oxidise succinate in the TCA cycle rather than diverting it to pyruvate. The consequence is that the fraction of pyruvate and oxaloacetate derived from the TCA cycle or from the ED pathway would vary significantly depending on whether the Crc protein is functional or not (see Fig. 17A and Fig. 18).

These flux changes derive from the greater activity of the PPP pathway and the greater inhibition of the ED pathway in the Crc-null strain than in the wild type. Since Crc strongly

inhibits the expression of the G6P isomerase (*pgi*) (Moreno et al., 2009b), this flux rerouting probably responds to the presumed higher levels of this enzyme in the Crc-null strain, which would allow carbon metabolites to flow through the PPP pathway, aided by a certain blockage of pyruvate metabolism imposed by the high levels of pyruvate provided by malic enzyme (Fig. 18). Thus, these results suggest that the Crc protein plays a significant role in the distribution of carbon flow when cells grow on a mixture of glucose and succinate.

The predicted flux distribution in the CrcZ/CrcY-null strain roughly resembled that of the wild type model (Fig. 17B), as anticipated from the low levels of CrcZ and CrcY sRNAs found in the wild type strain under co-feeding conditions (and which are indicative of relatively strong Crc/Hfq-dependent CCR) (Fig. 12). However, two important differences were seen. First, the greater GC secretion imposed on the CrcZ/CrcY-null flux model by the experimental evidence (Table 1) would slightly reduce the amount of 6PGC available. This agrees with the lower mRNA levels found for the genes encoding glycolytic enzymes such as Glk, GntK, KguK and KguD. As a consequence, the ED pathway was predicted to be 1.5 times less active than in the wild type strain. This was further supported by the lower mRNA levels observed for the *eda* and *edd* genes (2-fold and 1.6-fold reductions respectively). Second, succinate dehydrogenase was predicted to efficiently handle the higher rate of succinate uptake observed experimentally. However, the large amount of carbon incorporated would lead to an overflow of the TCA and, consequently, up to 40% of the malate produced was predicted to be funnelled to pyruvate by the malic enzyme MaeB (Fig. 17B and Fig. 18). This *in silico* prediction suggests that malic enzyme acts as a safety valve providing a balance between the levels of oxaloacetate and acetyl-CoA, compounds required to launch the TCA. No higher flux through pyruvate carboxylase (*oadA*, *accC-2*) was predicted, making a significant return of carbon to TCA unlikely. However, although part of the extra pyruvate being produced might be used to compensate for reduced ED pathway activity, the final destiny of this extra pyruvate is unclear. Its oxidation in the TCA is unlikely since the oxygen uptake rates found experimentally were similar in both strains (Table 1). Another possibility is its conversion to polyhydroxyalkanoates (PHAs) as storage compounds. However, the synthesis of PHA granules is inhibited by the Crc/Hfq system during exponential growth (La Rosa et al., 2014), inhibition that would be exacerbated in the CrcZ/CrcY-null strain. Thus, we favour the possibility of the extra pyruvate being spilled as secreted by-products. The increased flux through the malic enzyme MaeB to render pyruvate contrasts with the lower expression of the *maeB* gene (1.9-times) in the CrcZ/CrcY-null strain relative to the wild type indicated by the RNA-seq assays. However, even assuming a moderate reduction in the levels of this enzyme, they are probably still high enough to accommodate the flux predicted from succinate to malate in the CrcZ/CrcY-null model.

Thus, flux analysis of the CrcZ/CrcY-null model under co-feeding conditions supports the idea of mild CCR for the wild type strain when it has moderately low levels of CrcZ and CrcY sRNA (Fig. 12). The inactivation of these sRNAs seems to have only a minor impact on flux distribution after the lag phase has been overcome (Fig. 17B). However, the artificial increase in CCR generated by the inactivation of the *crcZ* and *crcY* genes appears to favour the metabolism of succinate over that of glucose, as suggested by the growth (Fig. 11A-B) and nutrient uptake data (Table 1). Interestingly, under these conditions the *crcZ*/*crcY* knockout strain apparently makes less efficient use of the carbon sources, as inferred from the large increase succinate uptake leading to only a small increase in the growth rate (Table 1 and Fig. 11). This suggests a higher rate of metabolite secretion (spilling), which is in part reflected in the in-

creased leakage of GC (Table 1). Thus, a proper modulation of the effect of Crc/Hfq by the CrcZ/CrcY under these conditions seems critical for optimising the efficient use of the available carbon sources.

Influence of Crc on ATP, NADH and NADPH levels

Central carbon metabolism is the source of precursors for the biosynthesis of building blocks and for the production of energy that is used in the anabolic processes that allow cell maintenance and growth. Some key enzymes of central metabolism generate ATP, NADH and NADPH that can be directly used to facilitate endergonic reactions and to feed reducing equivalents to the electron transport chain. Succinate, after being channelled to the TCA cycle, is transformed to malate, which can be converted either to oxaloacetate, generating NADH and reduced quinones (Mdh/Mqo enzymes, see Fig. 17), or to pyruvate through malic enzyme (MaeB), generating NADPH. The metabolism of glucose and gluconate also generates building blocks and NADPH. For example, glucose-6-phosphate dehydrogenase (Zwf-1; transforms G6P to 6PGC) and 6PGC dehydrogenase (Gnd; oxidises 6PGC to feed the PPP pathway) directly generate NADPH. As explained above, constraint-based flux analysis predicts that the Crc-null strain should have a higher flux through the enzymes that convert malate to oxaloacetate via pyruvate, and an increased activity of the PPP pathway and connecting reactions (Fig. 17A). This predicts that the mutant strain may have increased amounts of NADPH. Experimental determinations showed that this is in fact the case, with levels doubling when Crc was lacking (Fig. 19). The flux model also predicted a small increase in the activity of the ATP synthases in the Crc-null strain, and in fact the amounts of ATP detected in this strain were twice those seen in the wild type (Fig. 19). For the CrcZ-CrcY-null strain, the model predicted no changes in the activity of the PPP pathway and an increased flux through the malic enzyme. This suggests NADPH levels might be increased less than in the Crc-null strain, which was again experimentally verified (Fig. 19).

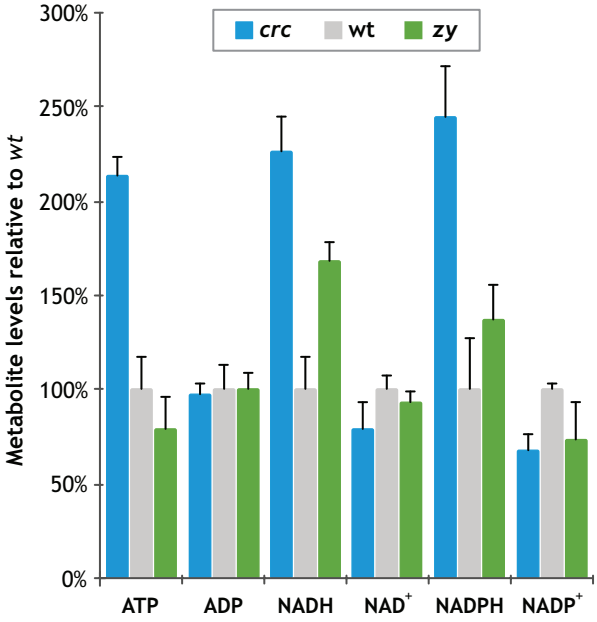

Fig. 19 Levels of ATP, ADP, NADH, NAD$^+$, NADPH and NADP$^+$
P. putida strain KT2440 (wild type) is indicated in light grey bars, its Crc-null derivative in light blue and its CrcZ/CrcY-null mutant derivative in green. Quantification was performed in cells cultivated in minimal salts medium containing both succinate and glucose, collected at mid-exponential phase (A_{600} = 0.6). Values are indicated as a percentage relative to the figure recorded for the wild type strain. Error bars indicate the standard deviation.

Conclusions

The present results show that succinate elicits a poor but detectable CCR response in *P. putida*, unlike the strong response this carbon source elicits in *P. aeruginosa,* a closely related species (MacGregor et al., 1992; Hester et al., 2000b; Valentini and Lapouge, 2013). Interestingly, the levels of the CrcZ and CrcY sRNAs, which are key elements in controlling CCR in *P. putida*, differed depending on whether cells were using succinate alone or with glucose. When succinate was the sole carbon source, CrcZ and CrcY sRNAs levels were relatively high, which is indicative of a weak Crc-dependent CCR. The same was true when glucose was the sole carbon source provided, although the growth rate attained was some 15% lower than that achieved with succinate. However, when both carbon sources were present, the amounts of CrcZ and CrcY decreased substantially, attaining levels indicative of a significantly Crc-dependent CCR (Fig. 12). Under these co-feeding conditions, cells co-metabolised both glucose and succinate, although the latter was consumed faster and the growth rate achieved was that corresponding to succinate when provided alone (Fig. 11 and Table 1). Flux analyses (Fig. 17), together with determinations of the metabolites consumed and excreted (Table 1), suggested that when both succinate and glucose are present, Crc organises a metabolism in which carbon compounds flow in opposite directions: from glucose to pyruvate on one hand, and from succinate to pyruvate on the other. Flux analyses also suggested that inactivating the *crc* gene leads to an increase in the amount of glucose being directed towards the PPP pathway, presumably because the transformation of 6PGC to pyruvate hits a bottleneck and metabolites are diverted to the PPP pathway. In fact, the Crc/Hfq system inhibits the expression of the genes involved in glucose uptake and in its initial transformation to 6PGC (del Castillo et al., 2007; Moreno et al., 2009b) this work); thus, inactivation the *crc* gene might facilitate an increase in the flow of glucose to 6PGC which, if inefficiently transformed to pyruvate, might be funnelled into the PPP pathway, a process likely facilitated by an increase in the level of G6P isomerase owed to the absence of Crc. Since this pathway serves to generate NADPH, stronger fluxes through the PPP pathway might be predicted to result in an increase in NADPH levels, as was in fact observed (Fig. 19). Flux analysis also indicated that the lack of the Crc protein allowed an increased flux of succinate towards pyruvate and oxaloacetate, processes that also generate NADPH.

Although flux analyses predicted that the inactivation of the *crc* gene would lead to a rise in the levels of ATP, NADH and NADPH over those seen in the wild type strain (increases that were experimentally observed), the metabolism of the cell became apparently less efficient. The growth rate decreased compared to the wild type strain, and more resources were apparently dedicated to the synthesis of ribosomal proteins despite the slower growth. When the CrcZ/CrcY-null strain, which has an artificially strong Crc/Hfq-dependent CCR, was initially cultivated in LB complete medium and then inoculated into minimal salts medium containing both succinate and glucose, the cells apparently ran into a metabolic conflict reflected in their inability to grow for several hours. After this lag time, the cells readapted their physiology in a way that is still unclear but that included Crc-dependent inhibition of the glucose uptake transport system (Fig. 15) and a much smaller impact on the expression of the low-affinity transporter for succinate (DctA; Fig. 16). Growth then resumed and glucose and succinate were

consumed simultaneously (Fig. 11C). About 33% of the glucose entering the cytoplasmic space was expelled back to the growth medium as GC, a value 50% higher than that observed for the wild type strain. However, part of the glucose was apparently metabolised, presumably entering the cell either as GC or 2KG, or through other unknown transporters switched on during the adaptation phase. Interestingly, succinate consumption was twice that seen in the wild type strain, suggesting that it was the main carbon source used, but this did not result in a growth rate significantly higher than that of the wild type. Overall, the results suggest that the activity of the Crc/Hfq regulatory system is carefully regulated by the CrcZ and CrcY sRNAs to optimise the co-metabolism of different carbon sources and to avoid imbalanced metabolic fluxes. The role of Crc -and consequently of CCR- is therefore wider than just favouring the assimilation of the most energetically favourable carbon source as commonly assumed; Crc also balances the fluxes of carbon compounds.

The results are consistent with the behaviour observed for *P. putida* KT2440 containing the TOL plasmid (which codes for a pathway for toluene assimilation) when confronted with a mixture of glucose and toluene. In this case, cells metabolised glucose and toluene simultaneously, although both substrates exerted a crossover CCR effect on the assimilation of the other compound (del Castillo and Ramos, 2007). The repression exerted by toluene on the expression of the glucose assimilation genes was reliant upon the Crc protein, while glucose repression of the toluene assimilation genes was channelled through the PtsN regulatory protein, but not through Crc. This observation is in line with previous reports on the way CCR controls the toluene assimilation genes (Cases et al., 1999; Velazquez et al., 2004; Aranda-Olmedo et al., 2006). The regulatory interplay between toluene and succinate was interpreted as indicating that cells counterbalance the amounts of total carbon taken up from each substrate, optimising the growth rate (del Castillo and Ramos, 2007). The present results also indicate that cells balance the flux of different carbon metabolites to optimise their growth and physiology, and that Crc has an important role in tuning this balance, even when working under a situation in which a large part of its influence is antagonised by the CrcZ and CrcY sRNAs.

Experimental procedures

Bacterial strains and culture media
Pseudomonas putida strains were cultivated at 30°C with vigorous shaking in LB medium (tryptone 10 g l^{-1}; yeast extract 5 g l^{-1}; NaCl 10 g l^{-1}), or in M9 minimal salts medium (Sambrook and Russell, 2001) with trace elements (Bauchop and Elsden, 1960) supplemented with either 20 mM succinate, 20 mM glucose, or both carbon sources at 20 mM each. The *P. putida* strains used were KT2440 (wild type) (Franklin et al., 1981), KTCRC (a KT2440 derivative containing an inactivated *crc* allele) (Hernandez-Arranz et al., 2013), and KT2440-ZY, which derives from KT2440 by deletion of the *crcZ* and *crcY* genes. This strain was obtained as previously described (Moreno et al., 2012), substituting the *crcZ* and *crcY* genes of strain KT2440 for inactivated *crcZ::tet* and *crcY::acc3* alleles using the suicide delivery plasmids pKNΔcrcZ-Tc and pKNΔcrcY-Gm (these are specifically designed for marker-exchange mutagenesis). The inactivation of *crcZ* and *crcY* in KT2440-ZY was confirmed by PCR. The absence of the corresponding sRNAs was assessed by real-time RT-PCR as described (Moreno et al., 2012). Antibiotics were added when needed at the following concentrations: tetracycline 10 μg ml^{-1} and gentamicin 10 μg ml^{-1}.

Analysis of extracellular metabolites
To determine the levels of extracellular metabolites in the culture supernatants, 1 ml of culture was taken at different times after inoculation and, after eliminating the cells by centrifugation, the supernatant was collected and frozen at -70°C until use. In all cases, three biological and two technical replicas were used. The rates of glucose and succinate consumption, as well as those of by-product formation, were determined by regression analysis during exponential growth. Glucose was quantified enzymatically using the Glucose (GO) Assay Kit (Sigma-Aldrich, St. Louis, USA) following the manufacturer's recommendations. Succinate concentration was determined using the succinic acid assay kit (Megazyme International Ireland, Bray, Ireland) following the microplate assay procedure indicated by the manufacturer. Gluconate was determined using the D-Gluconic Acid assay kit (Megazyme), employing the microplate assay procedure. Fumarate was quantified by high-pressure liquid chromatography (Gilson HPLC System), using an Aminex HPX-87H (Bio-Rad) column and a UV detector set at 210 nm. The liquid phase was 4 mM H_2SO_4 and the flow rate 0.6 ml/min at 55°C; dibasic sodium fumarate (Sigma-Aldrich) was used as a standard. HPLC was also used to evaluate the presence of fructose, pyruvate, formate, acetate, propionate and α-ketoglutarate in the culture supernatants.

Measurement of oxygen consumption
Pseudomonas putida strains KT2440, KTCRC and KT2440-ZY were grown in 50 ml flasks with strong aeration until reaching a turbidity (A_{600}) of 0.6. At this point, 0.5 ml of the cultures were diluted 1:2 with preheated fresh medium and the respiration rate measured using an oxygraph (Hansatech, United Kingdom) fitted with a Clark's type oxygen electrode, according to the manufacturer's instructions (Sevilla et al., 2013). The dry weight of the samples was used as the reference parameter. The consumption rate was expressed as mmol O_2 consumed per mg of cell dry weight per hour.

Analyses of intracellular compounds by gas chromatography-mass spectrometry
To determine the levels of ATP, ADP, NADH, NAD^+, NADPH and $NADP^+$ in the cells, liquid chromatography-tandem mass spectrometry was used as previously described (Luo et al., 2007; Fuhrer and Sauer, 2009). Briefly, 1 ml samples were withdrawn from exponentially growing cultures at an A_{600} of 0.6 and harvested by centrifugation at 14,000 x *g* for 20 sec. Cell pellets were immediately frozen in liquid N_2 until use. To prepare the samples for gas chromatography, the pellets were melted and subjected to extraction three times with 0.5 ml of 10 mM ammonium acetate (pH 7.2) in 60% ethanol at 70°C for 1 min. The supernatants were completely dried in a speed vac at 30°C and resuspended in 100 μl of 10 mM ammonium acetate (pH 7.2). Samples were analysed using a Varian HPLC system coupled with a triple quadrupole system (Varian LC/MS 1200L). Chromatographic separation was achieved using a Bruker Intensity Trio C18, 150 mm x 2.0 mm ID, S-3 μm, 12 nm column at a temperature of 45°C. The injected volume was 5 μl, and the mobile phase, at a flow rate of 200 μl/min, was a gradient of solutions A (100% methanol) and B (10 mM tributylamine, 15 mM acetate in 5% methanol). The gradient profile was: 0 min, 2% A; 0.6 min, 2% A; 0.8 min, 15% A; 4 min, 50% A; 6 min, 60% A; 8 min, 98% A; and 10 min, 98% A. Multiple-reaction monitoring settings were optimised individually for each metabolite. All samples were analysed using three biological and two technical replicates. HPLC-MS analyses were per-

formed at the Research Interdepartmental Service (SIdI) of the Autonomous University of Madrid, Madrid, Spain.

Real-time reverse-transcription PCR
Cells were grown in aerated flasks in the specified medium at 30ºC. At mid-exponential phase (A_{600} = 0.6), or at early stationary phase (A_{600} = 2.5), the cells were centrifuged and the pellets frozen at -70ºC. RNA was purified from each pellet using the RNeasy RNA purification kit (QIAGEN, Hilden, Germany) following the manufacturer's instructions. RNA integrity was checked by agarose gel electrophoresis. For the complete elimination of any contaminant DNA, RNA was treated with the RNase-Free DNase Set (QIAGEN, Inc., Valencia, CA, USA) and RNase-free DNase I (Turbo DNA-free, Ambion, Lifetechnologies, Grand Island, New York, USA) kits as specified by the supplier. The absence of DNA in the RNA samples was checked by real-time PCR as described earlier (Morales et al., 2006), using oligonucleotides for the *rpoN* gene. Three independent assays were performed. RNA samples (8 μg) were converted to cDNA by reverse transcription using the High Capacity cDNA kit (Applied Biosystems, Foster City, California, USA). Real-time PCR was performed using the SYBR Green PCR master mix (Applied Biosystems) and 0.2 μM of each primer in a 7500 Real-time PCR thermocycler (Applied Biosystems). The expression profile of CrcZ and CrcY was analysed by absolute quantitation using 25 ng and 0.25 ng of cDNA template. Standard curves were constructed by serial 10-fold dilutions of *P. putida* KT2440 genomic DNA, to obtain samples containing from 10^2 to 10^7 copies. The extension of PCR products was performed at 60°C. The primers used in the RT-PCR assays were 5'-acaaccaggcagagaacaacaa and 5'-cacgttgatctgtcgatccaa for *crcZ*, 5'-aaagcaggtcagcgctcaaa and 5'-tcggcttgtcctggtgttg for *crcY*.

Deep sequencing of transcripts
Cells were grown in aerated flasks containing M9 minimal salts medium supplemented with 20 mM succinate and 20 mM glucose as carbon sources. When the cultures reached a turbidity of 0.6 at 600 nm, cells were collected at 4ºC and immediately frozen at -70°C. Total RNA from each sample was purified using the RNeasy kit (QIAGEN). The RNase-Free DNase Set (QIAGEN) was used for the complete elimination of residual DNA from the samples. The quality of the RNAs was examined using an Agilent 2100 Bioanalyzer (Agilent Technologies, Inc., USA). RNA library construction and deep-sequencing were carried out by BGI (Shenzhen, China) using the Illumina mRNA sequencing sample preparation kit (cat. #RS-930–1001) and the Illumina HiSeq™ 2000 system (Illumina, Inc., San Diego, CA, USA). Reads generated by the sequencing machines were cleaned and mapped to the database of *Pseudomonas* gene sequences (NCBI reference sequence NC_002947, version NC_002947.3) using SOAP2 software (v. 2.21) (Li et al., 2009), and the resulting alignment visualised using IGV (Thorvaldsdottir et al., 2013) and Fiesta software (Oliveros, 2007). Two biological replicates of each sample were sequenced. More than $12x10^6$ reads were obtained for each sample, corresponding to $1.1x10^9$ base pairs sequenced, rendering an overall coverage of 177x (about 1 Gb of clean data). Fold-change and *P* values were calculated as described (Audic and Claverie, 1997); the *P* values were corrected by FDR (Benjamini et al., 2001). Genes with an RPKM value of <10 were considered not expressed. Genes with an absolute fold change of 1.8 (up or down) and an FDR of ≤0.001 were considered differentially expressed. The complete raw dataset is available at the Gene Expression Omnibus site of the NCBI (http://www.ncbi.nlm.nih.gov/geo) under accession code GSE63987.

Constraint-based analyses of metabolic fluxes
The model used for constraint-based analysis, named *i*JN1411 (J. Nogales, in preparation), is an updated version of model *i*JN746 for *P. putida* KT2440 (Nogales et al., 2008). *i*JN1411 accounts for 2826 metabolic and transport reactions, 2087 metabolites and 1411 genes, and provides the best available representation of *P. putida* metabolism. The growth of cells in a classical minimal salts medium under aerobic conditions was simulated *in silico* by allowing the free exchange of CO_2, H_2O, H^+, HCO_3^-, Na^+, NH_4^+, Pi, Fe^{2+} and SO_4^{2-} (Nogales et al., 2008). Flux balance analysis (Varma and Palsson, 1995; Orth et al., 2010) was used to make growth rate predictions and to determine initial flux distributions. Flux balance analysis is based on solving linear optimisation problems by maximising or minimising a given objective function **Z** subject to a set of constraints. The constraint $\mathbf{S \cdot v = 0}$ corresponds to a situation of steady-state mass conservation where the change in concentration of the metabolites as a function of time is zero. "S" is an *m* x *n* matrix containing all the stoichiometric coefficients in the model of *m* metabolites and *n* reactions, and the vector "v" has *n* elements that represent the individual flux values for each reaction. These fluxes

are additionally constrained by the imposed lower and upper limits "vl" and "vu". The output is a flux distribution that maximises or minimises the objective function. The growth rate was used as an objective function. All computational simulations were performed using the COBRA toolbox (Schellenberger et al., 2011) in the MATLAB environment (The MathWorks Inc.). Linear optimization problems were solved using the GNU Linear Programming Kit (GLPK) (http://www.gnu.org/software/glpk).

To construct condition specific metabolic models, the uptake rates of succinate and glucose experimentally determined for each strain, as well as the fumarate and gluconate secretion rates (Table 1), were used in *i*JN1411 as additional constraints. In addition, the gene expression datasets (mRNA levels) collected for each individual strain by RNA-Seq analyses were incorporated to constrain even further the solution space using the Gene Inactivity Moderated by Metabolism and Expression (GIMME) algorithm in COBRA Toolbox v2.0 (Schellenberger et al., 2011). As input, GIMME uses genome-scale reconstructions and expression data mapped on reactions, and builds reduced models by removing those reactions not available in the expression dataset while maintaining model functionality (e.g., *in silico* growth). It should be noted that GIMME considers which genes are expressed or not, but not the modifications in mRNA levels under different experimental conditions. A given gene was considered expressed when its RNA levels in the RNA-seq analysis were ≥10 RPKM.

The distribution of feasible fluxes in the condition-specific models was calculated using Markov chain Monte Carlo sampling (Schellenberger and Palsson, 2009) implemented in COBRA Toolbox v2.0 (Schellenberger et al., 2011). The objective function was unconstrained, allowing the computation of flux distributions independently of growth rates. The feasible flux distribution was obtained using the artificially centred *hit-and-run* algorithm as described previously (Lewis et al., 2010). For the wild type, Crc-null and CrcY/CrcZ-null models, mixed fractions of 0.529, 0.520 and 0.519 were respectively obtained, indicating that the solution space for each condition-specific model was uniformly sampled. The differential reaction activity was computed by assuming that the distributions of feasible fluxes for a given reaction (obtained from Markov chain Monte Carlo sampling) under two different conditions do not significantly overlap (Nam et al., 2014). The median value from the distribution was used as the most probable flux value.

Chapter 3

The Crc protein inhibits the production of polyhydroxyalkanoates under balanced carbon/nitrogen growth conditions

This chapter has been published as indicated below, but incorporates updates related to recents findings showing that Hfq binds the CA motifs present in Crc-regulated mRNAs (Moreno et al., 2015).

La Rosa, R., de la Pena, F., Prieto, M.A., and Rojo, F. (2014) The Crc protein inhibits the production of polyhydroxyalkanoates in *Pseudomonas putida* under balanced carbon/nitrogen growth conditions. *Environ Microbiol* **16**: 278-290.

Introduction

Free-living bacteria are frequently exposed to fluctuations in the availability of nutrients that can lead to nutritional imbalance. They respond to these changes with the help of regulatory mechanisms in order to adapt their metabolism accordingly. When carbon sources are present in excess but other inorganic nutrients (e.g. nitrogen) become limiting, many bacteria synthesize compounds such as polyhydroxyalkanoates (PHAs), triacylglycerols, wax esters or glycogen, which are stored as granules in the cytoplasm (Waltermann and Steinbuchel, 2005; Ren et al., 2010; Wilson et al., 2010). When the supply of the limiting nutrient is restored, the storage polymers can be depolymerised and used as carbon and energy sources. However, PHA metabolism is not a unidirectional process in which the PHA is either polymerised or depolymerised, but a bi-directional process in which there is a continuous cycle of synthesis and degradation. This helps adapt the carbon flow to the transient demand for metabolic intermediates, thus balancing carbon resources and better guaranteeing efficient growth (Ren et al., 2009; de Eugenio et al., 2010a; Ren et al., 2010; Escapa et al., 2012; Arias et al., 2013). This could be of great advantage in competitive niches in which nutritional conditions change rapidly.

PHAs are polyesters with physicochemical properties similar to those of plastics, with the advantages that they can be produced from renewable materials and can be biodegraded by microorganisms (Madison and Huisman, 1999; Luengo et al., 2003; Chen, 2009). PHAs have diverse properties depending on their structure, which in turn depends on the specific growth condition in which they are produced and on the bacterial species used. PHAs are biocompatible and potentially useful in medical applications such as production of sutures, scaffolds and implants, for controlled drug delivery and more simply for packaging purposes. The economic viability of their large-scale synthesis requires the detailed understanding and subsequent optimisation of their production and purification, areas in which significant progress has been made in the last years (Olivera et al., 2001; Luengo et al., 2003; Chen and Kazlauskas, 2011).

The synthesis of PHAs has been extensively studied in *Pseudomonas putida* KT2440 and recombinant strains with different genetic background are already used in large scale PHAs productions. Depending on the carbon source provided, *P. putida* can produce distinct types of medium-chain length PHAs. Due to its metabolic and genetic versatility *P. putida* is able to use different carbon sources for the synthesis of the polymer: fatty acids, glycerol, sugars and raw materials of different origin (Kenny et al., 2012; Escapa et al., 2013; Muhr et al., 2013; Poblete-Castro et al., 2014a; Poblete-Castro et al., 2014b). An exhaustive list of PHAs produced by distinct *P. putida* strains is presented in (Prieto et al., 2014). The PHA polymer is composed by a chains of (R)-3-hydroxyacyl-CoA monomers (Huisman et al., 1991) that can be derived from the β-oxidation, if fatty acids are used as carbon sources, or via *de novo* synthesis, if non-fatty acid related carbon sources are used (Escapa et al., 2012; Poblete-Castro et al., 2012; Escapa et al., 2013). PHAs are usually produced with highest yields when an imbalance between carbon and nitrogen sources is imposed, but they are produced as well, at lower yields, under balanced carbon/nitrogen conditions (Poblete-Castro et al., 2012). This points out the central role of PHAs as metabolic intermediates used by cells to optimize and regulate carbon metabolism when carbon sources are in excess.

In *P. putida* KT2440, the synthesis and degradation of PHAs depends on the genes of the *pha* cluster, which is organized into two operons, *phaC1ZC2D* and *phaIF* (Prieto et al., 2007; de Eugenio et al., 2010b) (Fig. 20).

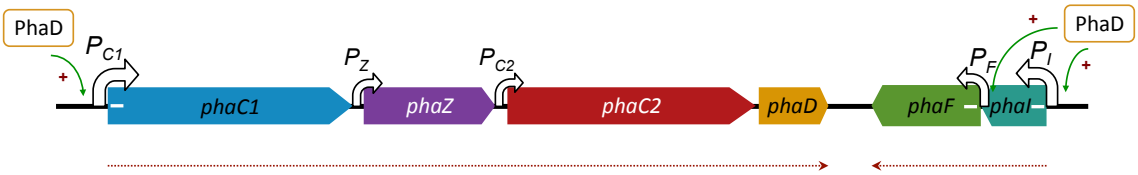

Fig. 20 Genetic organization of the *pha* cluster.
Bent open arrows indicate the position and orientation of the promoters P_{C1}, P_Z, P_{C2}, P_F and P_I, from which the *pha* genes are transcribed. The dashed lines indicate the *phaC1ZC2D* and *phaIF* polycistronic mRNAs which transcription depends on PhaD regulator.

The *phaC1* and *phaC2* genes code for two PHA polymerases that incorporate (R)-3-hydroxyacyl-CoA monomers into the PHA polymer (Huisman et al., 1991). Under laboratory conditions the PhaC1 polymerase is expressed at higher level and is the principal polymerase implied in granule formation (de Eugenio et al., 2010b). The *phaZ* gene codes for a depolymerase that allows the hydrolysis of PHAs; the products can then be fed into central metabolism (Fig. 21) (de Eugenio et al., 2007; de Eugenio et al., 2010a). PHA granules or carbonosomes are believed to be covered with a single layer of phospholipids, on the surface of which are found the PHA polymerases, the PHA depolymerase, the phasins PhaI and PhaF, and other proteins, such as the acyl-CoA synthetases (ACS1) that are related to monomer synthesis. Phasins serve as an interface between the granule and the cytoplasm, and are believed to facilitate other processes such as localization and segregation of the granules during cell division (Galan et al., 2011; Maestro et al., 2013; Jendrossek and Pfeiffer, 2014) (Fig. 21).

The expression of the *pha* genes relies on five promoters, P_{C1}, P_Z, P_{C2}, P_I and P_F ((de Eugenio et al., 2010b); see Fig. 20). The most active promoters, P_{C1} and P_I, are controlled by the PhaD protein, a transcriptional activator that responds to the presence of fatty acids in the growth medium (de Eugenio et al., 2010b). It is believed that the true effector of PhaD might be a CoA-intermediate of the fatty acid β-oxidation pathway. Promoters P_Z, P_{C2} and P_F are less active and do not respond to PhaD. Their role may be to ensure appropriate basal expression of the *phaZ*, *phaC2*, *phaD* and *phaF* genes when PHAs are produced at lower levels.

Some evidence suggests that the expression of the *pha* genes is under the influence of global regulatory networks, although the information available on this is very limited (Prieto et al., 2007; Velazquez et al., 2007; de Eugenio et al., 2010b; Ryan et al., 2013). Carbon Catabolite Repression, due to its role on regulation and optimization of metabolism, is one of the major global regulatory networks that could control and regulate the fluxes of carbon sources toward the synthesis or degradation of PHAs. Indeed sequences resembling the CA motifs can be predicted close to the translation initiation regions of the *phaC1*, *phaI* and *phaF* genes ((Browne et al., 2010); this work; Fig. 22). Therefore, the Crc/Hfq regulatory system might modulate the synthesis of PHAs, although experimental evidence was lacking.

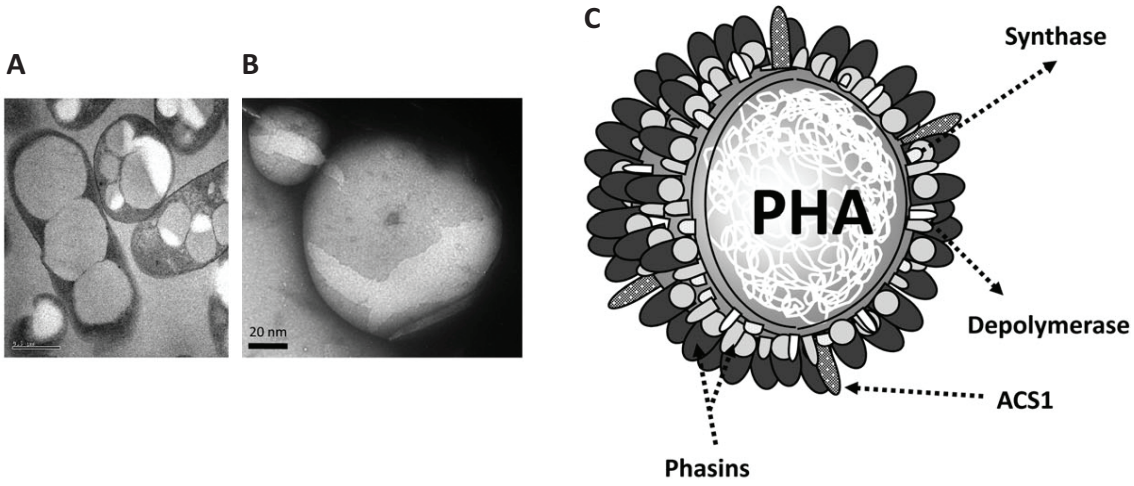

Fig. 21 The polyhydroxyalkanoate granules of *P. putida* KT2442.
(**A, B**) TEM images of mcl-PHA-producing cells (**A**) and of a PHA granule (**B**) from *P. putida* KT2442. (**C**) Model of PHA granule structure. Granules are composed of PHA coated by a monolayer of phospholipids and granule associated proteins (GAPs). The most abundant GAPs are the phasins, encoded by the *phaI* and *phaF* genes. The polymerases (or synthases) encoded by the *phaC1* and *phaC2* genes, the depolymerase encoded by the *phaZ* gene, and the acyl-CoA synthetase (ACS1), are also associated to the granule. Modified from (Galan et al., 2011).

The present work examines whether the Crc/Hfq proteins can recognize the CA motif present on *phaC1*, *phaI* and *phaF* mRNAs and if they can regulate translation of these genes. Moreover, the effect of inactivating the *crc* gene on the production and accumulation of PHAs in cells cultivated in different growth media was investigated. The influence of the carbon/nitrogen (C/N) ratio on CrcZ and CrcY sRNAs levels was also analysed to further examine the impact of Carbon Catabolite Repression on PHA synthesis.

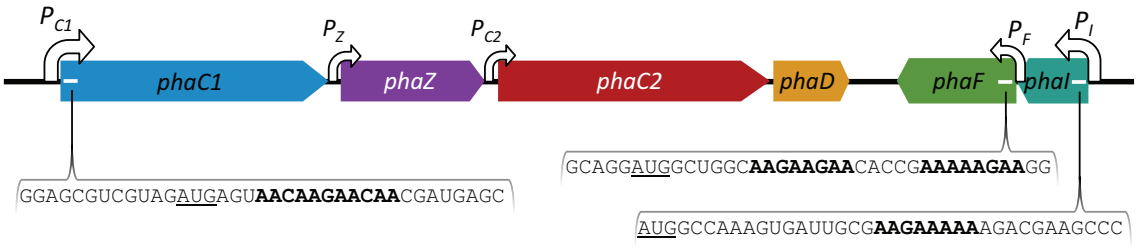

Fig. 22 Presence of sequences resembling CA motifs on the mRNA of genes of the *pha* cluster.
Bent open arrows indicate the position and orientation of the promoters P_{C1}, P_Z, P_{C2}, P_F and P_I, from which the *pha* genes are transcribed. The small white boxes on the *phaC1*, *phaF* and *phaI* genes denote the position of the presumed CA motifs indicative of Crc/Hfq-mediated catabolite repression; the sequence of the corresponding regions is indicated below, highlighting the CA motif (in bold) and the AUG initiation codon (underlined).

Results

Binding of the Crc/Hfq proteins to the translation initiation regions of *phaC1*, *phaI* and *phaF* mRNAs

The Hfq protein, with the help of Crc, is able to recognize and bind RNA molecules containing the unpaired AAnAAnAA motif (CA motif) typically located at, or close to, the translation initiation site of target mRNAs (Moreno et al., 2007; Moreno and Rojo, 2008; Moreno et al., 2009a; Sonnleitner and Blasi, 2014; Madhushani et al., 2015; Moreno et al., 2015). The mechanism through which Crc helps Hfq to bind RNA is still not fully understood, although it may imply an increase in the binding affinity of Hfq for the CA motifs. The *phaC1*, *phaF* and *phaI* genes contain sequences similar to a CA motif immediately downstream of the AUG start codon, within the coding region. In *phaF*, two such sites seem to be present separated by 5 nucleotides (Fig. 22). Purified Hfq protein can bind in vitro to short RNA oligonucleotides that contain a proper recognition sequence, process that is much more efficient in the presence of the Crc protein (Moreno et al., 2007; Moreno et al., 2009a; Moreno et al., 2015). The ability of the Crc/Hfq proteins to bind to the presumed sites at these three genes was tested in RNA band-shift assays using 26 nt-long radiolabelled RNA oligonucleotides containing the corresponding CA motifs (Fig. 23E). Two Crc protein preparations were used. The first one contained a Crc(6xHis) derivative and small amounts of the *E. coli* Hfq protein, which co-purifies with Crc(6xHis) and acts similarly to that of *P. putida* (Moreno et al., 2007). The second one included an untagged Crc that cannot bind RNA by itself, but helps the purified *P. putida* Hfq protein to bind RNA (Madhushani et al., 2015; Moreno et al., 2015). The Crc(6xHis)/Hfq mixture was able to bind the RNA oligonucleotide containing the *phaC1* target, generating a ribonucleoprotein complex (Fig. 23A). The addition of >100-fold excess of the same unlabelled oligonucleotide (indicated as 'Sp') led to the efficient inhibition of binding to the radiolabelled oligonucleotide. Moreover, no inhibition was seen when the same amount of an unrelated RNA fragment lacking a CA target (indicated as 'nSp' in A, and as 'Control' in B) was added (Fig. 23A). This shows that Crc/Hfq binding to the *phaC1* probe is specific. The ability of the purified untagged Crc and/or untagged Hfq proteins to bind the target RNA probes, when present individually or in combination, was also tested. As shown in Fig. 23B, binding to the *phaC1* RNA probe occurs only when both proteins are present. The Crc(6xHis)/Hfq mixture, instead, bound very poorly to the RNA oligonucleotides corresponding to *phaI* and *phaF* (Fig. 23C-D). Although some reduction in the amount of free RNA was detected, and a faint band corresponding to an ribonucleoprotein complex was visible at the highest Crc(6xHis)/Hfq concentrations tested, the affinity for these targets was very low. All together, these results suggest that Crc/Hfq could regulate translation of *phaC1* mRNA, but not that of *phaI* and *phaF* mRNAs.

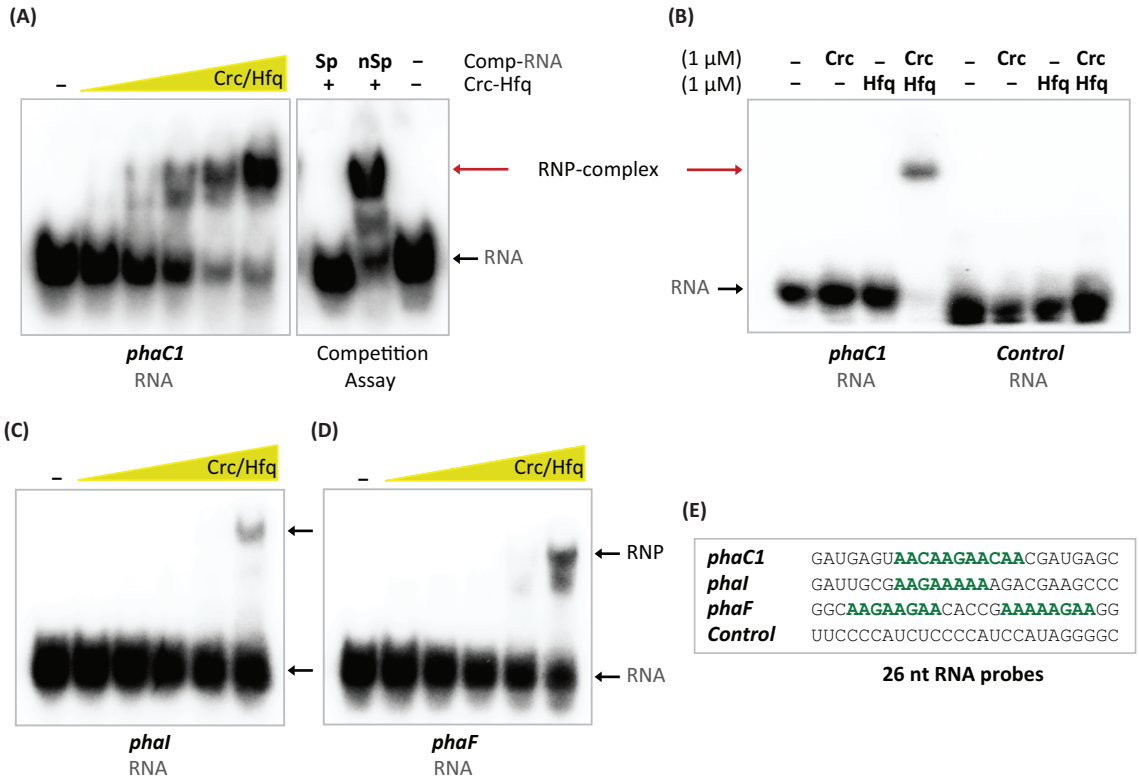

Fig. 23 Binding of Crc/Hfq to RNA oligonucleotides containing the putative CA motifs at *phaC1*, *phaI* and *phaF* mRNAs.
The ability of a Crc(6xHis)/Hfq mixture (93, 187, 375, 750 or 1500 nM) to bind *phaC1* (**A**), *phaI* (**C**) and *phaF* (**D**) radio-labelled RNA oligonucleotides was determined using band-shift assays. The binding specificity of the Crc(6xHis)/Hfq mixture to *phaC1* was determined in competition assays (**A**), performing the binding reactions in the presence of a >100-fold excess of the unlabelled *phaC1* RNA oligonucleotide (indicated as 'Sp'), or of an unlabelled RNA oligonucleotide lacking a CA motif (indicated as 'nSp' in A or 'Control' in B). The Crc(6xHis)/Hfq mixture was added at 750 nM. (**B**) The ability of the untagged Crc and/or untagged Hfq to bind the *phaC1* and the *Control* RNAs was tested using 1 µM of Crc and Hfq (expressed as Crc monomers and Hfq hexamers). (**E**) Sequences of the RNA oligonucleotides used (the CA motif is indicated in green). RNP indicates "ribonucleoprotein complex".

Crc/Hfq inhibit translation of *phaC1* mRNA, but not that of *phaI* and *phaF* mRNAs

The ability of Crc/Hfq to regulate the translation of the *phaC1*, *phaI* and *phaF* mRNAs, *in vivo*, was analysed using translational fusions of these genes to the *lacZ* reporter gene, fusions that contain the putative CA motifs (Fig. 24A; Fig. 26). The *phaC1'-'lacZ* fusion included the P_{C1} promoter and the downstream sequences up to the 11th codon of *phaC1*, followed by *lacZ* in-frame (Fig. 24B; 'Translational fusion'). The *phaI'-'lacZ* and *phaF'-'lacZ* fusions included the P_I or P_F promoters, respectively, plus the downstream sequences up to the 13th codon of *phaI* or *phaF*, followed by *lacZ* (Fig. 26). These three fusions were individually inserted into the Tn7 *att* site in the chromosome of *P. putida* strains KT2442 (wild type for *crc*) and KT2442-C1 (derived from KT2442 but containing an inactivated *crc::tet* allele), using a Tn7-based delivery system, as previously described (Silva-Rocha and de Lorenzo, 2011, 2014). The integration of the fusions at the Tn7 *att* site was verified by PCR assays (not shown). The obtained strains derived from KT2442 were named PC1 (containing the *phaC1'-'lacZ* fusion), PI (containing the

phaI'-'lacZ fusion) and PF (containing the *phaF'-'lacZ* fusion). Those derived from KT2442-C1 were named PC1C, PIC and PFC, respectively. The β-galactosidase activity of all these strains was tested in cells growing in complete LB medium, in LB supplemented with 10 mM octanoic acid (which induces PHA production), and in the minimal salts media 0.1N M63 and 1N M63, both supplemented with octanoic acid as the sole carbon source. The 0.1N M63 medium has an imbalanced C/N ratio (15 mM octanoic acid and 1.5 mM ammonium sulphate, resulting in a 40-fold molar excess of carbon relative to nitrogen), and is commonly used to study PHA production. In medium 1N M63, the carbon and nitrogen sources are balanced (7.5 mM octanoic acid and 15 mM ammonium sulphate; C/N ratio = 2) and PHAs are still produced but at lower level.

As previously indicated, the Crc/Hfq-dependent CCR is very strong when cells grow exponentially in a complete medium such as LB (Yuste and Rojo, 2001; Moreno et al., 2012; Valentini et al., 2014). If Crc/Hfq inhibit *phaC1*, *phaI* and *phaF* translation, the strains containing the inactive *crc::tet* allele should show higher β-galactosidase activity during exponential growth in LB than those with a wild type *crc* gene. In the cells harbouring the *phaC1'-'lacZ* fusion, low β-galactosidase activity was observed both in the presence (strain PC1) and absence (strain PC1C) of a functional Crc protein, although the activity observed in strain PC1C was twice that recorded for strain PC1 (Fig. 24A). The addition of octanoic acid to the growth medium clearly increased the levels of β-galactosidase, although the presence of a functional Crc protein reduced these to about one fifth those recorded when Crc was absent. The inhibitory effect of Crc vanished when the cells reached the stationary phase of growth (not shown), as previously reported. When cells were cultivated in the imbalanced 0.1N M63 medium containing octanoic acid, the activity of the *phaC1'-'lacZ* fusion was much greater than in the LB medium, and the Crc/Hfq system seemed to have no effect. In the balanced 1N M63 medium, however, the presence of a functional Crc protein reduced the β-galactosidase activity to less than half that seen in the *crc*-mutant strain. These results support the idea that Crc/Hfq inhibit the translation of *phaC1*, an effect that would be detected in the complete LB medium or in the mineral salts medium containing a balanced C/N ratio, but not in the imbalanced medium.

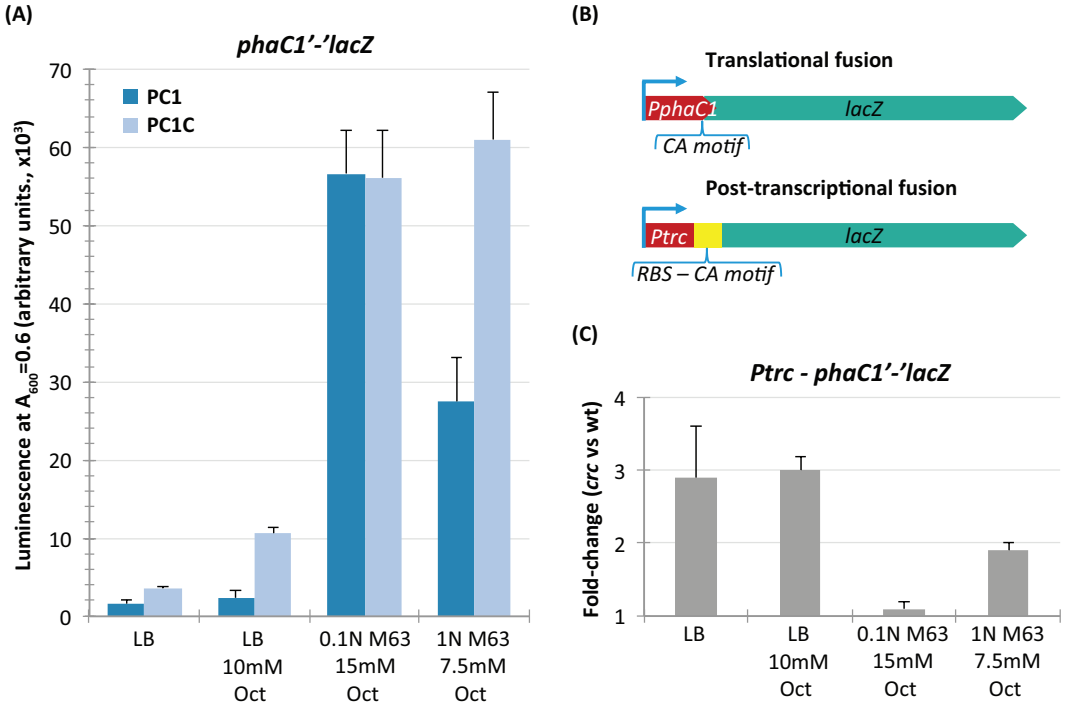

Fig. 24 Effect of Crc on the translation of *phaC1* mRNA *in vivo*.
The effect of Crc on the translation of *phaC1* mRNAs was determined using translational fusions of *phaC1* to the *lacZ* reporter gene (**A**) or using a post-transcriptional fusion in which the *phaC1'-'lacZ* translational fusion is expressed from the inducible and heterologous *Ptrc* promoter (**C**). (**B**) Schematic representation of the translational and post-transcriptional fusion of *phaC1* to *lacZ* reporter gene. In 'A' the bacterial strains used were PC1 (contains a *phaC1'-'lacZ* fusion and a wild-type *crc* gene) and PC1C (contains the *phaC1'-'lacZ* fusion and an inactive *crc::tet* allele). In 'C' *P. putida* strains KT2442 (wild-type) and KT2442-C1 (*crc*-mutant) contain the pC1PT plasmid that includes the *Ptrc-phaC1'-'lacZ* post-transcriptional fusion. (**C**) The figure shows the β-galactosidase activity observed in each case in the *crc*-mutant strain relative to that seen in the wild-type strain, expressed as fold-change. The β-galactosidase activity was evaluated in the absence or presence of 0.5 mM IPTG to induce transcription from the *Ptrc* promoter; the activity detected in the absence of IPTG was very low and is not indicated. In all cases cells were cultivated in LB, LB supplemented with 10 mM octanoic acid (LB Oct), 0.1N M63 containing 15 mM octanoic acid, or 1N M63 containing 7.5 mM octanoic acid. When cultures reached mid-exponential phase (A_{600} of 0.6), samples were collected, and the β-galactosidase activity was measured. Results correspond to the average of three independent assays; the standard deviation is indicated.

To further investigate whether Crc/Hfq inhibit the translation of *phaC1* mRNA, a plasmid was constructed containing a post-transcriptional reporter fusion, schematised in Fig. 24B (post-transcriptional fusion), in which the *phaC1'-'lacZ* translational fusion is immediately downstream of the heterologous *Ptrc* promoter, the activity of which can be induced by the addition of IPTG (isopropyl-β-D-thiogalactopyranoside). Since this construction lacks the native P_{C1} promoter, the expression of *phaC1'-'lacZ* is uncoupled from its native transcriptional regulator PhaD, therefore allowing to discard any possible indirect effect of Crc mutation on the transcription of *phaC1'-'lacZ*. The plasmid, named pC1PT, was introduced into *P. putida* strains KT2442 (wild type for *crc*) and KT2442-C1 (*crc*-mutant derivative). Cells were cultivated in LB medium or in M63 media as indicated previously. In the absence of IPTG, the levels of β-galactosidase detected were very low (data not shown). In the presence of 0.5 mM IPTG, expression of the *phaC1'-'lacZ* fusion was efficiently induced in all growth media tested. However, when cells were cultivated in LB, regardless of the presence or absence of octanoate, the

levels of β-galactosidase detected in the wild type strain at mid-exponential phase (A_{600} of 0.6) were about threefold lower than those seen in the *crc*-mutant strain. A clear but lower inhibitory effect of Crc/Hfq (about 2-fold) was also detected in the 1N M63 medium; no inhibition was detected when cells were cultivated in the 0.1N M63 medium (Fig. 24C). These results further support that Crc/Hfq inhibits translation of *phaC1* mRNA in a condition specific manner.

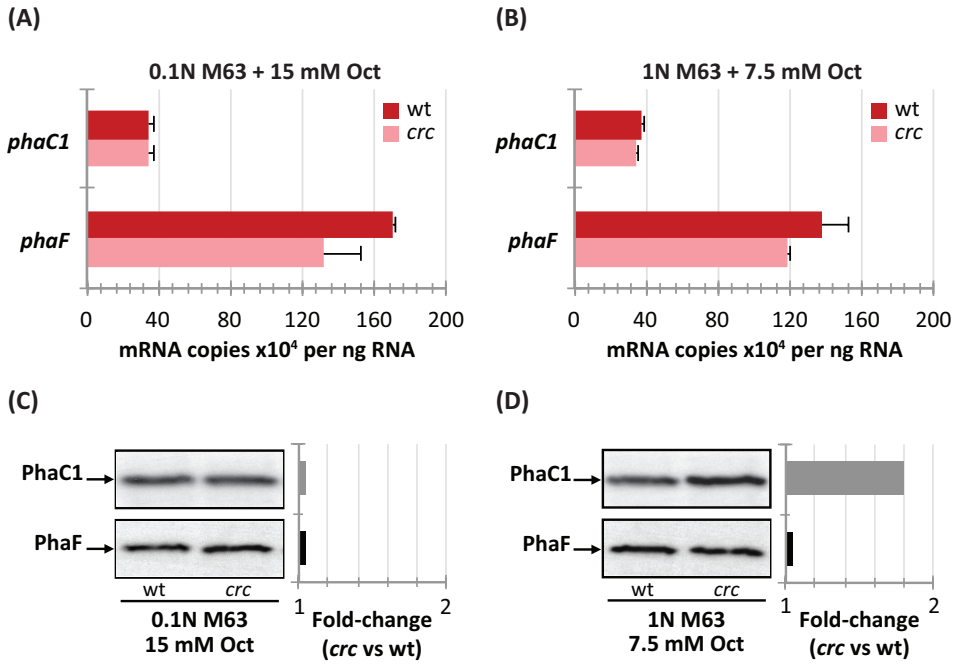

Fig. 25 Influence of Crc on the abundance of *phaC1* and *phaF* mRNAs and of PhaC1 and PhaF proteins.
(**A**, **B**) The levels of *phaC1* and *phaF* mRNAs in *P. putida* strains KT2442 (indicated as wt, red bars) and KT2442-C1 (indicated as *crc;* pink bars) were determined by real-time RT-PCR using total RNA samples obtained from cells growing exponentially (A_{600} = 0.6) in 0.1N M63 containing 15 mM of octanoic acid and in 1N M63 containing 7.5 mM octanoic acid. The values shown correspond to mRNA copies per ng of RNA. The standard deviation is indicated. (**C**, **D**) Total proteins from *P. putida* strains KT2442 (indicated as wt) and KT2442-C1 (indicated as *crc*), obtained from cells growing exponentially (A_{600} = 0.6) in 0.1N M63 and 1N M63 medium, were resolved by electrophoresis in a SDS-polyacrylamide gel. The presence of PhaC1 and PhaF proteins was detected by Western blotting using polyclonal antisera directed towards each of these two proteins. Proteins were revealed by chemiluminescence. The graph on the right shows the ratio of the signal intensity detected for each protein in the *crc* mutant strain relative to that detected in the wild-type strain.

To exclude any effect of the *crc* mutation on the transcription of *phaC1*, the amount of its mRNA was determined by real-time RT-PCR in strains KT2442 and KT2442-C1 cultivated in 0.1N M63 and in 1N M63 media supplemented with 15 mM and 7.5 mM, respectively, of octanoic acid. As shown in Fig. 25A-B, under the conditions tested the abundance of *phaC1* mRNA was very similar in the two strains. However, the use of a polyclonal antiserum directed against PhaC1 showed that the levels of PhaC1 protein were almost twice higher in the *crc*-deficient strain than in the wild type strain in 1N M63 medium (Fig. 25D). As expected, the same amount of PhaC1 protein was detected in 0.1N M63 medium (Fig. 25C). This indicates that Crc/Hfq inhibits the translation, but not the transcription, of *phaC1* under appropriate

growth conditions, and is consistent with the previous results obtained using the translational and post-transcriptional fusions (Fig. 24).

In accordance with the RNA shift assays, a different outcome was obtained when analysing Crc effect on the translation of *phaF* and *phaI* mRNAs. Irrespective of the growth medium used, the presence of Crc was unable to reduce the β-galactosidase activity of the *phaI'-'lacZ* and *phaF'-'lacZ* translational fusions (Fig. 26A-B). Moreover the levels of *phaF* mRNA (Fig. 25A-B) and PhaF protein (Fig. 25C-D) in cells growing in the 0.1N M63 and 1N M63 medium were similar in the *crc*-deficient and in the wild type strain, as determined respectively by real time RT-PCR and by western blot analysis using an anti-PhaF polyclonal antiserum (Fig. 25). Altogether these results suggest that Crc/Hfq system is unable to repress the translation of *phaI* and *phaF* mRNAs in all the conditions tested.

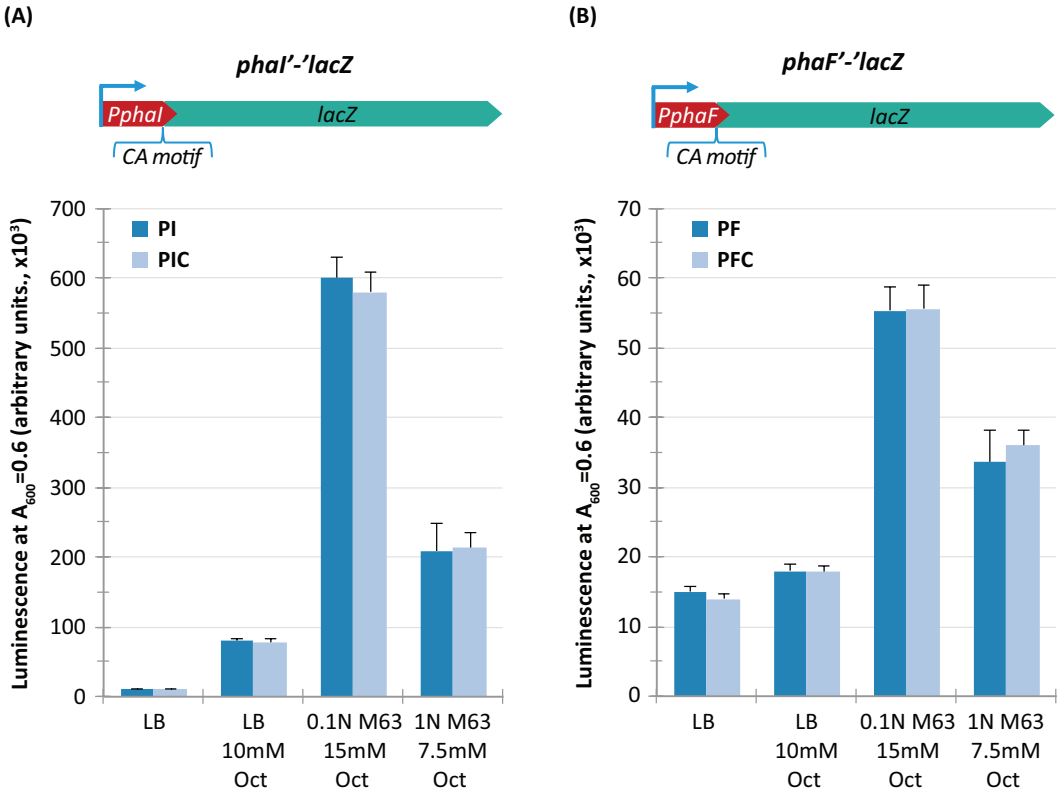

Fig. 26 Effect of Crc on the translation of *phaI* and *phaF* mRNAs.
The effect of Crc on the translation of *phaI* and *phaF* mRNAs was determined using translational fusions of *phaI* (**A**) and *phaF* (**B**) to the *lacZ* reporter gene. The schematic representation of the translational fusion is indicated. The bacterial strains used were PI (contains a *phaI'-'lacZ* fusion and a wild-type *crc* gene) and PIC (contains the *phaI'-'lacZ* fusion and an inactive *crc::tet* allele) and PF (contains a *phaF'-'lacZ* fusion and a wild-type *crc* gene) and PFC (contains the *phaF'-'lacZ* fusion and an inactive *crc::tet* allele). In all cases cells were cultivated in LB, LB supplemented with 10 mM octanoic acid (LB Oct), 0.1N M63 containing 15 mM octanoic acid, or 1N M63 containing 7.5 mM octanoic acid. When cultures reached mid-exponential phase (A_{600} of 0.6), samples were collected, and the β-galactosidase activity was measured. Results correspond to the average of three independent assays; the standard deviation is indicated.

It is noteworthy that the presence of octanoic acid induced the activity of promoters P_{C1} and P_1 in cells cultivated in LB medium (Fig. 24A and Fig. 26A), but not that of promoter P_F (Fig. 26B). A similar observation has been reported in cells grown in 0.1N M63 medium (de Eugenio et al., 2010b). In addition, the activity of promoter P_1 was much greater in cells growing in the 0.1N or 1N M63 media than in LB containing octanoate. The reason for this difference is not clear, but it suggests that additional regulatory elements related to carbon and nitrogen metabolism might control the activity of this promoter.

Levels of CrcZ and CrcY sRNAs under different C/N ratios

The levels of the two sRNAs (CrcZ and CrcY) that antagonize the Crc/Hfq-mediated repression vary substantially depending on the metabolic conditions, the nature and concentration of the carbon source being used, and the growth temperature (Sonnleitner et al., 2009; Moreno et al., 2012; Fonseca et al., 2013; Valentini et al., 2014). The levels of these sRNAs is high in cells growing in nutrient-poor growth media (in which the Crc/Hfq-mediated CCR is not needed) and much lower when cells grow in a rich media (where the CCR effect is strong). However, the influence of octanoic acid and the C/N ratio on CrcZ and CrcY levels remained unknown. To determine what this influence might be, real-time RT-PCR assays were used to determine the levels of these sRNAs in cells cultivated in the LB, 1N M63 and 0.1N M63 growth media containing octanoic acid. In cells growing exponentially in LB medium, addition of octanoic acid had little influence on the levels of CrcZ and CrcY (Fig. 27). In the imbalanced 0.1N M63 medium, however, the abundance of both CrcZ and CrcY was considerably greater, reaching total values (CrcZ+CrcY) some six times those seen in cells growing in LB medium (Fig. 27). In the cells growing in the balanced 1N M63 medium, the CrcZ+CrcY level was about 4.5 times that recorded in LB medium, a value about 25% lower than that observed in cells growing in the 0.1N M63 medium. These results fit well with the expression pattern of the *phaC1* gene in cells grown in these culture media, and suggest that in the balanced 1N M63 medium Crc/Hfq system is still partially able to inhibit translation of target RNAs, while in the imbalanced 0.1N M63 medium Crc-Hfq system is almost completely counteracted by CrcZ and CrcY and cannot, therefore, inhibit translation. In fact, in previous work (Fonseca et al., 2013) it was observed that culture conditions leading to CrcZ+CrcY levels intermediate between those seen under full-repression and no-repression conditions elicit the partial Crc-dependent repression of some genes.

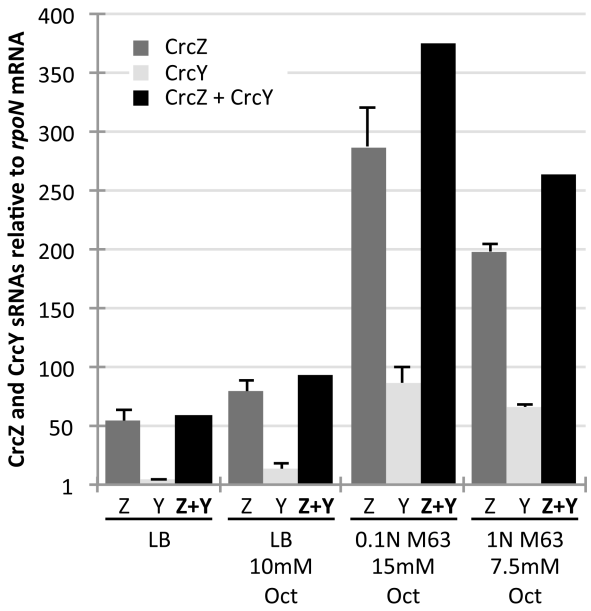

Fig. 27 Influence of octanoic acid on the levels of CrcZ and CrcY sRNAs.
The levels of the CrcZ and CrcY sRNAs, expressed relative to those of the *rpoN* mRNA, were determined by real-time RT-PCR in cells growing exponentially (A_{600} of 0.6) in LB medium, LB plus 10 mM octanoic acid (LB Oct), 0.1N M63 containing 15 mM octanoic acid, or 1N M63 containing 7.5 mM octanoic acid. Three independent assays were performed; the standard deviation is shown. 'Z + Y' stands for the total amount of CrcZ plus CrcY detected.

Inactivation of the *crc* gene leads to greater accumulation of PHA in LB medium

The inhibition imposed by Crc/Hfq system on the translation of the mRNA corresponding to the PhaC1 polymerase may affect PHA synthesis under certain conditions. During exponential growth in LB medium, PHAs were barely detectable irrespective of the presence or absence of octanoic acid or of the Crc protein (Fig. 28). In the stationary phase, however, significant amounts of PHAs were detected when 10 or 20 mM octanoic acid was present in the LB medium, but not if the concentration was reduced to 1 mM (Fig. 28). In the presence of 10 mM octanoic acid, and after 24 h of culture, the *crc*-mutant strain accumulated PHAs to the extent that they reached 30% of the cell dry weight (CDW) and there were about 0.9 mg of PHA per ml of culture. These values are higher than those recorded for the wild type strain (21.1 % of the CDW, 0.6 mg ml^{-1} PHA). When the concentration of octanoic was increased to 20 mM, the amount of PHA detected in the *crc*-mutant strain increased to about 63.5% of the CDW (and reached 2.5 mg ml^{-1}), much higher than that observed for the wild type strain (40.3% of the CDW, 1.5 mg ml^{-1} PHA; Fig. 28). Under these growth conditions, the total biomass generated in the wild type and *crc*-mutant strains was similar (3.7 and 3.8 mg ml^{-1} respectively). However, the residual biomass (PHA-free biomass) was significantly less in the *crc*-mutant strain (1.42 mg ml^{-1}) than in the parental strain (2.48 mg ml^{-1}), suggesting that Crc is involved in the control of the carbon flux to the PHA cycle or in biomass formation in C/N balanced media.

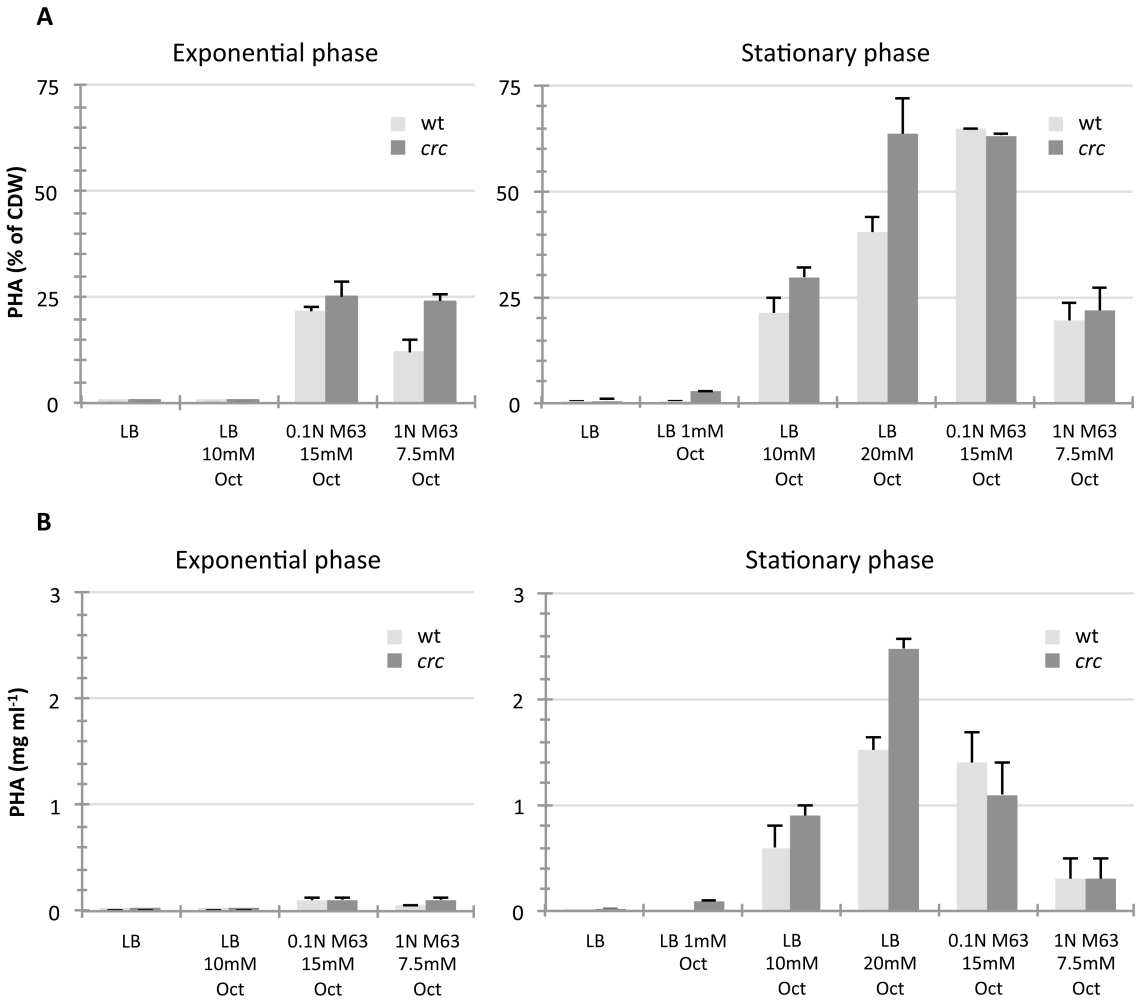

Fig. 28 Influence of the Crc protein on the production of PHAs.
Data correspond to the PHA accumulated in *P. putida* strains KT2442 (indicated as wt; light bars) and KT2442-C1 (indicated as *crc*; dark bars) cultivated in the indicated growth media (LB, LB with 1, 10 or 20 mM octanoic acid, 0.1 N M63 medium with 15 mM octanoic acid, or 1 N M63 medium with 7.5 mM octanoic acid), and collected either at mid-exponential phase (A_{600} = 0.6) or at the stationary phase (24 h of culture). The amount of PHA is expressed either as a percentage of total cell dry weight (**A**) or as mg per millilitre of culture (**B**).

In the imbalanced 0.1N M63 medium, both the wild type and the *crc* mutant cells accumulated PHAs up to about 20-25% of the CDW during exponential growth, an amount that increased to 65% of the CDW after 24 h in the stationary phase (Fig. 28). No differences were observed in terms of biomass production. The Crc regulator appeared to have no role in this growth medium, which is in agreement with the previous results (Fig. 24A-C Fig. 25A-C). However, the influence of Crc became apparent when the cells were cultivated in the balanced 1N M63 medium in which, during exponential growth, the amount of PHAs detected almost doubled when the *crc* gene was inactivated (Fig. 25B-D). This is consistent with the 50% reduction that Crc/Hfq imposed on the expression of the *phaC1'-'lacZ* and *Ptrc - phaC1'-'lacZ* fusions (Fig. 24A-C and Fig. 25A-C) in this balanced medium. In stationary phase cells, however,

this difference became less evident and similar amounts of PHAs were detected in the wild type and *crc*-mutant strains.

Discussion

Most studies on PHA metabolism in *P. putida* have been performed with cells growing under conditions of nutritional imbalance, in which the amount of carbon greatly exceeded that of nitrogen (the optimum conditions for PHA synthesis). Much less attention has been paid to PHA metabolism under conditions of nutritional balance, and in particular to the influence that the global regulation networks that modulate carbon fluxes might have on PHA metabolism. The results presented here show that, under balanced C/N conditions, the expression of the *pha* genes can be significant, but is negatively modulated by the global regulator Crc.

Although sequences resembling the canonical CA motifs that are indicative of Crc/Hfq regulation can be predicted close to the translation initiation regions of the *phaC1*, *phaI* and *phaF* mRNAs, the present results indicate that only the site at *phaC1* appears to be functional. *In vitro,* Crc/Hfq generated a stable and specific complex only on *phaC1* RNA. Translational fusions of *phaC1*, *phaI* and *phaF* to the *lacZ* reporter gene showed that the Crc/Hfq regulatory system can inhibit the translation of *phaC1* mRNA *in vivo*, but not that of *phaI* and *phaF* mRNAs. Moreover, the behaviour of a post-transcriptional fusion in which transcription of the *phaC1* is uncoupled from its native promoter, and driven instead from the heterologous *Ptrc* promoter, also supported that Crc/Hfq inhibit *phaC1* translation. In agreement to this, Crc had no influence on the levels of *phaC1* and *phaF* mRNAs, or on the amounts of PhaF protein, although it had an inhibitory effect on the levels of PhaC1 protein in the 1N M63 medium. This again indicates that the Crc/Hfq system regulates *phaC1* translation, but not that of *phaF*, and agrees with previous observations showing that not all RNA sequences apparently containing a CA motif are finally regulated by Crc/Hfq, the context and RNA structure around this motif being important as well (Moreno et al., 2009a; Hernandez-Arranz et al., 2013; Madhushani et al., 2015; Moreno et al., 2015). The strength of the inhibition imposed by Crc/Hfq on *phaC1* translation differed depending on the growth medium used. In cells growing in complete LB medium, a condition in which the effect of Crc-mediated CCR is very strong, the expression of *phaC1* was low but detectable, as deduced from the behaviour of the *phaC1'-'lacZ* translational fusion. The addition of octanoic acid to induce transcription of the *pha* genes was almost unable to stimulate the expression of the *phaC1'-'lacZ* translational fusion unless the *crc* gene was inactivated, in which case *phaC1* expression increased about five fold. It is worth noting that octanoic acid serves not only as an inducer of the *pha* genes, but also as a precursor of the PHA monomers (Huisman et al., 1989; Prieto et al., 2007; de Eugenio et al., 2010b). In cells growing exponentially in LB medium, PHAs were basically undetectable, even in the presence of octanoic acid, and in the strain lacking the Crc protein. This observation is consistent with low *phaC1* expression. A different pattern was observed when PHA production was analysed in cells that had already reached the stationary phase of growth, a time during which the effect of Crc/Hfq system fades because it is antagonized by the CrcZ and CrcY sRNAs. Under these conditions, the cells accumulated significant amounts of PHA if octanoic acid was added to the LB medium at sufficiently high concentrations (10-20 mM). Inactivation of the *crc* gene further increased PHA production by 42-57%, depending on the amount of octanoic acid present. It

seems, therefore, that during exponential growth in LB containing octanoic acid, expression of the *pha* genes is kept in check by Crc/Hfq. When Crc regulator is eliminated by mutation, the translation of *phaC1* mRNA and the amount of PHAs produced during exponential growth increases, although it only accumulates in small amounts. The PhaC1 protein accumulated during the exponential phase of growth in the *crc*-mutant strain probably explains why this strain shows larger amounts of PHA than the wild type in the stationary phase. When wild type cells reach the stationary phase of growth the effect of Crc/Hfq diminishes, thereby increasing the expression of *phaC1* and the accumulation of PHA. It is worth noting that PHAs did not accumulate if octanoic acid was absent or only present in low concentration, even if the *crc* gene was inactivated and the cells harvested in the stationary phase.

When cells were cultivated in an imbalanced minimal salts medium with a high C/N ratio and octanoic acid as the sole carbon source, the expression of *phaC1* during the exponential phase of growth was very high and was unaffected by Crc (as deduced from the activity of the *phaC1'-'lacZ* translational fusion). In agreement with this, PHA was clearly detected in exponentially growing cells, accounting for 20-25% of the CDW, an amount that increased to almost 65% in late-stationary phase cells. When cells were cultivated in a balanced mineral salts medium, clear Crc/Hfq repression of *phaC1* translation was seen in the exponential growth phase. The reduction in PhaC1 polymerase clearly affected PHA accumulation; the strain lacking a functional *crc* gene accumulated twice as much PHA as the wild type, reaching levels similar to those recorded with the imbalanced medium. In stationary phase cells in 1N M63 medium, and contrary to what occurred in cells cultivated in LB + 20 mM octanoic acid, the amount of PHA accumulated by the wild type strain was similar to that seen in the *crc*-mutant strain, presumably because Crc/Hfq-repression in the 1N M63 medium during exponential growth is not as strong as that generated by the LB medium, and its effects vanish soon as cells enter into the stationary phase of growth.

The present results suggest that Crc/Hfq-mediated CCR is influenced not only by the carbon source used, but also by the C/N ratio of the culture medium, a facet of Crc/Hfq regulation that had not been addressed before. In *P. putida*, Crc/Hfq-mediated repression is very weak when cells are grown in a minimal salts medium containing a balanced C/N ratio and an organic acid such as citrate as the carbon source (Yuste and Rojo, 2001; Valentini et al., 2014). However, the use of octanoic acid elicited a Crc/Hfq-dependent catabolite repression response in the minimal salts medium used here when the C/N ratio was balanced, but not if it was imbalanced. The combined levels of the CrcZ and CrcY sRNAs, which ultimately determine the strength of the Crc/Hfq-dependent repression, were rather high in cells growing exponentially in the imbalanced 0.1N M63 medium containing octanoic acid. Indeed, these levels were compatible with a situation in which Crc/Hfq system is strongly antagonized and no Crc/Hfq-mediated repression occurs. In the balanced 1N M63 medium, however, the levels of CrcZ+CrcY were about 30% lower, although still much higher than those seen in cells growing in LB medium. This suggests that in the balanced 1N M63 medium containing octanoic acid, the Crc/Hfq system is not fully antagonized by CrcZ and CrcY, and can inhibit translation of target mRNAs to some extent. This is supported by the Crc/Hfq-mediated repression of *phaC1* observed in this growth medium. Therefore, the combined results indicate that a high concentration of octanoic acid provokes a Crc/Hfq-dependent repression response only if the C/N ratio is properly balanced, the regulatory response being suppressed if the nitrogen source becomes limiting. This extends the role of the Crc protein in the optimisation of metabolism beyond that of the hierarchical utilization of

carbon sources. We propose that, in the balanced 1N M63 medium, the octanoic acid activates transcription of the *pha* genes, but that Crc acts to reduce the levels of PhaC1, reducing the flow of carbon towards PHA synthesis and favouring its use for cell growth. In an imbalanced medium, however, the lack of Crc/Hfq activity facilitates the diversion to PHA synthesis of all the carbon that cannot be used for cell growth. This idea, together with the lower residual biomass (PHA-free biomass) and increased PHA accumulation shown by the *crc*-mutant strain in LB medium containing octanoate, fully agrees with previous results suggesting that PHA metabolism is a critical route for synchronizing global carbon metabolism. In this earlier work, the lack of the PHA accumulation in a *phaC1*-mutant strain growing in an imbalanced medium containing octanoic acid was paralleled by an increase in the flux of carbon through the TCA cycle and by greater liberation of CO_2, therefore wasting the carbon not used to make biomass (Escapa et al., 2012).

Transcription of the CrcZ and CrcY sRNAs depends on the two-component sensor-regulator system formed by the CbrA and CbrB proteins (Sonnleitner et al., 2009; Moreno et al., 2012; Garcia-Maurino et al., 2013). This two-component system controls the uptake and assimilation of several amino acids as carbon and nitrogen sources and, together with the NtrB/NtrC proteins, is important for responding to changes in the C/N balance in Pseudomonads (Nishijyo et al., 2001; Zhang and Rainey, 2008; Amador et al., 2010). Therefore, the ability of Crc to regulate PHA synthesis will ultimately depend, at least in part, on the CbrA/CbrB system, although the exact signals to which the CbrA sensor protein responds are still unclear. The deeper understanding of the factors controlling PHA metabolism, obtained trough this work, may facilitate the development of bacterial strains able to accumulate large amounts of PHA when growing at the expense of cheap carbon sources, thereby reducing the costs associated with the production of PHAs useful as bioplastics. In fact, the present work shows that the addition of octanoic acid and the inactivation of the *crc* gene can lead to a dramatic increase in PHA production in cells grown in LB medium. The strength of Crc/Hfq inhibition, however, can be predicted to vary significantly depending on the growth medium used.

Experimental procedures

Bacterial strains and culture media
Escherichia coli and *P. putida* strains were routinely grown at 37°C and 30°C, respectively. Lysogeny broth (LB) was used as a complete growth medium (Sambrook and Russell, 2001), supplemented where indicated with octanoic acid (1, 10 or 20 mM, as specified). The defined minimal media used were 1N M63 (13.6 g of KH_2PO_4 l^{-1}, 2 g of $(NH_4)_2SO_4$ l^{-1}, 0.5 mg of $FeSO_4 \cdot 7\ H_2O$ l^{-1}, adjusted to pH 7.0 with KOH) and 0.1N M63 (Moldes et al., 2004), which is a nitrogen-limited variation of 1N M63 containing a tenth of the concentration of $(NH_4)_2SO_4$ (0.2 g l^{-1}). Both media were supplemented with 1 mM $MgSO_4$ and a solution of trace elements (1000 x composition: $FeSO_4 \cdot 7H_2O$, 2.78 g l^{-1}; $MnCl_2 \cdot 4H_2O$, 1.98 g l^{-1}; $CoSO_4 \cdot 7H_2O$, 2.81 g l^{-1}; $CaCl_2 \cdot 2H_2O$, 1.47 g l^{-1}; $CuCl_2 \cdot 2H_2O$, 0.17 g l^{-1}; $ZnSO_4 \cdot 7H_2O$, 0.29 g l^{-1}). Octanoic acid was added as the carbon source (7.5 mM for 1N M63 and 15 mM for 0.1 M63, respectively) to achieve a C/N ratio of 2 (mol/mol) for the non-limited medium, and of 40 for the medium containing a low concentration of the nitrogen source. Antibiotics were added when needed at the following concentrations: gentamicin 10 mg ml^{-1}, streptomycin 50 mg ml^{-1}, chloramphenicol 34 mg ml^{-1}, ampicillin 100 mg ml^{-1}, tetracycline 10 mg ml^{-1}. *P. putida* KT2442 is a spontaneous rifampicin-resistant derivative of strain KT2440 (Franklin et al., 1981). *Pseudomonas putida* KT2442-C1 derives from strain KT2442 by replacing the *crc* gene by an inactive *crc::tet* allele (Ruiz-Manzano et al., 2005). *Pseudomonas putida* strains PC1, PI and PF contain the translational fusions *phaC1'-'lacZ*, *phaI'-'lacZ* and *phaF'-'lacZ* respectively at the Tn7 *att* site (see below). Strains PC1C, PIC and PFC are like strains PC1, PI and PF, respectively, but contain an inactive *crc::tet* allele.

Protein purification
The purification of the *P. putida* Crc(6xHis), was performed as a fusion with a 6xHis tag at the C-terminus as indicated in (Moreno et al., 2007). The purification mixture contained the E. coli Hfq protein that act similarly of the P. putida Hfq protein. In the text the mixture is indicated as "Crc(6xHis)/Hfq". The *P. putida* untagged Crc and untagged Hfq were purified separately using the Impact-CN intein system as described (Moreno et al., 2015), and were kindly provided by Renata Moreno.

RNA band shift assays
The binding reactions involved labelled RNA (0.1 nM), 1 µg of yeast tRNA and the indicated amounts of Crc(6xHis)/Hfq or untagged Crc and Hfq proteins, and were performed in 20 µl volumes of 10 mM Hepes-KOH, pH 7.9, 35 mM KCl, 2 mM $MgCl_2$. After 30 min at 20°C, 3 µl of loading buffer (60% glycerol, 0.025% xylene cyanol) were added and the samples loaded onto a non-denaturing 6% (29:1 acrylamide/bisacrylamide) polyacrylamide gel containing TBM buffer (45 mM Tris-HCl, pH 8.3, 43 mM boric acid, 2 mM $MgCl_2$, 5% glycerol). Electrophoresis was performed at 4°C using TBM as the running buffer. RNA oligonucleotides (synthesized by Sigma) were labelled with T4 polynucleotide kinase and (γ^{32}P)-ATP and purified in MicroSpin G-25 columns (GE Healthcare).

Translational fusions of phaC1, phaI and phaF to lacZ
To obtain a translational fusion of *phaC1* with the *lacZ* reporter gene, a 295 bp DNA fragment containing promoter P_{C1} and the DNA region coding for the first 11 amino acid residues of PhaC1 (containing the CA regulatory motif) was amplified by PCR using *P. putida* KT2442 genomic DNA as the template plus primers 5'-gcggaattcggcctgcggggtttagag and 5'-gcgggatcccgctgtagctcatcgttgttc. The DNA fragment obtained was digested with EcoRI and BamHI and cloned between the same sites of plasmid pUJ9 (Herrero et al., 1990), immediately upstream of the promoterless *lacZ* reporter gene to create an in-frame translational fusion. The resulting plasmid (named pUJ9C1) was digested with NotI and the excised 3.5 kb fragment containing the *phaC1'-'lacZ* fusion was cloned into the NotI site of the Tn7-based delivery vector pNBTN7 (Silva-Rocha and de Lorenzo, 2011, 2014). The corresponding plasmid, named pTN7C1, was transferred to *P. putida* strains KT2442 and KT2442-C1 by tetra-partite mating using *E. coli* CC118λpir (pTnS1) as the supplier of Tn7 transposase and *E. coli* HB101 (pRK600) as the transfer function donor, as previously described (Silva-Rocha and de Lorenzo, 2011, 2014). The strains obtained were named PC1 (derived from KT2442) and PC1C (derived from KT2442-C1). The correct insertion of the transposon at the *att* Tn7 site of the P. putida genome was checked using primer pairs Tn7RF (5'-atgaccaatggcgaaggc) plus Tn7RR (5'-atatttcgaccccacgcc) and Tn7LF (5'-cctaggcggccccaacc) plus Tn7LR

(5'-gccagcccatgatactgc). A similar strategy was used to construct the *phaI'-'lacZ* and *phaF'-'lacZ* translational fusions. The 493 nt DNA fragment corresponding to *phaI'* 5'-end was obtained with oligonucleotides 5'-cgcgaattcgccagaaaatgcctgagaagctc and 5'-cgcggatccagggcttcgtctttttttcttcgc. The 271 nt DNA fragment corresponding to the *phaF* 5'-end was generated with oligonucleotides 5'-cgcgaattcccagcttgacgaagtcggtga and 5'-cgcggatccgagctgccttctttttcggtg. The plasmids obtained, pTN7I and pTN7F, were transferred to *P. putida* strains KT2442 and KT2442-C1 as described above, obtaining strains PI and PF (derived from KT2442), or PIC and PFC (derived from KT2442-C1).

Post-transcriptional fusion of phaC1 to lacZ

A post-transcriptional *Ptrc-phaC1'-'lacZ* fusion in which the *phaC1'-'lacZ* reporter construction is transcribed from the heterologous IPTG-inducible *Ptrc* promoter was constructed as follows. A DNA fragment containing *phaC1'-'lacZ* (including the *phaC1* ribosome binding sequence but lacking the P_{C1} promoter) was PCR amplified with oligonucleotides 5'- aaaggtaccaggacaacggagcgtcgtag (hybridizes immediately upstream of *phaC1* and contains a restriction site for KpnI) and 5'- ttattaagcttttatttttgacaccagacca (hybridizes downstream of 'lacZ and includes a restriction site for HindIII), using plasmid pUJ9C1 as template. The DNA fragment was digested with KpnI and HindIII endonucleases and cloned between the same sites of plasmid pSEVA424 (Silva-Rocha et al., 2013; Martinez-Garcia et al., 2015), in such a way that the *phaC1'-'lacZ* fusion can be transcribed from the *Ptrc* promoter of the vector. The plasmid obtained was named pC1PT. The nucleotide sequence of the PCR-amplified construction was verified to assure the absence of spurious mutations.

β-galactosidase assay

β-galactosidase activity was measured by chemiluminescence using the Galacto-Light Plus™ System (Applied Biosystems), following the manufacturer's instructions. Reactions were performed in 96-well plates as described previously (Moreno et al., 2009a; Valls et al., 2011). Results were analysed using a luminometer (TECAN Infinite 200); the values shown (expressed in arbitrary units) correspond to the luminescence observed normalized relative to absorbance at 600 nm. Three independent experiments were performed.

RNA purification

Cells were grown in aerated flasks in the specified medium at 30°C. At mid-exponential phase (A_{600} = 0.6), the cells were centrifuged and the pellets frozen at -70°C. RNA was purified from each pellet using the RNeasy RNA purification kit (QIAGEN) following the manufacturer's instructions. RNA was treated with RNase-free DNase I (Turbo DNA-free, Ambion), as specified by the supplier. The absence of DNA in the RNA samples was checked by real-time PCR as described earlier (Morales et al., 2006), using oligonucleotides for the *rpoN* gene. RNA integrity was checked by agarose gel electrophoresis. Three independent assays were performed.

Real time PCR

RNA samples (8 μg) were reverse transcribed to cDNA using the High Capacity cDNA kit (Applied Biosystems). Real-time PCR was performed using SYBR Green PCR master mix (Applied Biosystems) and 0.2 μM of each primer in a 7500 Real-time PCR thermocycler (Applied Biosystems). The expression profile of *phaC1* and *phaF* was analyzed by absolute quantitation using 25 ng and 0.25 ng of cDNA template. Standard curves were constructed by serial 10-fold dilutions from 10^7 to 10^2 copies of P. putida KT2442 genomic DNA. The levels of the CrcZ and CrcY sRNAs were analyzed by relative quantization as previously described (Livak and Schmittgen, 2001; Morales et al., 2006). Results were normalized relative to those obtained for the *rpoN* gene since its expression in P. putida remains constant throughout the growth phase under the conditions used (Cases et al., 1996; Yuste et al., 2006). The extension of PCR products was performed at 60°C. The primers used in the RT-PCR assays were 5′-acaaccaggcagagaacaacaa and 5'-cacgttgatctgtcgatccaa for *crcZ*, 5'-aaagcaggtcagcgctcaaa and 5′-tcggcttgtcctggtgttg for *crcY*, 5'-tcgacccggagctggata and 5'- cggctcgaactgctggat for *rpoN*, 5'-ccaccgcagatcaacaagttc and 5'-gcgagcgcaggcagaa for *phaC1*, and 5'-ggagcgaacttgaagaagcc and 5'-cgtggccagtcgaagagctag for *phaF*.

Western blotting

Cells were grown in the specified growth media and, at mid-exponential phase (A_{600} = 0.6), cells were collected, freeze-dried and lyophilized. The lyophilized pellets were suspended in 50 mM Tris-HCl pH 7 and total proteins were resolved in an SDS-polyacrylamide gel. 40 μg of total cell extract, excluding PHAs, were loaded onto the gel. The proteins were transferred to a nitrocellulose membrane and detected with the ECL Western Blotting Detection Kit (Amersham Biosciences) according to the protocol described by the manufacturer, using as primary antibodies a polyclonal anti-PhaC1 serum (1:5,000 dilution), or a polyclonal anti-PhaF serum (1:20,000 dilution). Membranes were treated with a secondary anti-rabbit antibody conjugated to peroxidase (Amersham-Pharmacia Biotech) and developed by chemiluminescence. The signal intensity was quantified using a ChemiDoc XRS+ image detector and the Quantity One software (BioRad).

Gas chromatography-mass spectrometry analysis for PHA

PHA monomer composition and cellular PHA contents were determined by GC-MS of the methanolysed polyester. Methanolysis was performed by suspending 5-10 mg of lyophilised aliquots in 0.5 ml of chloroform and 2 ml of methanol containing 15% sulphuric acid and 0.5 mg/ml 3-methylbenzoic acid (internal standard), incubating the samples at 80ºC for 7 h. After cooling, 1 ml of demineralised water and 1 ml of chloroform were added, and the organic phase containing the resulting methyl esters analysed by GC-MS (Lageveen et al., 1988; de Eugenio et al., 2010a). An Agilent series 7890A apparatus coupled to a 5975C MS detector (EI, 70 eV) and a split-splitless injector were used in this analysis. An aliquot (1 μl) of the organic phase was injected into the gas chromatograph at a split ratio of 1:20. Separation of compounds was achieved using an HP-5 MS capillary column (5% phenyl-95% methyl siloxane, 30 m x 0.25 mm film thickness). Helium was used as the carrier gas at a flow rate of 1 ml min^{-1}. The injector and transfer line temperatures were set at 275°C and 300°C respectively. The oven temperature programme was: initial temperature 80ºC for 2 min, then from 80°C to 150°C at a rate of 5°C min^{-1}, at which temperature it was held for 1 min. The mass spectra were recorded in full scan mode (m/z 40-550). 3-Hydroxy-butyric acid methyl ester was resolved using the selected ion monitoring mode (SIM).

Conclusions

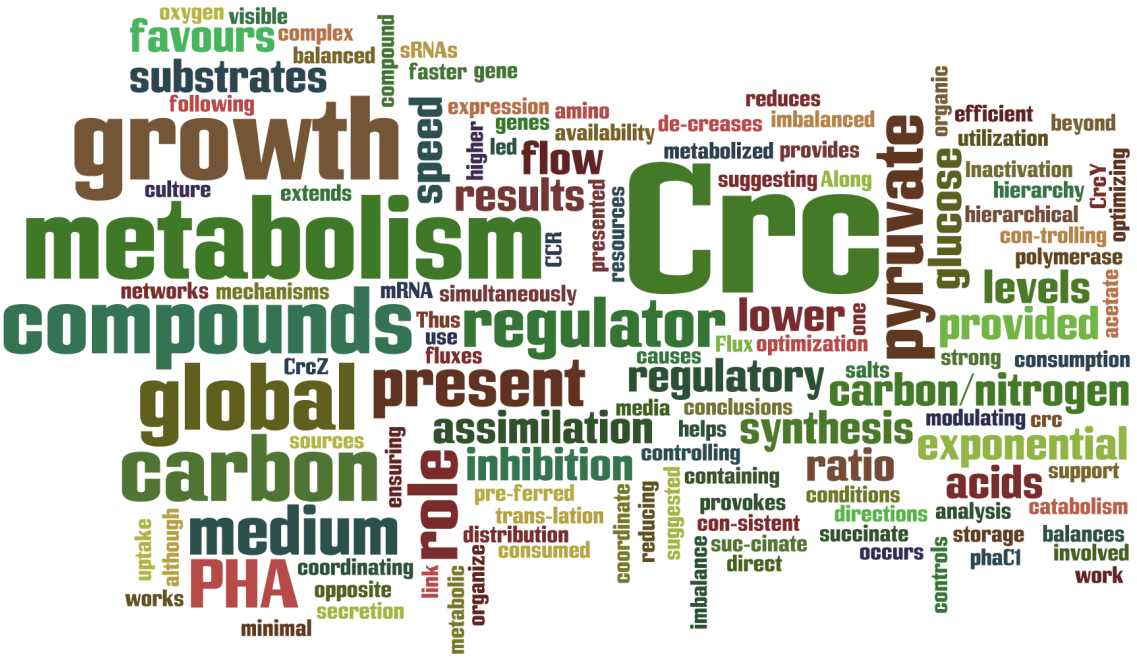

The work presented has led to the following conclusions:

1. During exponential growth in a complex medium, conditions in which CCR is strong, the Crc global regulator favours a higher growth speed with lower oxygen consumption. Along with other regulatory mechanisms, Crc controls the hierarchy of assimilation of the organic acids and amino acids present in the culture medium, modulating the expression of genes involved in their uptake and catabolism. Inactivation of the *crc* gene causes a metabolic imbalance, which decreases growth speed and provokes the secretion of acetate and pyruvate. These results are consistent with a role of the Crc regulator in the optimization of metabolism.

2. When provided simultaneously in a minimal salts medium, succinate is consumed faster than glucose, although both compounds are metabolized. The levels of the CrcZ and CrcY sRNAs are lower when both substrates are present than when only one of them is provided. Since these sRNAs antagonize the effect of Crc, the results presented suggest a role for Crc in coordinating the metabolism of succinate and glucose. Flux distribution analysis suggested that, when both substrates are present, Crc works to organize a metabolism in which carbon compounds flow in opposite directions: from glucose to pyruvate, and from succinate to pyruvate. Thus, these results support that Crc not only favours the assimilation of preferred compounds, but balances carbon fluxes, optimizing metabolism and growth.

3. The Crc global regulator reduces PHA synthesis during exponential growth in media containing a balanced carbon/nitrogen ratio. This occurs through a direct inhibition of the translation of the *phaC1* mRNA, reducing the levels of PHA polymerase. No inhibition is visible when the carbon/nitrogen ratio is imbalanced. This extends the role of Crc beyond that of controlling the hierarchical utilization of carbon sources and provides a link between the global regulatory networks controlling carbon flow and the synthesis of PHA, a storage compound that helps to coordinate global metabolism to the availability of resources, ensuring their efficient use.

Conclusiones

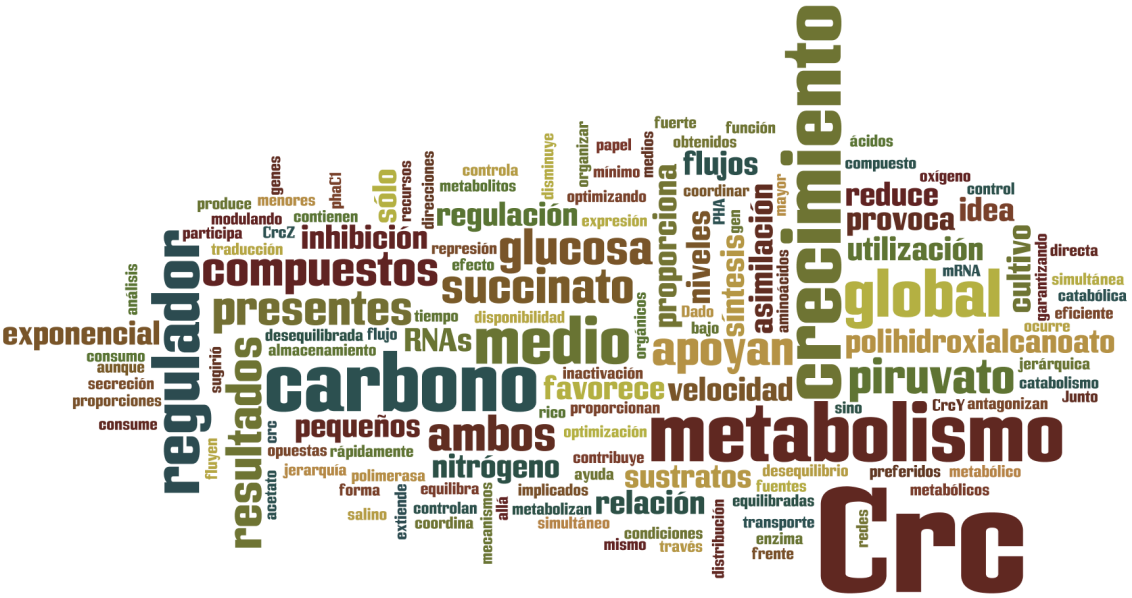

El trabajo presentado ha llevado a las siguientes conclusiones:

1. Durante el crecimiento exponencial en un medio rico, condiciones en las que la represión catabólica es fuerte, el regulador global Crc favorece una mayor velocidad de crecimiento con un consumo de oxígeno más bajo. Junto con otros mecanismos de regulación, Crc controla la jerarquía de asimilación de los ácidos orgánicos y aminoácidos presentes en el medio de cultivo, modulando la expresión de genes implicados en el transporte y catabolismo de estos compuestos. La inactivación del gen *crc* provoca un desequilibrio metabólico que disminuye la velocidad de crecimiento y provoca la secreción de acetato y piruvato. Estos resultados apoyan la idea de que el regulador Crc participa en la optimización del metabolismo.

2. Cuando se proporcionan de forma simultánea en un medio mínimo salino, el succinato se consume más rápidamente que la glucosa, aunque ambos compuestos se metabolizan al mismo tiempo. Los niveles de los RNAs pequeños CrcZ y CrcY son menores cuando ambos sustratos están presentes que cuando se proporciona sólo uno de ellos. Dado que estos RNAs pequeños antagonizan el efecto de Crc, los resultados obtenidos apoyan la idea de que Crc coordina el metabolismo simultáneo de succinato y glucosa. El análisis de la distribución de flujos metabólicos sugirió que, cuando ambos sustratos están presentes, Crc contribuye a organizar un metabolismo en el cual los metabolitos fluyen en direcciones opuestas: desde la glucosa hasta el piruvato, y desde el succinato hasta piruvato. Por lo tanto, estos resultados apoyan que Crc no sólo favorece la asimilación de compuestos preferidos, sino que equilibra los flujos de carbono, optimizando el metabolismo y el crecimiento.

3. El regulador global Crc reduce la síntesis de polihidroxialcanoato durante el crecimiento exponencial en medios que contienen proporciones equilibradas de carbono frente a nitrógeno. Esto ocurre a través de una inhibición directa de la traducción del mRNA de *phaC1*, lo que reduce los niveles del enzima PHA polimerasa. Esta inhibición no se produce cuando el medio de cultivo tiene una relación desequilibrada de carbono y nitrógeno. Esto extiende el papel del regulador Crc más allá del control de la utilización jerárquica de fuentes de carbono, y proporciona un relación entre las redes de regulación global que controlan el flujo de carbono y la síntesis de polihidroxialcanoato, un compuesto de almacenamiento que ayuda a coordinar el metabolismo global en función de la disponibilidad de recursos , garantizando su utilización eficiente.

References


metabolism
repression
catabolite
regulator
Crc
polyhydroxyalkanoate
systemglobal
Mol
metabolic
regulation
pathway
expression
carbon
Biol
Appl
Biotechnol
Prieto
genes
catabolic
plasmid
RNA
amino
degradation
control
analysis
M.A
Rev
et
al
Chem
B.O
Nat
KT2440
pathways
Sauer
Chavarria
characterization
involved
protein
regulatory
response
Role
growth
I.F
bacteria
using
polyhydroxyalkanoates
Opin
Marques
promoter
Catabolite
role
medium
production
Thiele
P.V
Escapa
inhibits
biochemical
two-component
Sanz
Kim
controls
Res
Hfq
Pflüger-Grau
KT2442
Cases
genome-scale
Bagdasarian
Luengo
J.G
cloning
bacterial
Canosa
evidence
toluene
phosphotransferase
Huisman
RNAs
Pu
Behrends
G.W
small
proteins
Timmis
CrcZ
gene
networks
uptake
acids
utilization
Sonnleitner
Haas
pWW0
Witholt
data
models
Silva-Rocha
Eugenio
transcriptional
FEMS
M.M
Microbiology
BMC
Fuhrer
flux
H.D
del
integration
aromatic
Williams
PLoS
central
catabolism
Carbon
Valentini
J.M
A.M
acid
transport
acidic
K.N
Duque
Galan
Rohm
glycerol
TOL
Curr
microbial
alkane
PHA

Abdou, L., Chou, H.T., Haas, D., and Lu, C.D. (2011) Promoter recognition and activation by the global response regulator CbrB in Pseudomonas aeruginosa. *J Bacteriol* **193**: 2784-2792.

Aiba, H. (2007) Mechanism of RNA silencing by Hfq-binding small RNAs. *Curr Opin Microbiol* **10**: 134-139.

Amador, C.I., Canosa, I., Govantes, F., and Santero, E. (2010) Lack of CbrB in Pseudomonas putida affects not only amino acids metabolism but also different stress responses and biofilm development. *Environ Microbiol* **12**: 1748-1761.

Aranda-Olmedo, I., Ramos, J.L., and Marques, S. (2005) Integration of signals through Crc and PtsN in catabolite repression of Pseudomonas putida TOL plasmid pWW0. *Appl Environ Microbiol* **71**: 4191-4198.

Aranda-Olmedo, I., Marin, P., Ramos, J.L., and Marques, S. (2006) Role of the ptsN gene product in catabolite repression of the Pseudomonas putida TOL toluene degradation pathway in chemostat cultures. *Appl Environ Microbiol* **72**: 7418-7421.

Arias, S., Bassas-Galia, M., Molinari, G., and Timmis, K.N. (2013) Tight coupling of polymerization and depolymerization of polyhydroxyalkanoates ensures efficient management of carbon resources in Pseudomonas putida. *Microb Biotechnol* **6**: 551-563.

Arias-Barrau, E., Olivera, E.R., Luengo, J.M., Fernandez, C., Galan, B., Garcia, J.L. et al. (2004) The homogentisate pathway: a central catabolic pathway involved in the degradation of L-phenylalanine, L-tyrosine, and 3-hydroxyphenylacetate in Pseudomonas putida. *J Bacteriol* **186**: 5062-5077.

Audic, S., and Claverie, J.M. (1997) The significance of digital gene expression profiles. *Genome Res* **7**: 986-995.

Bauchop, T., and Elsden, S.R. (1960) The growth of micro-organisms in relation to their energy supply. *J Gen Microbiol* **23**: 457-469.

Becker, S.A., and Palsson, B.O. (2008) Context-specific metabolic networks are consistent with experiments. *PLoS Comput Biol* **4**: e1000082.

Beckonert, O., Keun, H.C., Ebbels, T.M., Bundy, J., Holmes, E., Lindon, J.C., and Nicholson, J.K. (2007) Metabolic profiling, metabolomic and metabonomic procedures for NMR spectroscopy of urine, plasma, serum and tissue extracts. *Nat Protoc* **2**: 2692-2703.

Behrends, V., Williams, H.D., and Bundy, J.G. (2014) Metabolic footprinting: extracellular metabolomic analysis. *Methods Mol Biol* **1149**: 281-292.

Behrends, V., Ebbels, T.M., Williams, H.D., and Bundy, J.G. (2009) Time-resolved metabolic footprinting for nonlinear modeling of bacterial substrate utilization. *Appl Environ Microbiol* **75**: 2453-2463.

Behrends, V., Geier, B., Williams, H.D., and Bundy, J.G. (2013a) Direct assessment of metabolite utilization by Pseudomonas aeruginosa during growth on artificial sputum medium. *Appl Environ Microbiol* **79**: 2467-2470.

Behrends, V., Bell, T.J., Liebeke, M., Cordes-Blauert, A., Ashraf, S.N., Nair, C. et al. (2013b) Metabolite profiling to characterize disease-related bacteria: gluconate excretion by Pseudomonas aeruginosa mutants and clinical isolates from cystic fibrosis patients. *J Biol Chem* **288**: 15098-15109.

Benjamini, Y., Drai, D., Elmer, G., Kafkafi, N., and Golani, I. (2001) Controlling the false discovery rate in behavior genetics research. *Behav Brain Res* **125**: 279-284.

Browne, P., Barret, M., O'Gara, F., and Morrissey, J.P. (2010) Computational prediction of the Crc regulon identifies genus-wide and species-specific targets of catabolite repression control in Pseudomonas bacteria. *BMC Microbiol* **10**: 300.

Busch, A., Lacal, J., Silva-Jimenez, H., Krell, T., and Ramos, J.L. (2010) Catabolite repression of the TodS/TodT two-component system and effector-dependent transphosphorylation of TodT as the basis for toluene dioxygenase catabolic pathway control. *J Bacteriol* **192**: 4246-4250.

Cascieri, T., and Mallette, M.F. (1976) Peptide utilization by Pseudomonas putida and Pseudomonas maltophilia. *J Gen Microbiol* **92**: 283-295.

Cases, I., and de Lorenzo, V. (2005) Promoters in the environment: transcriptional regulation in its natural context. *Nat Rev Microbiol* **3**: 105-118.

Cases, I., de Lorenzo, V., and Perez-Martin, J. (1996) Involvement of sigma 54 in exponential silencing of the Pseudomonas putida TOL plasmid Pu promoter. *Mol Microbiol* **19**: 7-17.

Cases, I., Perez-Martin, J., and de Lorenzo, V. (1999) The IIANtr (PtsN) protein of Pseudomonas putida mediates the C source inhibition of the sigma54-dependent Pu promoter of the TOL plasmid. *J Biol Chem* **274**: 15562-15568.

Cases, I., Velazquez, F., and de Lorenzo, V. (2001) Role of ptsO in carbon-mediated inhibition of the Pu promoter belonging to the pWW0 Pseudomonas putida plasmid. *J Bacteriol* **183**: 5128-5133.

Chavarria, M., Nikel, P.I., Perez-Pantoja, D., and de Lorenzo, V. (2013a) The Entner-Doudoroff pathway empowers Pseudomonas putida KT2440 with a high tolerance to oxidative stress. *Environ Microbiol* **15**: 1772-1785.

Chavarria, M., Kleijn, R.J., Sauer, U., Pfluger-Grau, K., and de Lorenzo, V. (2012) Regulatory tasks of the phosphoenolpyruvate-phosphotransferase system of Pseudomonas putida in central carbon metabolism. *MBio* **3**.

Chavarria, M., Fuhrer, T., Sauer, U., Pfluger-Grau, K., and de Lorenzo, V. (2013b) Cra regulates the cross-talk between the two branches of the phosphoenolpyruvate : phosphotransferase system of Pseudomonas putida. *Environ Microbiol* **15**: 121-132.

Chavarria, M., Durante-Rodriguez, G., Krell, T., Santiago, C., Brezovsky, J., Damborsky, J., and de Lorenzo, V. (2014) Fructose 1-phosphate is the one and only physiological effector of the Cra (FruR) regulator of Pseudomonas putida. *FEBS Open Bio* **4**: 377-386.

Chen, G.Q. (2009) A microbial polyhydroxyalkanoates (PHA) based bio- and materials industry. *Chem Soc Rev* **38**: 2434-2446.

Chen, G.Q., and Kazlauskas, R. (2011) Chemical biotechnology in progress. *Curr Opin Biotechnol* **22**: 747-748.

Chubukov, V., Gerosa, L., Kochanowski, K., and Sauer, U. (2014) Coordination of microbial metabolism. *Nat Rev Microbiol* **12**: 327-340.

Chubukov, V., Uhr, M., Le Chat, L., Kleijn, R.J., Jules, M., Link, H. et al. (2013) Transcriptional regulation is insufficient to explain substrate-induced flux changes in Bacillus subtilis. *Mol Syst Biol* **9**: 709.

Csete, M., and Doyle, J. (2004) Bow ties, metabolism and disease. *Trends Biotechnol* **22**: 446-450.

Daniels, C., Godoy, P., Duque, E., Molina-Henares, M.A., de la Torre, J., Del Arco, J.M. et al. (2010) Global regulation of food supply by Pseudomonas putida DOT-T1E. *J Bacteriol* **192**: 2169-2181.

de Eugenio, L.I., Garcia, P., Luengo, J.M., Sanz, J.M., Roman, J.S., Garcia, J.L., and Prieto, M.A. (2007) Biochemical evidence that phaZ gene encodes a specific intracellular medium chain length polyhydroxyalkanoate depolymerase in Pseudomonas putida KT2442: characterization of a paradigmatic enzyme. *J Biol Chem* **282**: 4951-4962.

de Eugenio, L.I., Escapa, I.F., Morales, V., Dinjaski, N., Galan, B., Garcia, J.L., and Prieto, M.A. (2010a) The turnover of medium-chain-length polyhydroxyalkanoates in Pseudomonas putida KT2442 and the fundamental role of PhaZ depolymerase for the metabolic balance. *Environ Microbiol* **12**: 207-221.

de Eugenio, L.I., Galan, B., Escapa, I.F., Maestro, B., Sanz, J.M., Garcia, J.L., and Prieto, M.A. (2010b) The PhaD regulator controls the simultaneous expression of the pha genes involved in polyhydroxyalkanoate metabolism and turnover in Pseudomonas putida KT2442. *Environ Microbiol* **12**: 1591-1603.

De Lay, N., Schu, D.J., and Gottesman, S. (2013) Bacterial small RNA-based negative regulation: Hfq and its accomplices. *J Biol Chem* **288**: 7996-8003.

del Castillo, T., and Ramos, J.L. (2007) Simultaneous catabolite repression between glucose and toluene metabolism in Pseudomonas putida is channeled through different signaling pathways. *J Bacteriol* **189**: 6602-6610.

del Castillo, T., Duque, E., and Ramos, J.L. (2008) A set of activators and repressors control peripheral glucose pathways in Pseudomonas putida to yield a common central intermediate. *J Bacteriol* **190**: 2331-2339.

del Castillo, T., Ramos, J.L., Rodriguez-Herva, J.J., Fuhrer, T., Sauer, U., and Duque, E. (2007) Convergent peripheral pathways catalyze initial glucose catabolism in Pseudomonas putida: genomic and flux analysis. *J Bacteriol* **189**: 5142-5152.

Deutscher, J. (2008) The mechanisms of carbon catabolite repression in bacteria. *Curr Opin Microbiol* **11**: 87-93.

Dinamarca, M.A., Ruiz-Manzano, A., and Rojo, F. (2002) Inactivation of cytochrome o ubiquinol oxidase relieves catabolic repression of the Pseudomonas putida GPo1 alkane degradation pathway. *J Bacteriol* **184**: 3785-3793.

Duetz, W.A., Marques, S., de Jong, C., Ramos, J.L., and van Andel, J.G. (1994) Inducibility of the TOL catabolic pathway in Pseudomonas putida (pWW0) growing on succinate in continuous culture: evidence of carbon catabolite repression control. *J Bacteriol* **176**: 2354-2361.

Duetz, W.A., Marques, S., Wind, B., Ramos, J.L., and van Andel, J.G. (1996) Catabolite repression of the toluene degradation pathway in Pseudomonas putida harboring pWW0 under various conditions of nutrient limitation in chemostat culture. *Appl Environ Microbiol* **62**: 601-606.

Escapa, I.F., del Cerro, C., Garcia, J.L., and Prieto, M.A. (2013) The role of GlpR repressor in Pseudomonas putida KT2440 growth and PHA production from glycerol. *Environ Microbiol* **15**: 93-110.

Escapa, I.F., Garcia, J.L., Buhler, B., Blank, L.M., and Prieto, M.A. (2012) The polyhydroxyalkanoate metabolism controls carbon and energy spillage in Pseudomonas putida. *Environ Microbiol* **14**: 1049-1063.

Feist, A.M., Herrgard, M.J., Thiele, I., Reed, J.L., and Palsson, B.O. (2009) Reconstruction of biochemical networks in microorganisms. *Nat Rev Microbiol* **7**: 129-143.

Feist, A.M., Henry, C.S., Reed, J.L., Krummenacker, M., Joyce, A.R., Karp, P.D. et al. (2007) A genome-scale metabolic reconstruction for Escherichia coli K-12 MG1655 that accounts for 1260 ORFs and thermodynamic information. *Mol Syst Biol* **3**: 121.

Filiatrault, M.J., Stodghill, P.V., Wilson, J., Butcher, B.G., Chen, H., Myers, C.R., and Cartinhour, S.W. (2013) CrcZ and CrcX regulate carbon source utilization in *Pseudomonas syringae* pathovar tomato strain DC3000. *RNA Biol* **10**: 245-255.

Fonseca, P., Moreno, R., and Rojo, F. (2013) Pseudomonas putida growing at low temperature shows increased levels of CrcZ and CrcY sRNAs, leading to reduced Crc-dependent catabolite repression. *Environ Microbiol* **15**: 24-35.

Franklin, F.C., Bagdasarian, M., Bagdasarian, M.M., and Timmis, K.N. (1981) Molecular and functional analysis of the TOL plasmid pWWO from Pseudomonas putida and cloning of genes for the entire regulated aromatic ring meta cleavage pathway. *Proc Natl Acad Sci U S A* **78**: 7458-7462.

Frimmersdorf, E., Horatzek, S., Pelnikevich, A., Wiehlmann, L., and Schomburg, D. (2010) How Pseudomonas aeruginosa adapts to various environments: a metabolomic approach. *Environ Microbiol* **12**: 1734-1747.

Fuhrer, T., and Sauer, U. (2009) Different biochemical mechanisms ensure network-wide balancing of reducing equivalents in microbial metabolism. *J Bacteriol* **191**: 2112-2121.

Galan, B., Dinjaski, N., Maestro, B., de Eugenio, L.I., Escapa, I.F., Sanz, J.M. et al. (2011) Nucleoid-associated PhaF phasin drives intracellular location and segregation of polyhydroxyalkanoate granules in Pseudomonas putida KT2442. *Mol Microbiol* **79**: 402-418.

Garcia-Maurino, S.M., Perez-Martinez, I., Amador, C.I., Canosa, I., and Santero, E. (2013) Transcriptional activation of the CrcZ and CrcY regulatory RNAs by the CbrB response regulator in *Pseudomonas putida*. *Mol Microbiol* **89**: 189-205.

Gorke, B., and Stulke, J. (2008) Carbon catabolite repression in bacteria: many ways to make the most out of nutrients. *Nat Rev Microbiol* **6**: 613-624.

Hernandez-Arranz, S., Moreno, R., and Rojo, F. (2013) The translational repressor Crc controls the Pseudomonas putida benzoate and alkane catabolic pathways using a multi-tier regulation strategy. *Environ Microbiol* **15**: 227-241.

Hernández-Arranz, S., Moreno, R., and Rojo, F. (2013) The translational repressor Crc controls the *Pseudomonas putida* benzoate and alkane catabolic pathways using a multi-tier regulation strategy. *Environ Microbiol* **15**: 227-241.

Herrero, M., de Lorenzo, V., and Timmis, K.N. (1990) Transposon vectors containing non-antibiotic resistance selection markers for cloning and stable chromosomal insertion of foreign genes in gram-negative bacteria. *J Bacteriol* **172**: 6557-6567.

Hester, K.L., Madhusudhan, K.T., and Sokatch, J.R. (2000a) Catabolite repression control by crc in 2xYT medium is mediated by posttranscriptional regulation of bkdR expression in Pseudomonas putida. *J Bacteriol* **182**: 1150-1153.

Hester, K.L., Lehman, J., Najar, F., Song, L., Roe, B.A., MacGregor, C.H. et al. (2000b) Crc is involved in catabolite repression control of the bkd operons of Pseudomonas putida and Pseudomonas aeruginosa. *J Bacteriol* **182**: 1144-1149.

Hoch, J.A. (2000) Two-component and phosphorelay signal transduction. *Curr Opin Microbiol* **3**: 165-170.

Holmqvist, E., and Vogel, J. (2013) A small RNA serving both the Hfq and CsrA regulons. *Genes Dev* **27**: 1073-1078.

Holtel, A., Marques, S., Mohler, I., Jakubzik, U., and Timmis, K.N. (1994) Carbon source-dependent inhibition of xyl operon expression of the Pseudomonas putida TOL plasmid. *J Bacteriol* **176**: 1773-1776.

Hoshino, T., and Kose, K. (1990) Cloning, nucleotide sequences, and identification of products of the Pseudomonas aeruginosa PAO bra genes, which encode the high-affinity branched-chain amino acid transport system. *J Bacteriol* **172**: 5531-5539.

Hoshino, T., Kose-Terai, K., and Sato, K. (1992) Solubilization and reconstitution of the Pseudomonas aeruginosa high affinity branched-chain amino acid transport system. *J Biol Chem* **267**: 21313-21318.

Huisman, G.W., de Leeuw, O., Eggink, G., and Witholt, B. (1989) Synthesis of poly-3-hydroxyalkanoates is a common feature of fluorescent pseudomonads. *Appl Environ Microbiol* **55**: 1949-1954.

Huisman, G.W., Wonink, E., Meima, R., Kazemier, B., Terpstra, P., and Witholt, B. (1991) Metabolism of poly(3-hydroxyalkanoates) (PHAs) by *Pseudomonas oleovorans*. Identification and sequences of

genes and function of the encoded proteins in the synthesis and degradation of PHA. *J Biol Chem* **266**: 2191-2198.

Hyduke, D.R., Lewis, N.E., and Palsson, B.O. (2013) Analysis of omics data with genome-scale models of metabolism. *Mol Biosyst* **9**: 167-174.

Jendrossek, D., and Pfeiffer, D. (2014) New insights in the formation of polyhydroxyalkanoate granules (carbonosomes) and novel functions of poly(3-hydroxybutyrate). *Environ Microbiol* **16**: 2357-2373.

Jimenez, J.I., Minambres, B., Garcia, J.L., and Diaz, E. (2002) Genomic analysis of the aromatic catabolic pathways from Pseudomonas putida KT2440. *Environ Microbiol* **4**: 824-841.

Kenny, S.T., Runic, J.N., Kaminsky, W., Woods, T., Babu, R.P., and O'Connor, K.E. (2012) Development of a bioprocess to convert PET derived terephthalic acid and biodiesel derived glycerol to medium chain length polyhydroxyalkanoate. *Appl Microbiol Biotechnol* **95**: 623-633.

Kiely, P.D., O'Callaghan, J., Abbas, A., and O'Gara, F. (2008) Genetic analysis of genes involved in dipeptide metabolism and cytotoxicity in Pseudomonas aeruginosa PAO1. *Microbiology* **154**: 2209-2218.

Kim, J., and Park, W. (2014) Oxidative stress response in Pseudomonas putida. *Appl Microbiol Biotechnol* **98**: 6933-6946.

La Rosa, R., Nogales, J., and Rojo, F. (2015) The Crc/CrcZ-CrcY global regulatory system helps the integration of gluconeogenic and glycolytic metabolism in Pseudomonas putida. *Environ Microbiol*.

La Rosa, R., de la Pena, F., Prieto, M.A., and Rojo, F. (2014) The Crc protein inhibits the production of polyhydroxyalkanoates in Pseudomonas putida under balanced carbon/nitrogen growth conditions. *Environ Microbiol* **16**: 278-290.

Lageveen, R.G., Huisman, G.W., Preusting, H., Ketelaar, P., Eggink, G., and Witholt, B. (1988) Formation of Polyesters by Pseudomonas oleovorans: Effect of Substrates on Formation and Composition of Poly-(R)-3-Hydroxyalkanoates and Poly-(R)-3-Hydroxyalkenoates. *Appl Environ Microbiol* **54**: 2924-2932.

Lewis, N.E., Nagarajan, H., and Palsson, B.O. (2012) Constraining the metabolic genotype-phenotype relationship using a phylogeny of in silico methods. *Nat Rev Microbiol* **10**: 291-305.

Lewis, N.E., Hixson, K.K., Conrad, T.M., Lerman, J.A., Charusanti, P., Polpitiya, A.D. et al. (2010) Omic data from evolved E. coli are consistent with computed optimal growth from genome-scale models. *Mol Syst Biol* **6**: 390.

Li, R., Yu, C., Li, Y., Lam, T.W., Yiu, S.M., Kristiansen, K., and Wang, J. (2009) SOAP2: an improved ultrafast tool for short read alignment. *Bioinformatics* **25**: 1966-1967.

Linares, J.F., Moreno, R., Fajardo, A., Martinez-Solano, L., Escalante, R., Rojo, F., and Martinez, J.L. (2010) The global regulator Crc modulates metabolism, susceptibility to antibiotics and virulence in Pseudomonas aeruginosa. *Environ Microbiol* **12**: 3196-3212.

Livak, K.J., and Schmittgen, T.D. (2001) Analysis of relative gene expression data using real-time quantitative PCR and the 2(-Delta Delta C(T)) Method. *Methods* **25**: 402-408.

Luengo, J.M., Garcia, B., Sandoval, A., Naharro, G., and Olivera, E.R. (2003) Bioplastics from microorganisms. *Curr Opin Microbiol* **6**: 251-260.

Luo, B., Groenke, K., Takors, R., Wandrey, C., and Oldiges, M. (2007) Simultaneous determination of multiple intracellular metabolites in glycolysis, pentose phosphate pathway and tricarboxylic acid cycle by liquid chromatography-mass spectrometry. *J Chromatogr A* **1147**: 153-164.

MacGregor, C.H., Wolff, J.A., Arora, S.K., Hylemon, P.B., and Phibbs, P.V., Jr. (1992) Catabolite repression control in *Pseudomonas aeruginosa*. In *Pseudomonas, molecular biology and biotechnology*. Galli, E., Silver, S., and Witholt, B. (eds). Washington, D.C: American Society for Microbiology, pp. 198-206.

Madhushani, A., Del Peso-Santos, T., Moreno, R., Rojo, F., and Shingler, V. (2015) Transcriptional and translational control through the 5'-leader region of the dmpR master regulatory gene of phenol metabolism. *Environ Microbiol* **17**: 119-133.

Madison, L.L., and Huisman, G.W. (1999) Metabolic engineering of poly(3-hydroxyalkanoates): from DNA to plastic. *Microbiol Mol Biol Rev* **63**: 21-53.

Maestro, B., Galan, B., Alfonso, C., Rivas, G., Prieto, M.A., and Sanz, J.M. (2013) A new family of intrinsically disordered proteins: structural characterization of the major phasin PhaF from Pseudomonas putida KT2440. *PLoS One* **8**: e56904.

Martinez-Garcia, E., Aparicio, T., Goni-Moreno, A., Fraile, S., and de Lorenzo, V. (2015) SEVA 2.0: an update of the Standard European Vector Architecture for de-/re-construction of bacterial functionalities. *Nucleic Acids Res* **43**: D1183-1189.

Milojevic, T., Grishkovskaya, I., Sonnleitner, E., Djinovic-Carugo, K., and Blasi, U. (2013) The Pseudomonas aeruginosa catabolite repression control protein Crc is devoid of RNA binding activity. *PLoS One* **8**: e64609.

Moldes, C., Garcia, P., Garcia, J.L., and Prieto, M.A. (2004) In vivo immobilization of fusion proteins on bioplastics by the novel tag BioF. *Appl Environ Microbiol* **70**: 3205-3212.

Monod, J. (1941) Recherches sur la croissance des cultures bactériennes. In. Paris: Hermann.

Morales, G., Ugidos, A., and Rojo, F. (2006) Inactivation of the Pseudomonas putida cytochrome o ubiquinol oxidase leads to a significant change in the transcriptome and to increased expression of the CIO and cbb3-1 terminal oxidases. *Environ Microbiol* **8**: 1764-1774.

Morales, G., Linares, J.F., Beloso, A., Albar, J.P., Martinez, J.L., and Rojo, F. (2004) The Pseudomonas putida Crc global regulator controls the expression of genes from several chromosomal catabolic pathways for aromatic compounds. *J Bacteriol* **186**: 1337-1344.

Moreno, R., and Rojo, F. (2008) The target for the Pseudomonas putida Crc global regulator in the benzoate degradation pathway is the BenR transcriptional regulator. *J Bacteriol* **190**: 1539-1545.

Moreno, R., Fonseca, P., and Rojo, F. (2010) The Crc global regulator inhibits the Pseudomonas putida pWW0 toluene/xylene assimilation pathway by repressing the translation of regulatory and structural genes. *J Biol Chem* **285**: 24412-24419.

Moreno, R., Fonseca, P., and Rojo, F. (2012) Two small RNAs, CrcY and CrcZ, act in concert to sequester the Crc global regulator in Pseudomonas putida, modulating catabolite repression. *Mol Microbiol* **83**: 24-40.

Moreno, R., Ruiz-Manzano, A., Yuste, L., and Rojo, F. (2007) The Pseudomonas putida Crc global regulator is an RNA binding protein that inhibits translation of the AlkS transcriptional regulator. *Mol Microbiol* **64**: 665-675.

Moreno, R., Marzi, S., Romby, P., and Rojo, F. (2009a) The Crc global regulator binds to an unpaired A-rich motif at the Pseudomonas putida alkS mRNA coding sequence and inhibits translation initiation. *Nucleic Acids Res* **37**: 7678-7690.

Moreno, R., Martinez-Gomariz, M., Yuste, L., Gil, C., and Rojo, F. (2009b) The Pseudomonas putida Crc global regulator controls the hierarchical assimilation of amino acids in a complete medium: evidence from proteomic and genomic analyses. *Proteomics* **9**: 2910-2928.

Moreno, R., Hernandez-Arranz, S., La Rosa, R., Yuste, L., Madhushani, A., Shingler, V., and Rojo, F. (2015) The Crc and Hfq proteins of Pseudomonas putida cooperate in catabolite repression and formation of ribonucleic acid complexes with specific target motifs. *Environ Microbiol* **17**: 105-118.

Morita, T., Maki, K., and Aiba, H. (2005) RNase E-based ribonucleoprotein complexes: mechanical basis of mRNA destabilization mediated by bacterial noncoding RNAs. *Genes Dev* **19**: 2176-2186.

Muhr, A., Rechberger, E.M., Salerno, A., Reiterer, A., Malli, K., Strohmeier, K. et al. (2013) Novel description of mcl-PHA biosynthesis by Pseudomonas chlororaphis from animal-derived waste. *J Biotechnol* **165**: 45-51.

Muller, C., Petruschka, L., Cuypers, H., Burchhardt, G., and Herrmann, H. (1996) Carbon catabolite repression of phenol degradation in Pseudomonas putida is mediated by the inhibition of the activator protein PhlR. *J Bacteriol* **178**: 2030-2036.

Nakazawa, T. (2002) Travels of a Pseudomonas, from Japan around the world. *Environ Microbiol* **4**: 782-786.

Nam, H., Campodonico, M., Bordbar, A., Hyduke, D.R., Kim, S., Zielinski, D.C., and Palsson, B.O. (2014) A systems approach to predict oncometabolites via context-specific genome-scale metabolic networks. *PLoS Comput Biol* **10**: e1003837.

Nelson, K.E., Weinel, C., Paulsen, I.T., Dodson, R.J., Hilbert, H., Martins dos Santos, V.A. et al. (2002) Complete genome sequence and comparative analysis of the metabolically versatile Pseudomonas putida KT2440. *Environ Microbiol* **4**: 799-808.

Nikel, P.I., Kim, J., and de Lorenzo, V. (2014) Metabolic and regulatory rearrangements underlying glycerol metabolism in Pseudomonas putida KT2440. *Environ Microbiol* **16**: 239-254.

Nishijyo, T., Haas, D., and Itoh, Y. (2001) The CbrA-CbrB two-component regulatory system controls the utilization of multiple carbon and nitrogen sources in *Pseudomonas aeruginosa*. *Mol Microbiol* **40**: 917-931.

Nogales, J., Palsson, B.O., and Thiele, I. (2008) A genome-scale metabolic reconstruction of Pseudomonas putida KT2440: iJN746 as a cell factory. *BMC Syst Biol* **2**: 79.

O'Toole, G.A., Gibbs, K.A., Hager, P.W., Phibbs, P.V., and Kolter, R. (2000) The Global Carbon Metabolism Regulator Crc Is a Component of a Signal Transduction Pathway Required for Biofilm Development by Pseudomonas aeruginosa. *Journal of Bacteriology* **182**: 425-431.

Ochs, M.M., Lu, C.D., Hancock, R.E., and Abdelal, A.T. (1999) Amino acid-mediated induction of the basic amino acid-specific outer membrane porin OprD from Pseudomonas aeruginosa. *J Bacteriol* **181**: 5426-5432.

Olivera, E.R., Carnicero, D., Jodra, R., Minambres, B., Garcia, B., Abraham, G.A. et al. (2001) Genetically engineered Pseudomonas: a factory of new bioplastics with broad applications. *Environ Microbiol* **3**: 612-618.

Oliveros, J.C. (2007) FIESTA@BioinfoGP. An interactive server for analyzing DNA microarray experiments with replicates. http://bioinfogp.cnb.csic.es/tools/FIESTA.

Orth, J.D., Thiele, I., and Palsson, B.O. (2010) What is flux balance analysis? *Nat Biotechnol* **28**: 245-248.

Palmer, K.L., Aye, L.M., and Whiteley, M. (2007) Nutritional cues control Pseudomonas aeruginosa multicellular behavior in cystic fibrosis sputum. *J Bacteriol* **189**: 8079-8087.

Patil, K.R., Akesson, M., and Nielsen, J. (2004) Use of genome-scale microbial models for metabolic engineering. *Curr Opin Biotechnol* **15**: 64-69.

Petruschka, L., Burchhardt, G., Muller, C., Weihe, C., and Herrmann, H. (2001) The cyo operon of Pseudomonas putida is involved in carbon catabolite repression of phenol degradation. *Mol Genet Genomics* **266**: 199-206.

Pfluger-Grau, K., and Gorke, B. (2010) Regulatory roles of the bacterial nitrogen-related phosphotransferase system. *Trends Microbiol* **18**: 205-214.

Pfluger-Grau, K., and de Lorenzo, V. (2014) From the phosphoenolpyruvate phosphotransferase system to selfish metabolism: a story retraced in Pseudomonas putida. *FEMS Microbiol Lett* **356**: 144-153.

Pfluger-Grau, K., Chavarria, M., and de Lorenzo, V. (2011) The interplay of the EIIA(Ntr) component of the nitrogen-related phosphotransferase system (PTS(Ntr)) of Pseudomonas putida with pyruvate dehydrogenase. *Biochim Biophys Acta* **1810**: 995-1005.

Poblete-Castro, I., Binger, D., Oehlert, R., and Rohde, M. (2014a) Comparison of mcl-Poly(3-hydroxyalkanoates) synthesis by different Pseudomonas putida strains from crude glycerol: citrate accumulates at high titer under PHA-producing conditions. *BMC Biotechnol* **14**: 110.

Poblete-Castro, I., Rodriguez, A.L., Lam, C.M., and Kessler, W. (2014b) Improved production of medium-chain-length polyhydroxyalkanoates in glucose-based fed-batch cultivations of metabolically engineered Pseudomonas putida strains. *J Microbiol Biotechnol* **24**: 59-69.

Poblete-Castro, I., Escapa, I.F., Jager, C., Puchalka, J., Lam, C.M., Schomburg, D. et al. (2012) The metabolic response of P. putida KT2442 producing high levels of polyhydroxyalkanoate under single- and multiple-nutrient-limited growth: highlights from a multi-level omics approach. *Microb Cell Fact* **11**: 34.

Potvin, E., Sanschagrin, F., and Levesque, R.C. (2008) Sigma factors in Pseudomonas aeruginosa. *FEMS Microbiol Rev* **32**: 38-55.

Price-Whelan, A., Dietrich, L.E., and Newman, D.K. (2007) Pyocyanin alters redox homeostasis and carbon flux through central metabolic pathways in Pseudomonas aeruginosa PA14. *J Bacteriol* **189**: 6372-6381.

Prieto, M.A., de Eugenio, L.I., Galán, B., Luengo, J.M., and Witholt, B. (2007) Synthesis and degradation of polyhydroxyalkanoates. In *Pseudomonas, vol V: a Model System in Biology*. Ramos, J.L., and Filloux, A. (eds): Springer, pp. 397-428.

Prieto, M.A., Escapa, I.F., Martinez, V.V., Dinjaski, N., Herencias, C., de la Pena, F. et al. (2014) A holistic view of polyhydroxyalkanoate metabolism in Pseudomonas putida. *Environ Microbiol*.

Regenhardt, D., Heuer, H., Heim, S., Fernandez, D.U., Strompl, C., Moore, E.R., and Timmis, K.N. (2002) Pedigree and taxonomic credentials of Pseudomonas putida strain KT2440. *Environ Microbiol* **4**: 912-915.

Ren, Q., de Roo, G., Witholt, B., Zinn, M., and Thony-Meyer, L. (2010) Influence of growth stage on activities of polyhydroxyalkanoate (PHA) polymerase and PHA depolymerase in Pseudomonas putida U. *BMC Microbiol* **10**: 254.

Ren, Q., de Roo, G., Ruth, K., Witholt, B., Zinn, M., and Thony-Meyer, L. (2009) Simultaneous accumulation and degradation of polyhydroxyalkanoates: futile cycle or clever regulation? *Biomacromolecules* **10**: 916-922.

Revelles, O., Espinosa-Urgel, M., Fuhrer, T., Sauer, U., and Ramos, J.L. (2005) Multiple and interconnected pathways for L-lysine catabolism in Pseudomonas putida KT2440. *J Bacteriol* **187**: 7500-7510.

Roca, A., and Ramos, J.L. (2009) In vivo role of FdhD and FdmE in formate metabolism in Pseudomonas putida: Redundancy and expression in the stationary phase. *Environ Microbiol Rep* **1**: 208-213.

Roca, A., Rodriguez-Herva, J.J., and Ramos, J.L. (2009) Redundancy of enzymes for formaldehyde detoxification in Pseudomonas putida. *J Bacteriol* **191**: 3367-3374.

Roca, A., Rodriguez-Herva, J.J., Duque, E., and Ramos, J.L. (2008) Physiological responses of Pseudomonas putida to formaldehyde during detoxification. *Microb Biotechnol* **1**: 158-169.

Rojo, F. (2010) Carbon catabolite repression in Pseudomonas : optimizing metabolic versatility and interactions with the environment. *FEMS Microbiol Rev* **34**: 658-684.

Ruiz-Manzano, A., Yuste, L., and Rojo, F. (2005) Levels and activity of the Pseudomonas putida global regulatory protein Crc vary according to growth conditions. *J Bacteriol* **187**: 3678-3686.

Ryan, W.J., O'Leary, N.D., O'Mahony, M., and Dobson, A.D. (2013) GacS-dependent regulation of polyhydroxyalkanoate synthesis in Pseudomonas putida CA-3. *Appl Environ Microbiol* **79**: 1795-1802.

Saha, R., Chowdhury, A., and Maranas, C.D. (2014) Recent advances in the reconstruction of metabolic models and integration of omics data. *Curr Opin Biotechnol* **29**: 39-45.

Sambrook, J., and Russell, D.W. (2001) *Molecular cloning: a laboratory manual*. Cold Spring Harbor, N.Y.: Cold Spring Harbor Laboratory.

Schellenberger, J., and Palsson, B.O. (2009) Use of randomized sampling for analysis of metabolic networks. *J Biol Chem* **284**: 5457-5461.

Schellenberger, J., Que, R., Fleming, R.M., Thiele, I., Orth, J.D., Feist, A.M. et al. (2011) Quantitative prediction of cellular metabolism with constraint-based models: the COBRA Toolbox v2.0. *Nat Protoc* **6**: 1290-1307.

Schleissner, C., Olivera, E.R., Fernandez-Valverde, M., and Luengo, J.M. (1994) Aerobic catabolism of phenylacetic acid in Pseudomonas putida U: biochemical characterization of a specific phenylacetic acid transport system and formal demonstration that phenylacetyl-coenzyme A is a catabolic intermediate. *J Bacteriol* **176**: 7667-7676.

Sevilla, E., Alvarez-Ortega, C., Krell, T., and Rojo, F. (2013) The Pseudomonas putida HskA hybrid sensor kinase responds to redox signals and contributes to the adaptation of the electron transport chain composition in response to oxygen availability. *Environ Microbiol Rep* **5**: 825-834.

Sezonov, G., Joseleau-Petit, D., and D'Ari, R. (2007) Escherichia coli physiology in Luria-Bertani broth. *J Bacteriol* **189**: 8746-8749.

Sharma, R., Sahu, B., Ray, M., and Deshmukh, M. (2015) Backbone and stereospecific 13C methyl Ile (δ1), Leu and Val side-chain chemical shift assignments of Crc. *Biomolecular NMR Assignments* **9**: 75-79.

Silva-Rocha, R., and de Lorenzo, V. (2011) A composite feed-forward loop I4-FFL involving IHF and Crc stabilizes expression of the XylR regulator of Pseudomonas putida mt-2 from growth phase perturbations. *Mol Biosyst* **7**: 2982-2990.

Silva-Rocha, R., and de Lorenzo, V. (2014) Chromosomal integration of transcriptional fusions. *Methods Mol Biol* **1149**: 479-489.

Silva-Rocha, R., Martinez-Garcia, E., Calles, B., Chavarria, M., Arce-Rodriguez, A., de Las Heras, A. et al. (2013) The Standard European Vector Architecture (SEVA): a coherent platform for the analysis and deployment of complex prokaryotic phenotypes. *Nucleic Acids Res* **41**: D666-675.

Singh, B., and Rohm, K.H. (2008) Characterization of a Pseudomonas putida ABC transporter (AatJMQP) required for acidic amino acid uptake: biochemical properties and regulation by the Aau two-component system. *Microbiology* **154**: 797-809.

Sonawane, A., Kloppner, U., Derst, C., and Rohm, K.H. (2003a) Utilization of acidic amino acids and their amides by pseudomonads: role of periplasmic glutaminase-asparaginase. *Arch Microbiol* **179**: 151-159.

Sonawane, A., Kloppner, U., Hovel, S., Volker, U., and Rohm, K.H. (2003b) Identification of Pseudomonas proteins coordinately induced by acidic amino acids and their amides: a two-dimensional electrophoresis study. *Microbiology* **149**: 2909-2918.

Sonawane, A.M., Singh, B., and Rohm, K.H. (2006) The AauR-AauS two-component system regulates uptake and metabolism of acidic amino acids in Pseudomonas putida. *Appl Environ Microbiol* **72**: 6569-6577.

Sonnleitner, E., and Blasi, U. (2014) Regulation of Hfq by the RNA CrcZ in Pseudomonas aeruginosa carbon catabolite repression. *PLoS Genet* **10**: e1004440.

Sonnleitner, E., Abdou, L., and Haas, D. (2009) Small RNA as global regulator of carbon catabolite repression in *Pseudomonas aeruginosa*. *Proceedings of the National Academy of Sciences* **106**: 21866-21871.

Sonnleitner, E., Valentini, M., Wenner, N., Haichar, F.Z., Haas, D., and Lapouge, K. (2012) Novel targets of the CbrAB/Crc carbon catabolite control system revealed by transcript abundance in Pseudomonas aeruginosa. *PLoS One* **7**: e44637.

Sudarsan, S., Dethlefsen, S., Blank, L.M., Siemann-Herzberg, M., and Schmid, A. (2014) The functional structure of central carbon metabolism in Pseudomonas putida KT2440. *Appl Environ Microbiol* **80**: 5292-5303.

Tamber, S., Ochs, M.M., and Hancock, R.E. (2006) Role of the novel OprD family of porins in nutrient uptake in Pseudomonas aeruginosa. *J Bacteriol* **188**: 45-54.

Thony, B., and Hennecke, H. (1989) The -24/-12 promoter comes of age. *FEMS Microbiol Rev* **5**: 341-357.

Thorvaldsdottir, H., Robinson, J.T., and Mesirov, J.P. (2013) Integrative Genomics Viewer (IGV): high-performance genomics data visualization and exploration. *Brief Bioinform* **14**: 178-192.

Trias, J., and Nikaido, H. (1990) Protein D2 channel of the Pseudomonas aeruginosa outer membrane has a binding site for basic amino acids and peptides. *J Biol Chem* **265**: 15680-15684.

Ugidos, A., Morales, G., Rial, E., Williams, H.D., and Rojo, F. (2008) The coordinate regulation of multiple terminal oxidases by the Pseudomonas putida ANR global regulator. *Environ Microbiol* **10**: 1690-1702.

Valentini, M., and Lapouge, K. (2013) Catabolite repression in Pseudomonas aeruginosa PAO1 regulates the uptake of C4 -dicarboxylates depending on succinate concentration. *Environ Microbiol* **15**: 1707-1716.

Valentini, M., Storelli, N., and Lapouge, K. (2011) Identification of C(4)-dicarboxylate transport systems in Pseudomonas aeruginosa PAO1. *J Bacteriol* **193**: 4307-4316.

Valentini, M., Garcia-Maurino, S.M., Perez-Martinez, I., Santero, E., Canosa, I., and Lapouge, K. (2014) Hierarchical management of carbon sources is regulated similarly by the CbrA/B systems in Pseudomonas aeruginosa and Pseudomonas putida. *Microbiology* **160**: 2243-2252.

Valls, M., Silva-Rocha, R., Cases, I., Munoz, A., and de Lorenzo, V. (2011) Functional analysis of the integration host factor site of the sigma(54) Pu promoter of Pseudomonas putida by in vivo UV imprinting. *Mol Microbiol* **82**: 591-601.

Varma, A., and Palsson, B.O. (1995) Parametric sensitivity of stoichiometric flux balance models applied to wild-type Escherichia coli metabolism. *Biotechnol Bioeng* **45**: 69-79.

Velazquez, F., di Bartolo, I., and de Lorenzo, V. (2004) Genetic evidence that catabolites of the Entner-Doudoroff pathway signal C source repression of the sigma54 Pu promoter of Pseudomonas putida. *J Bacteriol* **186**: 8267-8275.

Velazquez, F., Pfluger, K., Cases, I., De Eugenio, L.I., and de Lorenzo, V. (2007) The phosphotransferase system formed by PtsP, PtsO, and PtsN proteins controls production of polyhydroxyalkanoates in Pseudomonas putida. *J Bacteriol* **189**: 4529-4533.

Vilchez, S., Manzanera, M., and Ramos, J.L. (2000a) Control of expression of divergent Pseudomonas putida put promoters for proline catabolism. *Appl Environ Microbiol* **66**: 5221-5225.

Vilchez, S., Molina, L., Ramos, C., and Ramos, J.L. (2000b) Proline catabolism by Pseudomonas putida: cloning, characterization, and expression of the put genes in the presence of root exudates. *J Bacteriol* **182**: 91-99.

Vinuselvi, P., Kim, M.K., Lee, S.K., and Ghim, C.M. (2012) Rewiring carbon catabolite repression for microbial cell factory. *BMB Rep* **45**: 59-70.

Vogel, J., and Luisi, B.F. (2011) Hfq and its constellation of RNA. *Nat Rev Microbiol* **9**: 578-589.

Waltermann, M., and Steinbuchel, A. (2005) Neutral lipid bodies in prokaryotes: recent insights into structure, formation, and relationship to eukaryotic lipid depots. *J Bacteriol* **187**: 3607-3619.

Wilson, W.A., Roach, P.J., Montero, M., Baroja-Fernandez, E., Munoz, F.J., Eydallin, G. et al. (2010) Regulation of glycogen metabolism in yeast and bacteria. *FEMS Microbiol Rev* **34**: 952-985.

Winsor, G.L., Lam, D.K., Fleming, L., Lo, R., Whiteside, M.D., Yu, N.Y. et al. (2011) Pseudomonas Genome Database: improved comparative analysis and population genomics capability for Pseudomonas genomes. *Nucleic Acids Res* **39**: D596-600.

Wolff, J.A., MacGregor, C.H., Eisenberg, R.C., and Phibbs, P.V., Jr. (1991) Isolation and characterization of catabolite repression control mutants of Pseudomonas aeruginosa PAO. *J Bacteriol* **173**: 4700-4706.

Yuste, L., and Rojo, F. (2001) Role of the crc gene in catabolic repression of the Pseudomonas putida GPo1 alkane degradation pathway. *J Bacteriol* **183**: 6197-6206.

Yuste, L., Canosa, I., and Rojo, F. (1998) Carbon-source-dependent expression of the *PalkB* promoter from the *Pseudomonas oleovorans* alkane degradation pathway. *J Bacteriol* **180**: 5218-5226.

Yuste, L., Hervas, A.B., Canosa, I., Tobes, R., Jimenez, J.I., Nogales, J. et al. (2006) Growth phase-dependent expression of the Pseudomonas putida KT2440 transcriptional machinery analysed with a genome-wide DNA microarray. *Environ Microbiol* **8**: 165-177.

Zhang, X.X., and Rainey, P.B. (2008) Dual involvement of CbrAB and NtrBC in the regulation of histidine utilization in *Pseudomonas fluorescens* SBW25. *Genetics* **178**: 185-195.

Supplementary Materials

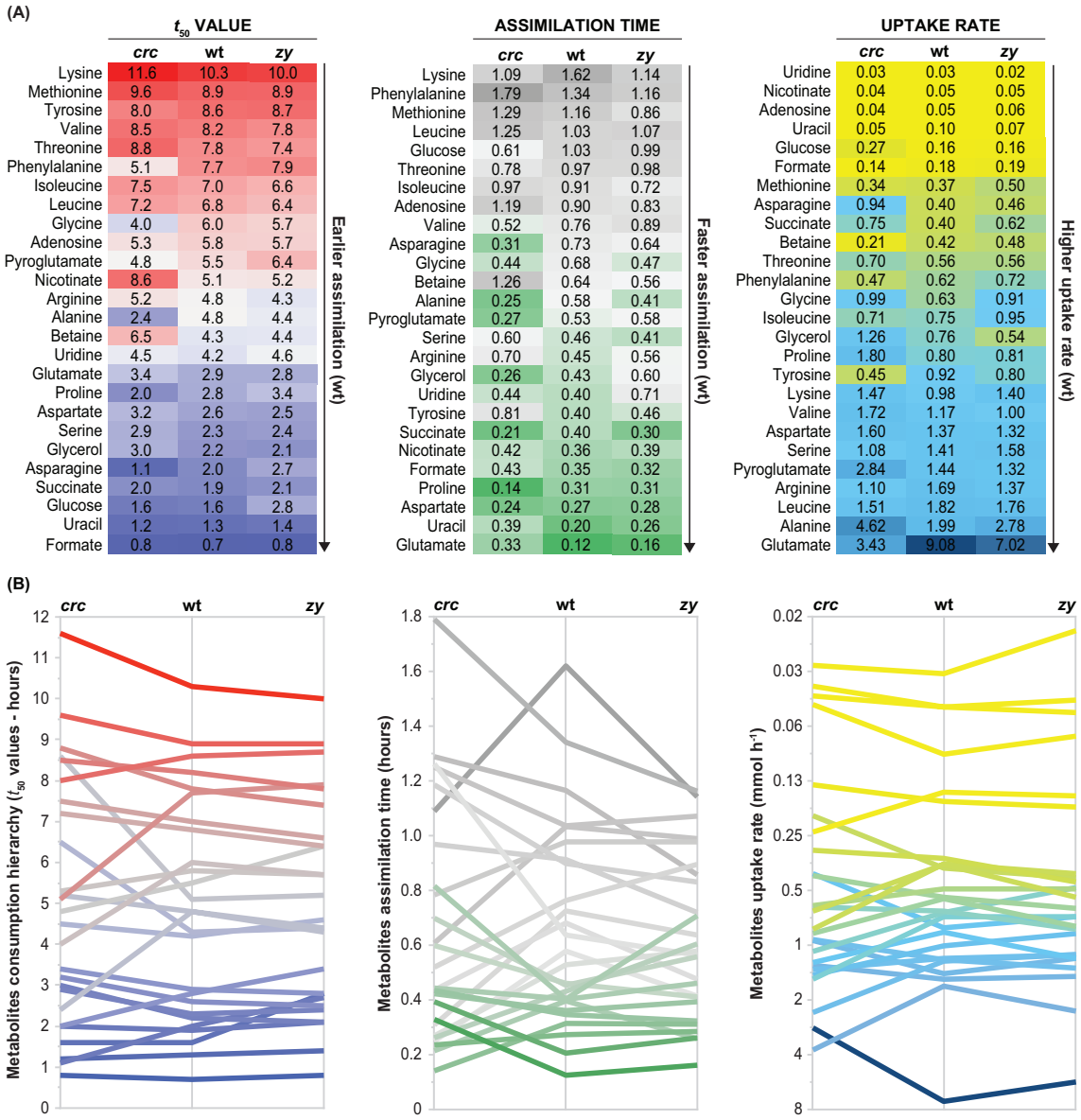

Fig. S1 Parameters for the assimilation of the detected compounds.
(**A**) Heat maps of the "t_{50}" values, "assimilation times" and "uptake rates" derived from the sigmoid fits of concentration data ordered from the highest to the lowest (t_{50} and assimilation time) and from the lowest to the highest (uptake rate). Values correspond to *P. putida* strains KT2440 (wild type, indicated as 'wt'), KTCRC (Crc-null derivative of KT2440, indicated as '*crc*') and KT2440-ZY (CrcZ- and CrcY-null derivative of KT2440, indicated as '*zy*'). Values corresponding to the t_{50} (time at which the concentration has changed by half) and the assimilation time (time needed to detect a decrease in the relative concentration from 75% to 25% of the starting value) are indicated in hours. Uptake rates, indicated as mmol h^{-1}, correspond to the decreased in concentration of each compound (from the 75% to 25% of its initial value) relative to the time period of the decrease. (**B**) Parallel plots of the t_{50} values, assimilation times and uptake rates. Each line represents a metabolite and follows the order as indicated in (A).

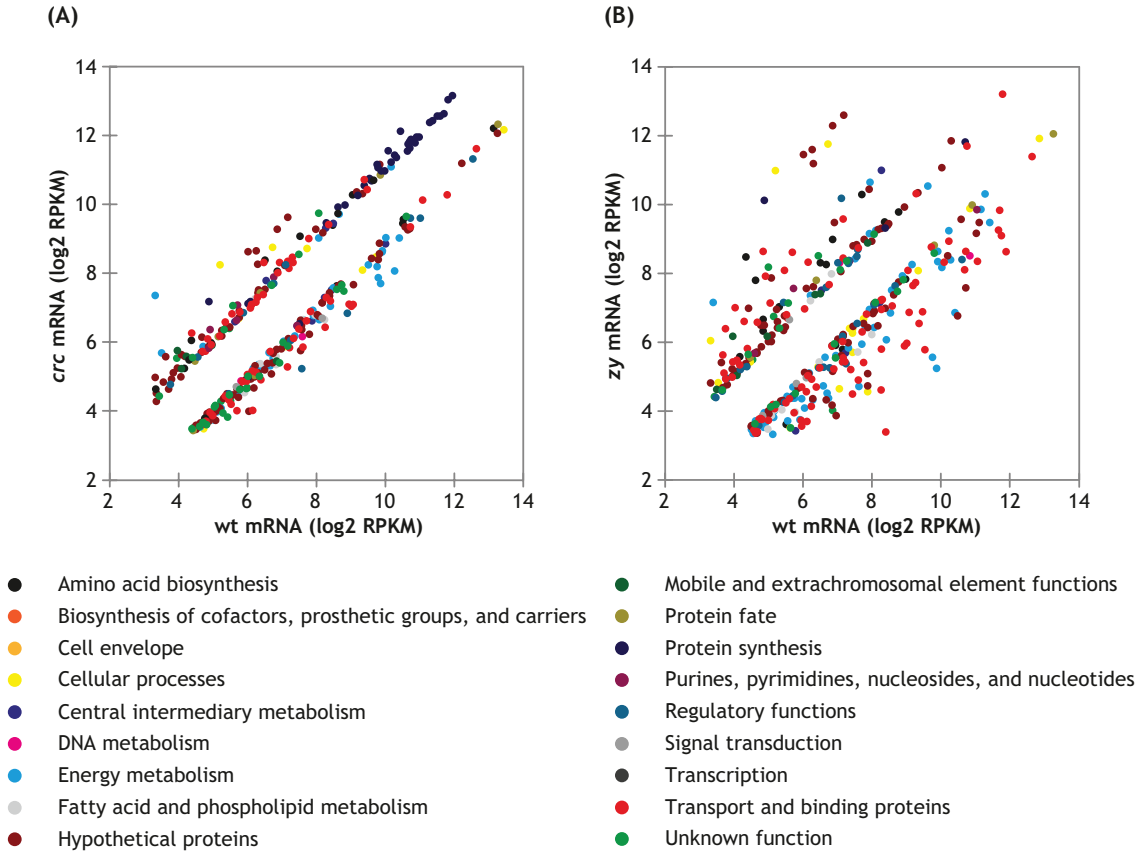

Fig. S2 Scattered plots of the differentially expressed genes.
Genes showing increased or reduced mRNA levels upon inactivation of the *crc* gene (**A**), or of the *crcZ* and *crcY* genes (**B**). Only those genes presenting an absolute fold-change of >1.8, and with a *P* value (corrected for FDR) of <0.001, are represented. Values derive from RNA-Seq assays (Table S1), and are indicated as RPKM (reads per kilobase per million reads). In the Crc-null strain, 7.4% of the genes were differentially expressed compared to the wild type, a value that increased to 8.2% for the CrcZ/CrcY-null strain.

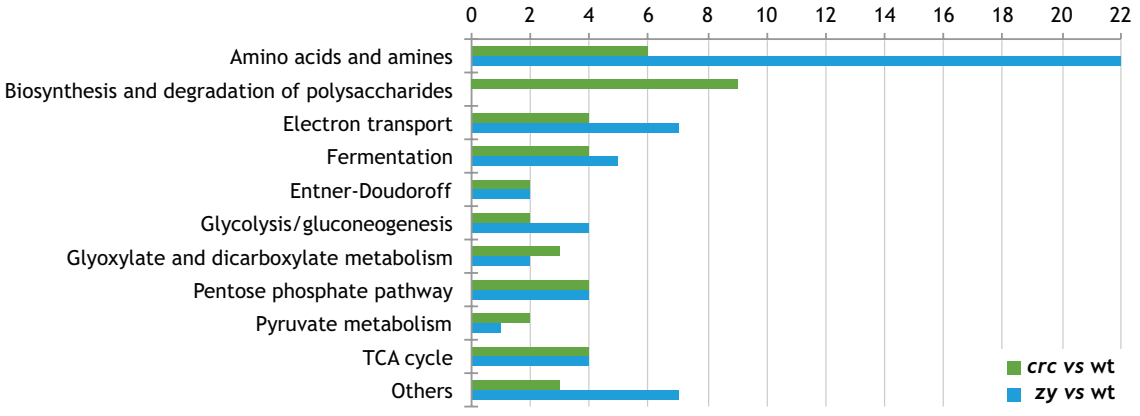

Fig. S3 Genes belonging to the functional category of energy metabolism.
In green genes that show elevated or reduced mRNA levels upon inactivation of the *crc* gene, or in blue of the *crcZ* and *crcZ* genes, and divided into sub-categories. The scale on top indicates "number of genes".

Table S1: List of the genes showing increased or reduced mRNA levels upon inactivation of the *crc* gene (*crc*/wt spreadsheet), or of the *crcZ* and *crcY* genes (*zy*/wt spreadsheet), as indicated by RNA-Seq analyses.
The table includes only those genes presenting an absolute fold-change of > 1.8, with a P-value (corrected for FDR) of < 0.001 and an RNA abundance of > 10 reads per kilobase per million reads (RPKM). The spreadsheets labelled as 'operons' include those genes that were observed to be differentially expressed (highlighted in yellow) and that are part of computationally predicted operons (as indicated at the Pseudomonas Genome Database, http://www.pseudomonas.com; Winsor et al., 2011).

Table S1 can be downloaded from the following webpage:
http://onlinelibrary.wiley.com/doi/10.1111/1462-2920.12812/suppinfo

Annexes: published papers